Review

Highly oriented hydrogels for tissue regeneration: design strategies, cellular mechanisms, and biomedical applications

Jiuping Wu[1,2#], Zhihe Yun[3#], Wenlong Song[4], Tao Yu[3], Wu Xue[3], Qinyi Liu[3✉], Xinzhi Sun[1✉]

1. Department of Orthopedics, The First Affiliated Hospital of Zhengzhou University, Zhengzhou 450052, China.
2. Translational Medicine Center, The First Affiliated Hospital of Zhengzhou University, Zhengzhou 450052, China.
3. Department of Orthopedics, The Second Hospital of Jilin University, Changchun 130041, China.
4. State Key Laboratory of Supramolecular Structure and Materials, College of Chemistry, Jilin University, Changchun 130023, China.

#These authors contributed equally to this work.

✉ Corresponding authors: Qinyi Liu, Email: qinyi@jlu.edu.cn; Xinzhi Sun Email: sunxinzhi2023@163.com.

Abstract

Many human tissues exhibit a highly oriented architecture that confers them with distinct mechanical properties, enabling adaptation to diverse and challenging environments. Hydrogels, with their water-rich "soft and wet" structure, have emerged as promising biomimetic materials in tissue engineering for repairing and replacing damaged tissues and organs. Highly oriented hydrogels can especially emulate the structural orientation found in human tissue, exhibiting unique physiological functions and properties absent in traditional homogeneous isotropic hydrogels. The design and preparation of highly oriented hydrogels involve strategies like including hydrogels with highly oriented nanofillers, polymer-chain networks, void channels, and microfabricated structures. Understanding the specific mechanism of action of how these highly oriented hydrogels affect cell behavior and their biological applications for repairing highly oriented tissues such as the cornea, skin, skeletal muscle, tendon, ligament, cartilage, bone, blood vessels, heart, etc., requires further exploration and generalization. Therefore, this review aims to fill that gap by focusing on the design strategy of highly oriented hydrogels and their application in the field of tissue engineering. Furthermore, we provide a detailed discussion on the application of highly oriented hydrogels in various tissues and organs and the mechanisms through which highly oriented structures influence cell behavior.

1. Introduction

Tissue engineering (TE), which was first defined in 1993, is an interdisciplinary field that combines the principles of life science and engineering in vitro with the ultimate goal of developing biological substitutes or entire tissues and organs for use in basic research on physiological processes and translational therapies aimed at repairing, preserving or enhancing tissue function [1]. To achieve this, bionic scaffolds have been designed using various strategies to provide cells with biochemical and/or biophysical cues replicating the in vivo cellular survival environment, aiming to regulate cellular behavior toward proliferation and differentiation for tissue repair and regeneration. As such, emulating the structural and physicochemical properties of natural tissues or organs is paramount in TE.

Hydrogel, a cross-linked polymer network containing water, has emerged as a promising candidate for biomedical TE applications owing to its biocompatibility, ease of functionalization, and ability to mimic the chemical and biophysical properties of various structures in vivo [2-4]. However, traditional

hydrogels' poor mechanical properties and brittleness, which impede their wider use **(Table 1)**, have led researchers to explore and develop numerous approaches to address these limitations over the past decades. For instance, double-network [5], nanocomposite [6], dynamically cross-linked [7], and polyampholyte [8] hydrogels have shown great potential in improving the mechanical properties of hydrogels. However, as TE research advances, it has become clear that these efforts are insufficient to replicate natural tissues; replicating the structure of natural tissues and organs is also crucial in pursuing bionics.

Table 1. Mechanical properties and applicable clinical applications of traditional hydrogels and highly oriented hydrogels.

	Highly Oriented Hydrogel	Traditional Hydrogels
Properties	• A special type of hydrogel, based on the distribution of internal components • With highly oriented structure (Most important properties) • Anisotropic mechanical properties • For special application purposes	• Mechanical property (Comparatively soft materials) • Water-absorbing quality (Wet materials) • Biocompatibility • Biodegradability • Swellability • Stimuli sensitivity ("Smart" materials) • Based on different purposes and applications, special properties will be highlighted
Clinical applications	• Main applications for tissue repair and regeneration of oriented tissues, such as cartilage, bone, skeletal muscle, tendons, myocardium, nerves, blood vessels, and cornea, et al.	• Main applications for tissue repair and regeneration of soft tissues, such as muscle, skin, nerves, blood vessels, et al. • With special mechanical properties enhanced, also used in tissue repair and regeneration of hard tissues, such as bone, cartilage, tendon, et al.

Natural biological tissues such as cartilage [9], bone [10], skeletal muscle [11], tendons [12], myocardium [13], nerves [14], blood vessels [15, 16], and cornea [17] exhibit highly oriented structures that bestow them with distinctive mechanical properties, which are fundamental to their biological function **(Figure 1)**. For example, the layered, highly oriented cartilage structure confers different tasks to each layer, allowing them to work in synergy to dissipate compressive loads and absorb impact [9]. Similarly, the highly oriented arrangement of collagen fibers in skeletal muscle imparts superior mechanical properties [11]. The importance of highly oriented microenvironments in the body for regulating cell behavior and tissue development demonstrates the need to construct highly oriented 3D hydrogels in vitro to replicate natural tissues' unique mechanical properties and functions. This approach enhances

hydrogels' mimicry of natural tissues and broadens their applications [18].

Recent studies have reported on a variety of highly oriented hydrogels, which can be broadly summarized as (i) highly oriented nanofillers hydrogels obtained using strategies such as magnetic/electric fields [19, 20] and mechanical forces [21], (ii) hydrogels with a highly oriented polymer-chain network obtained by strategies such as mechanical forces [22] and ion diffusion [23], (iii) hydrogels with highly oriented void channels prepared by strategies such as directed freezing/ice templates [24], and (iv) highly oriented hydrogels with microfabricated structures using strategies such as 3D printing [25], and (v) other highly oriented hydrogels prepared by special methods **(Figure 2)**. This paper aims to review each of these strategies, discussing their unique strengths and limitations and the progress of research.

In addition, although hydrogels have been widely used in TE and regenerative medicine, the specific mechanism of action of how hydrogels affect cell behavior is still not fully understood. Similarly, the mechanism of how highly oriented hydrogels affect specific cell behaviors and promote tissue repair and regeneration is unknown, with only limited literature suggesting that they can regulate specific cellular behaviors by influencing cell physiological processes such as cell adhesion, proliferation, migration, and differentiation [26, 27]. Although their cytological mechanisms are not well understood, studies have confirmed that highly oriented hydrogels are effective for structural and functional tissue repair and regeneration, especially for highly oriented tissues such as nerve [28], skeletal muscle [29], tendon [30], ligament [31], cartilage [32], bone [33], blood vessels [34], heart [35], etc., by mimicking their structure. However, the extensive literature on the biological applications of highly oriented hydrogels remains to be summarized and reviewed.

Several exceptional previously published reviews exist on anisotropic hydrogels, ranging from comprehensive reviews covering their diverse applications across various fields to reports focusing on their use in a specific TE domain [36-41]. Additionally, some reviews delve into specific preparation strategies for anisotropic hydrogels in TE applications [42, 43]. Nancy Khuu et al. [44] reviewed the synthesis, characterization, and physical properties of anisotropic hydrogels for use in TE; however, they did not provide an overview of recent advances in TE applications. This review aims to fill that gap by focusing on the design strategy of highly oriented hydrogels and their application in TE **(Table 2)**. In particular, we provide a detailed discussion of

the applications of highly oriented hydrogels in different tissues and organs and the mechanisms by which highly oriented structures may influence cell behavior. This comprehensive review provides valuable insights into the progress and challenges in preparing highly oriented hydrogels and their potential applications in TE. By understanding the strengths and weaknesses of each strategy, researchers can more effectively develop novel approaches to prepare highly oriented hydrogels with improved properties and functionalities, leading to better outcomes for TE applications.

2. Design and Preparation of Highly Oriented Hydrogels

Scientists have designed and reported several types of highly oriented structural hydrogels. These include nanofiller hydrogels obtained through magnetic/electrical fields, mechanical forces, self-assembly, and other methods; polymer-chain network hydrogels can be prepared through mechanical forces, ion diffusion, and other methods; void channel hydrogels can be obtained through sacrificial template methods such as directed freezing; hydrogels with microfabricated structures can be created through techniques such as 3D printing; and lastly, other specialized techniques can be used to prepare highly oriented hydrogels.

2.1. Highly Oriented Nanofillers Hydrogels

A common method for preparing highly oriented hydrogels is to disperse highly oriented nanofiller materials within them. Various methods, including magnetic/electrical fields, mechanical forces, directed freezing, and self-assembly, can control the distribution and orientation of the filler material. This section presents the principles and recent advances of these different methods and discusses their respective advantages and disadvantages.
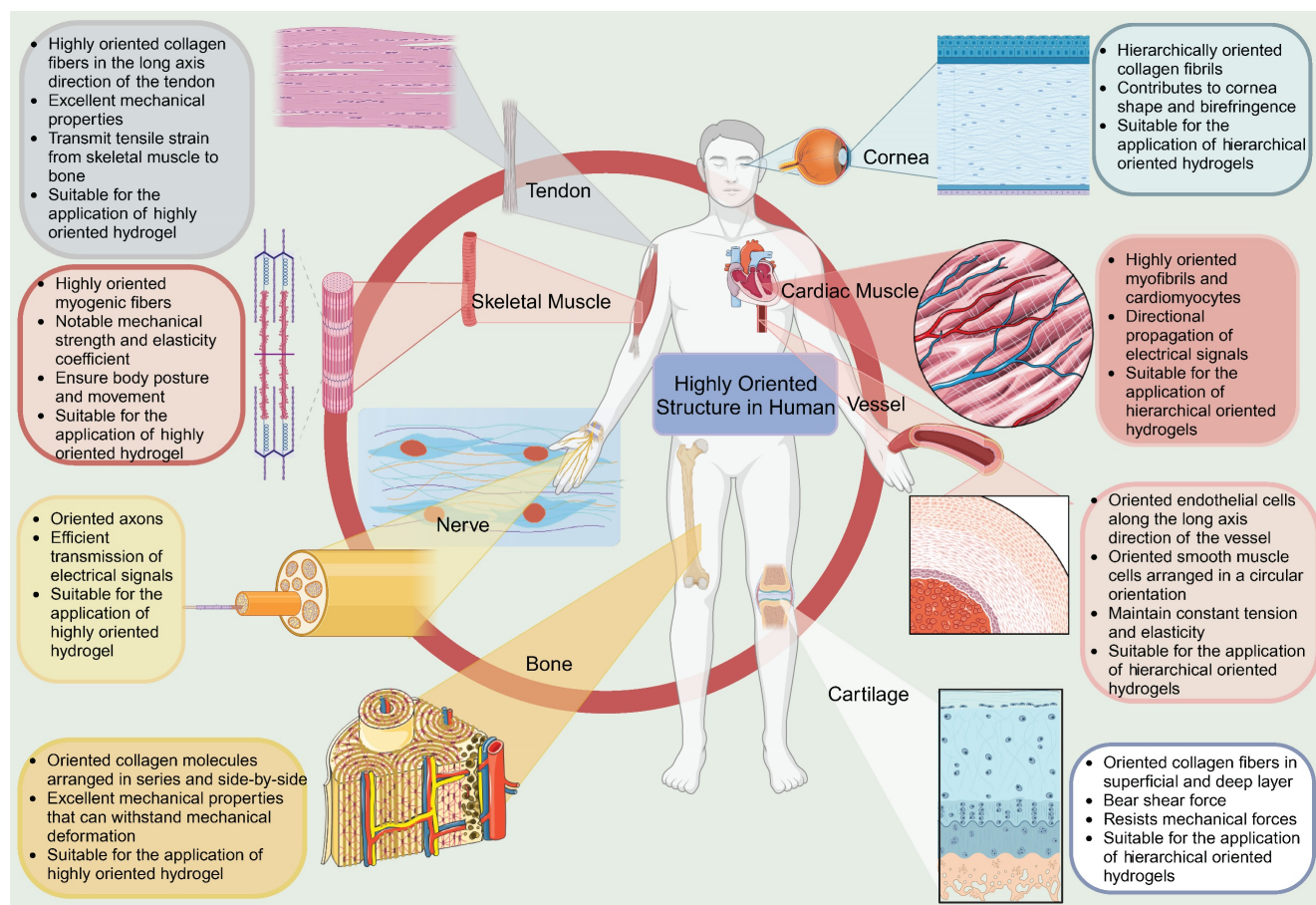
Figure 1. Highly oriented tissues and organs in the human body (Figure was created with Biorender.com).
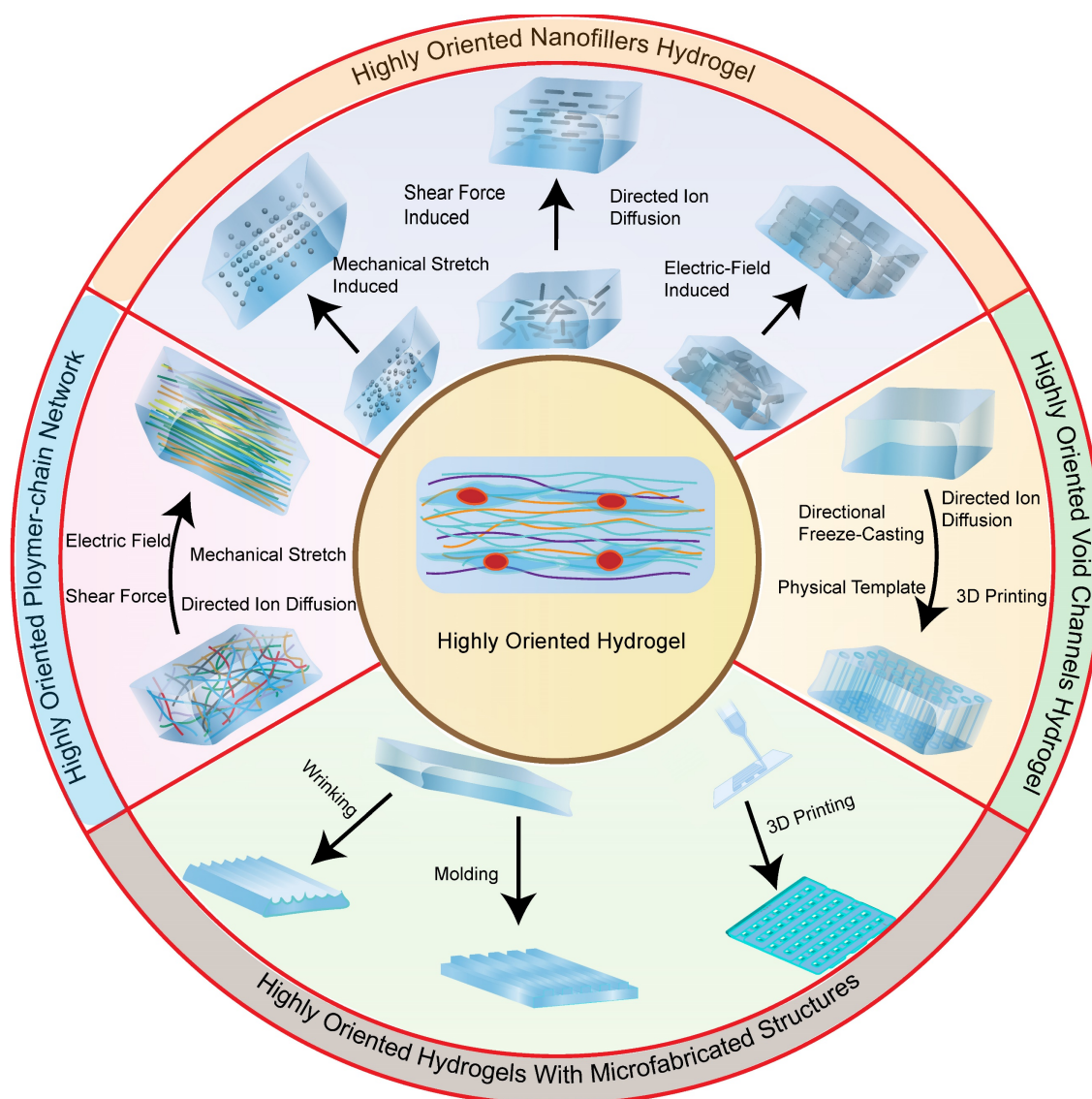
Figure 2. Classification of highly oriented hydrogels, which can be broadly summarized as highly oriented nanofillers hydrogels obtained using strategies such as magnetic/electric fields and mechanical force, highly oriented polymer-chain network hydrogels obtained by strategies such as mechanical force and ion diffusion, highly oriented void channels hydrogels prepared by strategies such as directed freezing/ice template, and highly oriented hydrogels with microfabricated structures using strategies such as 3D printing.

2.1.1. Magnetic-Field-Induced Highly Oriented Nanofillers Hydrogels

Magnetic highly oriented hydrogels are prepared by controlling the distribution of magnetic field-responsive materials in the hydrogel using a magnetic field to obtain an oriented structure. Magnetism-responsive electrons in the filler material allow for the formation of a highly oriented morphology in the external magnetic field, which is then fixed in the 3D hydrogel during the gelation process, resulting in a highly oriented structure that is maintained after the withdrawal of the external magnetic field [38]. This composite hydrogel is highly oriented and magnetic, while also exhibiting excellent biocompatibility, which is particularly important in TE. Its preparation, involving magnetically respon-sive materials, both magnetic and non-magnetic, and

an external magnetic field, offers a non-invasive and therefore advantageous alternative to other methods of creating highly oriented hydrogels.

2.1.1.1. Magnetically Responsive Materials

Magnetically responsive materials can be categorized into two types: magnetic and non-magnetic materials. Among magnetic materials, magnetic nanoparticles (MNPs) are extensively employed for TE repair due to their remarkable magnetic responsiveness [42, 45-52]. The MNPs used for biomedical applications include iron oxide-based MNPs such as hematite (α-Fe_2O_3), magnetite (γ-Fe_2O_3), and magnetite (Fe_3O_4), transition metal ferrites such as $CoFe_2O_4$, $MnFe_2O_4$, and transition metal alloys like FePT, which are incorporated into hydrogels [53-57]. Iron oxide-based MNPs have been approved by the FDA for clinical use due to their

good biocompatibility, high magnetization ability, low toxicity, easy preparation, and low cost. Consequently, they have gained significant attention in biomedical applications such as TE and drug delivery, and are more commonly used than other types of MNPs [42, 58-66].

Table 2. Comparison of different highly oriented hydrogels and their applications in tissue engineering.

Highly Oriented hydrogel	Strategy		Advantages		Challenges		Applications in tissue engineering
Highly oriented nanofillers hydrogels	•	Magnetic-Field-Induced	• •	Remote control Nanofillers of different dimensions (0D, 1D, 2D)	• •	Non-magnetic fillers require high-intensity magnetic fields Safety of different magnetic fillers in tissue engineering	Tendon [19, 29, 31], Skin [81], Bone [110], Cartilage [309], Nerve [51, 368, 373]
	•	Electric-Field-Induced	• •	Fast and easy preparation Nanofillers of different dimensions (0D, 1D, 2D)	• •	Noncontact strategy Electrochemical stability of the material	Cardiac Muscle [129, 130], Nerve [375]
	•	Mechanical force-Induced	• • •	Fast and simple preparation Easy processing Excellent mechanical properties	• •	Unevenly distributed shear forces Precise control	Cardiac Muscle [152, 153], Cartilage [152], Tendon [154, 177], Skeletal Muscle [170], Nerve [380], Vessel [409]
	•	Directed freezing	• •	Easy processing Large-scale fabrication	• • •	Time/energy-consuming during freezing Low temperature environment below zero Precise control	Nerve [374]
	•	Self-assembly	•	No external force required	• • •	Large-scale fabrication Easy processing Precise control	Skeletal Muscle [170], Nerve [390]
Hydrogels with highly oriented polymer-chain network	•	Mechanical Stretch Induced	• • • •	Fast and simple preparation Easy processing Excellent mechanical properties Good reproducibility	• •	Precise control Huge mechanical force	Tendon [177, 180, 184], Bone [181, 321, 322], Cardiac Muscle [35]
	•	Directed Ion Diffusion	•	Easy processing	•	Non-homogeneous	Vessel [186]
	•	Shear Force Induced	•	Easy processing	• •	Unevenly distributed shear forces Precise control	Bone [188, 189, 192], Skeletal Muscle [190], Tendon [190], Nerve [14, 28, 383], Cardiac Muscle [192]
	•	Electric-Field-Induced	•	Fast and easy preparation	• •	Noncontact strategy Electrochemical stability of the material	Vessel [194], Bone [195], Nerve [196]
Hydrogels with highly oriented void channels	•	Directional Freeze-Casting	• • • •	Easy processing Controllable pore size Controllable pore arrangement Large-scale fabrication	• • •	Time/energy-consuming during freezing Low temperature environment Uncontrollable pore shape	Bone [307, 318], Cartilage [32, 307, 308], Nerve [202]
	•	physical template/molding	• •	Easy processing Personalized assembly	•	Low mechanical strength	Nerve [211-215]
	•	Directed Ion Diffusion	•	Easy processing	•	Low mechanical strength	Vessel [186]
	•	3D Printing	• • • • •	Precise control Complex architectures Rapid prototyping Scalability Versatile	• • •	Limited to printable hydrogels Expensive Resolution	Nerve [14, 219], Cornea [393]
Highly oriented hydrogels with microfabricated structures	•	3D Printing	• • • • • •	Precise control Complex architectures Rapid prototyping Scalability Versatile Personalization	• • •	Limited to printable hydrogels Expensive Resolution	Skin [25], Skeletal Muscle [192, 346], Cardiac Muscle [192, 355, 357], Tendon [227, 332], Nerve [364, 369, 381], Disc [226], Bone [319, 320], Cornea [394, 395], Vessel [34, 408]
	•	Molding	• •	Easy processing Personalized assembly	•	Template's design and prepared	Cardiac Muscle [228, 356], Nerve [231], Skeletal Muscle [231]
	•	Wrinkling	• •	Fast and easy preparation Easy processing	•	Precise control	Bone [240]
Special highly oriented hydrogels	•	Biotemplating	•	Excellent mechanical properties	•	In vivo degradation	Disc [418], Cartilage Muscle [312], Bone [33]
	•	Filamented Light biofabrication	• • •	Ultrahigh aspect ratios Complex architectures Rapid production	•	Expensive	Tendon, Skeletal Muscle [30]
	•	Embed highly oriented structure in hydrogel	•	Personalized assembly	•	Complicated	Cartilage [245, 310, 311], Cardiac Muscle [246]
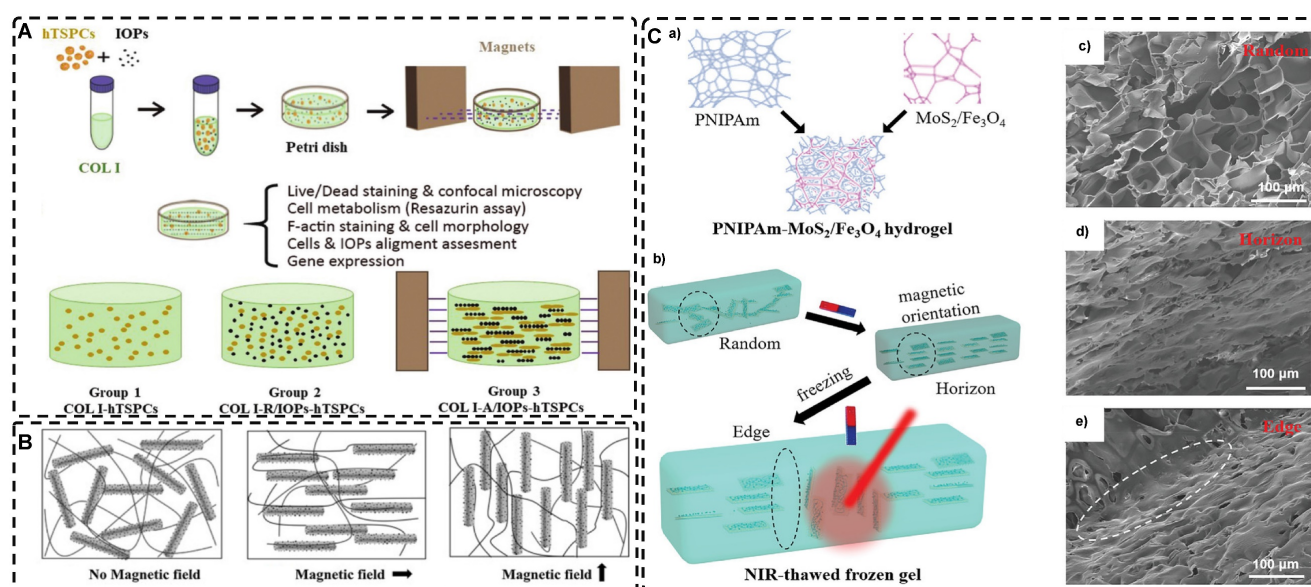
Figure 3. Fabrication of highly oriented hydrogels based on 0D nanoparticles (A), 1D nanotubes (B) and 2D nanosheets (C) in an external magnetic field. A). Schematic illustration of the formation of anisotropic hTSPC-nanocomposite hydrogel induced by the addition of paramagnetic iron oxide nanoparticles (IOPs) under exposure to magnetic field and cartoon of the three study groups. Adapted with permission from [19], copyright 2021, Royal Society of Chemistry. B) Schematic representation of 1D nanorods in hydrogel oriented under an external magnetic field. Adapted with permission from [81], copyright 2020, Elsevier. C) Schematic representation of a) the fabrication of PNIPAm-MoS₂/Fe₃O₄ hydrogel and b) programming the orientation of MoS₂/Fe₃O₄ under the magnetic field followed by NIR light-treatment of frozen hydrogels. Representative SEM images of PNIPAm-MoS₂/Fe₃O₄ hydrogels under different conditions. Adapted with permission from [93], copyrights 2022, Wiley-VCH.

The arrangement of MNPs into highly oriented hydrogels depends on various properties such as the size, shape, and saturation magnetic strength of MNPs, as well as the strength and shape of the magnetic field [67]. These factors have a significant impact on the physicochemical properties and magnetic responsiveness of the final hydrogels, which in turn are influenced by the method of MNP synthesis [47, 59, 68]. Currently, the three main synthesis methods for MNPs are physical, chemical, or biological [69]. Chemical synthesis methods such as sol-gel, solvothermal synthesis, co-precipitation, and thermal decomposition account for the majority of all MNPs produced as they deliver better particle quality and higher homogeneity. Compared to chemical synthesis methods, physical synthesis methods including thermal evaporation, pulsed laser deposition and grinding produce less than 10% of all MNPs. Biological synthesis methods as the third synthesis method for MNPs include using microorganisms, enzymes, fungi, plants and plant extracts. Similarly, biological synthesis methods are also used for the preparation of only a small amount of MNPs [42, 58, 70]. Among the chemical methods, the thermal decomposition method has better application potential than the simple, fast, cheap, and high-yield co-precipitation method, as it allows for better control over the shape and size of MNPs [42].

The size of MNPs is one of the most influential factors that affect their properties. When the particle diameter is less than a well-defined size (D_{cr}), the particles become single domain and have uniform magnetization, regardless of the presence of an external magnetic field [42, 71]. Further reduction in diameter to less than a certain critical size (D_{sp}) results in particles entering the superparamagnetic regime, where the magnetic moment becomes thermally unstable and changes spontaneously and rapidly in the absence of an external magnetic field [72, 73]. Superparamagnetic particles have zero magnetization in the absence of an external magnetic field and exhibit magnetic responsiveness only in the presence of such a field, making them highly remote-controllable in practical applications [74]. Additionally, they have little tendency to form aggregates, which, along with their low toxicity, make highly oriented hydrogels of superparamagnetic state MNPs promising for TE applications [42, 70, 75].

Magnetic nanomaterials of various dimensions (0D, 1D, 2D) can be magnetically assembled and oriented in a pre-hydrogel solution under the influence of an external magnetic field. The 0D MNPs typically form a chain-like oriented structure when exposed to a magnetic field[19, 76-80]. Recently, Xu et al. [19] successfully produced highly oriented nanocomposite hydrogels that consist of type I collagen and oriented MNPs **(Figure 3A)**. Compared to pristine type I collagen and isotropic hydrogels, human Tendon Stem/Progenitor Cells (hTSPCs) had a higher value-added rate in highly oriented hydrogels, resulting in significant upregulation of tendon-related genes and good potential for clinical

translation. Zhang et al. [80] also reported the self-assembly of SiO_2-coated Fe_3O_4 nanoparticles into highly oriented unconfined filled arrays in a pre-hydrogel solution. The MNPs conferred magnetic and photothermal properties to the highly oriented hydrogels, resulting in self-healing properties, and their results showed that the viability of cells is not affected by the temperature changes induced by light and alternating magnetic fields.

Magnetic 1D nanorods or nanowires and 2D nanosheets may facilitate better orientation compared to magnetic spherical particles [81, 82]. Several studies have reported the preparation of highly oriented hydrogels based on 1D nanomaterials utilizing magnetic fields [71, 81, 83-88]. Rincón-Iglesias et al. [83] synthesized highly monodisperse ferrimagnetic Fe_3O_4 nanorods with adjustable size by solvothermal synthesis and varied the amount of hexadecylamine capping ligands. Subsequently, the nanorods were coated with gold shells and doped into agarose hydrogels, to obtain hydrogels with anisotropic magnetic and optical properties. These hydrogels have applications in fields such as regenerative medicine, cancer ablation, local therapy, and sensors due to their magneto-thermal and photothermal properties. Shi et al. [81] dispersed silica nanorods coated with Fe_3O_4 in a sol-gel state type I collagen and aligned the nanorods along the magnetic field with a weak magnetic field (<100 mT) generated by two plate-like magnets **(Figure 3B)**. Next, the sol-gel state was transformed into the gel state at 37°C to prepare a highly oriented hydrogel that facilitates the directional growth of normal human dermal fibroblasts.

Similarly, recent studies have shown that 2D magnetic nanosheets can create highly oriented structures when subjected to an external magnetic field [89-94]. Dai et al. [91] accomplished the formation of two-dimensional magnetic nanosheet structures (MDS) by interleaving γ-Fe_2O_3 nano-particles between two silicate layers. They then rotated the magnetic field (± 260 mT) to obtain a range of highly oriented poly(N-isopropylacrylamide) (PNIPAm) nanocomposite hydrogels. These MDS structures exhibit controlled anisotropy in optical and mechanical properties due to their sandwich structure, high aspect ratio, high charge density, and responsiveness to light and magnetic fields. Additionally, they exhibit anisotropic responses to temperature or light irradiation. Chen et al. [93] developed a novel programmable hydrogel that is magneto-thermally responsive and highly oriented **(Figure 3C)**. They anchored thermally sensitive PNIPAm and Fe_3O_4 magnetic nanoparticles onto the surface of MoS_2 nanosheets and then embedded them in 3D-printed hydrogel cubes. They controlled the orientation of the 2D nanosheets by applying a magnetic field. In a separate study, Yan et al. [92] prepared a highly oriented hydrogel using catechol-mediated precipitation of Fe_3O_4 nanoparticles encapsulated on the surface of dialdehyde cellulose-polydopamine (DAC-PDA) nanomaterials, cross-linked with PAM chains under a magnetic field. The hydrogel possessed high electrical conductivity, strong adhesion, and biocompatibility, making it a promising candidate for various advanced applications, especially for flexible wearable sensors. The above examples demonstrate the wide range of current applications of magnetic materials in the preparation of highly oriented hydrogels and their potential for future use in TE.

Non-magnetic materials exhibit an extremely weak response to external magnetic stimuli and can be categorized as either antimagnetic or paramagnetic [42, 95]. Several non-magnetic materials, including peptides [96, 97], protein fibers such as fibrin and collagen [98-101], cellulose nanocrystals [31, 102, 103], carbon nanotubes [88, 104], graphene [105, 106], and rare earth elements [107], have been explored for the preparation of highly oriented structural hydrogels. For instance, Radvar et al. [96] designed peptides that contained phenylalanine residues at the C-terminus and fabricated hydrogels with highly oriented nanofiber alignment through the self-assembly of peptides with hyaluronic acid. By exploiting the antimagnetic properties of phenylalanine residues under magnetic fields (12T, 6T, 1T), they achieved highly oriented hydrogels. Echave et al. [31] incorporated cellulose nanocrystals (CNC) into a gelatin network and utilized the antimagnetic properties of CNC to create highly oriented hydrogels that mimicked the alignment of tendon tissues under a magnetic field. The preparation of highly oriented hydrogels using antimagnetic materials is promising but challenging; most non-magnetic materials require high-intensity external magnetic fields, which can be unsafe for clinical TE, limiting their practical use.

2.1.1.2. External Magnetic Field

For TE, magnetic fields can be categorized as static or alternating, depending on whether they are constant or continuously varying in amplitude and direction. Typically, static magnetic fields, generated with two parallel permanent magnets for a more uniform effect than single magnets, are used to generate the orientation of magnetic hydrogels. The size, composition, and purity of the magnets can be varied to control the magnitude of the static field [108]. To date, several studies have employed static magnetic fields to orient MNPs in hydrogels along the

magnetic field lines [76-80]. Alternating magnetic fields can also be used to prepare highly oriented hydrogels [77, 109]. Hu et al. [77] demonstrated this using a high-frequency (400 kHz) alternating magnetic field to orient MNPs into chains in a hydrogel matrix, enhancing its magneto-thermal properties. This technique allows control over thermogenesis by adjusting the angle between the hydrogel's structure and the magnetic field, making it suitable for controlled drug release.

In addition, a magnetic field can guide the orientation arrangement of MNPs directly to assist in 3D printing or electrostatic spinning techniques. Hu et al. [110] also created hydrogels with oriented structures at both hundred microns and ~10 microns by combining 3D printing with MNPs induced by magnetic fields. These MNPs were sized similarly to adipose tissue-derived stem cells (ADSCs), allowing ADSCs to better sense the orientation structure and promote their differentiation towards osteogenesis **(Figure 4A-G)**. Johnson et al. [51] used oleic acid-coated superparamagnetic iron oxide nanoparticles doped into poly-l-lactic acid (PLLA) to prepare small conduits of aligned magnetic fibers through electrospinning. These small conduits were combined with collagen and fibrinogen hydrogel solutions, and then prepared under magnetic fields to form a highly oriented hydrogel that directed the

growth of primary dorsal root ganglion. Wang et al. [29] prepared monodisperse magnetic controlled short nanofibers (MSNFs) using an advanced coaxial electrospinning-cyrocutting method and further designed an injectable oriented MSNF/Gel nanofiber hydrogel scaffold **(Figure 4H)** that guided the 3D alignment and mimicry of cells with macroscopic and microscopic biological structures in vitro, demonstrating great potential in promoting skeletal muscle regeneration in vivo.

In fact, designing oriented hydrogels by orienting magnetic materials in hydrogel matrices with low-intensity magnetic fields has been a preferred method [42, 111]. This approach enhances biocompatibility, orientation, and magnetic responsiveness while also providing unique advantages in remote control, bionanotechnology, and mechanical properties. Randomly oriented MNPs can transit from superparamagnetic to weakly ferromagnetic; the alignment of MNPs changes their magnetic properties, explained by dipolar moments, creating local magnetic order that persists even without an external magnetic field [112]. This enables MNPs to generate a micro-magnetic driving forces between the hydrogel scaffold and the cells, activating cell surface-sensitive receptors, ion channels and triggering mechanotransduction pathways for remote cell stimulation for remote cell stimulation to
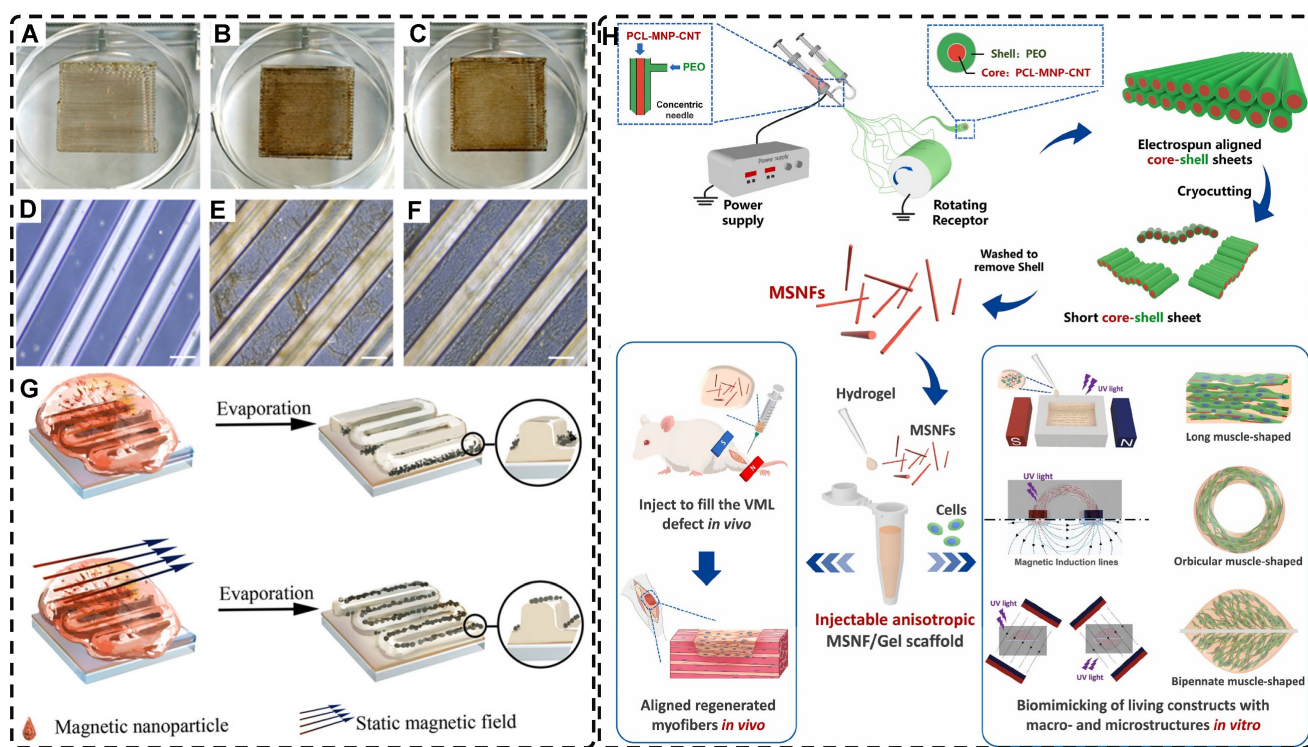
Figure 4. A-F) Macroscopic and microscopic images of MNP-, MNP+MNA-, and MNP+MNA+. G) Schematic diagram of hydrogels with oriented structures by combining 3D printing with MNPs induced by magnetic fields. Adapted with permission from [110], copyright 2021, Nature Publishing Group. H) Schematic illustration of injectable oriented MSNF/Gel nanofiber hydrogel scaffold for biomimicking of living constructs with macro- and micro-structures in vitro and aligned regenerated myofibers in vivo. Adapted with permission from [29], copyright 2022, Elsevier.

influence cell growth [59, 112-114]. Several studies have shown that the bionic oriented structure of magnetic highly oriented hydrogels enhances cellular localization, proliferation, and differentiation, making them an excellent candidate for TE e.g., tendon regeneration, skin regeneration, and nerve regeneration [19, 29, 76, 81, 84, 85, 115, 116].

The biosafety and fate of biomimetic hydrogels in living organisms are critical for TE. Iron oxide-based MNPs, commonly used in MRI, drug delivery, thermal therapy etc., are recognized for their biosafety and eventual metabolism by the host immune system following in vivo administration [117-121]. However, MNPs' effects and pharmacokinetics vary based on size, shape, chemical composition, and surface coating. Magnetic hydrogels interact differently with cells or tissues depending on their intended use, and comprehensive data are necessary to ensure their controlled, stable, safe, and effective use in clinical TE [122, 123]. Future TE studies should consider as many of these factors as possible to demonstrate the potential and promising future of highly oriented hydrogels induced by magnetic fields in conjunction with other ordered manufacturing methods.

2.1.2. Electric-Field-Induced Highly Oriented Nanofiller Hydrogels

Applying an external electric field induces the distributed polarization of free electrons on particles, generating an electric dipole moment. This phenomenon enables the electric field to manipulate the alignment and assembly of materials in solution that have permanent or induced dipole moments, in addition to the magnetic field. The migration of dispersed particles in a fluid under a uniform electric field is referred to as electrophoresis (EP), while the migration of particles in a non-uniform electric field is referred to as dielectrophoresis (DEP) [124-126]. Using different pre-gel media and electro-responsive building blocks of varying sizes, oriented structures with diverse orientations can be obtained by driving them with EP or DEP under different external electric fields. These oriented structures are then immobilized in the hydrogel matrix via a sol-to-gel state transition.

Electric fields, like magnetic fields, can induce materials of different morphologies to assemble into oriented structures in hydrogels. Morales et al. [127] and Zhang et al. [20] aligned 0D polystyrene particles into chains of different orientations using DEP forces under an alternating current (AC) electric field, creating endoskeleton-like particle chains, resulting in composite hydrogels with unique mechanical, optical, and anisotropic properties compared to isotropic hydrogels. Potential applications of these hydrogels include the development of soft robots and smart materials. Recently, Chiang et al. [128] designed graphene oxide/filament-poly-L-lysine layer-assembled PLGA 0D porous microcapsules (PM) loaded with NT-3 **(Figure 5A)**, arranged in linear or triangular highly oriented structures within photocrosslinked gelatin methacrylic acid (GelMA) hydrogels by DEP. These triangular hydrogels can form a gradient distribution of NT-3 that could significantly guide the migration of NSCs and enhance spinal cord injury repair. Such spatially highly oriented 4D hydrogels have great potential to replace 3D hydrogels in bionic TE for better mimicking the pericellular microenvironment.

Carbon nanotubes, commonly used as 1D filler materials in hydrogel substrates, can be assembled into oriented composite hydrogels under the influence of an external electric field [129, 130]. Ahadian et al. [129] utilized DEP to align carbon nanotubes (CNTs) within GelMA hydrogels under a 2 MHz AC electric field at 20 V, resulting in oriented hydrogels that achieved superior maturation of muscle myofibers compared to hydrogels with randomly distributed CNTs **(Figure 5B)**. Moreover, their oriented GelMA-CNT hydrogels, prepared under a 1 MHz AC electric field at 20 V, promoted the differentiation of mouse embryoid bodies (EBs) to cardiomyocytes more efficiently than isotropic hydrogels [130]. Notably, cells on the oriented hydrogels exhibited enhanced migration and differentiation after applying electrical stimulation in the direction of orientation, which is attributed to the excellent electrical conductivity.

Electric fields have also been used to orient 2D graphene nanosheets as hydrogel filler materials [131, 132]. Yang et al. [131] achieved an anodically oriented arrangement of negatively charged 2D graphene oxide (GO) through EP under a DC electric field, which resulted in a bionic gradient-oriented structure after cross-linking gelation in poly(N-isopropyl-acrylamide) hydrogels **(Figure 5C)**. Its near-infrared light response and programmable motion make it a promising candidate for artificial muscles and soft brakes. MXenes are a new class of 2D materials that consist of transition metal carbides, nitrides or carbonitrides with the general formula of M $_{n+1}$X$_n$ (n = 1–3), where M represents an early transition metal (such as Sc, Ti, Zr, Hf, V, Nb, Ta, Cr, Mo) and X is either carbon or nitrogen [133-135]. Using the electric field-assisted forced-assembly technique, Dutta et al. [136] were able to obtain hydrogels with aligned Ti$_3$C$_2$T$_x$ Mxene nanosheets. The gelation process depended on the type of metal electrode and redox potential, and adjusting the electric field distribution allowed for various sheet-like alignments, useful for

capacitors and hot water evaporators. MXene's oriented structure also promoted cell adhesion, proliferation, and guided growth, highlighting its potential in biomedicine TE [137]. Zhu et al. [138] induced highly charged nanosheets (Hectorite $[Na_{0.5}]^{inter}[Li_{0.5}Mg_{2.5}]^{oct}[Si_4]^{teter}O_{10}F_2$) to form complex oriented structures in a pre-hydrogel matrix using patterned electrodes etched on glass substrates. Subsequently, these structures were immobilized by UV photopolymerization to form highly oriented bionic hydrogels that can deform in a directed way under external stimuli, which is compelling for applications in artificial muscles and soft brakes. Furthermore, the controllable patterned distribution of electric fields could be applied to orienting other charged particles through electrophoresis.

Several studies have shown that external electric fields can be utilized for straightforward, cost-effective, and flexible assembly of materials into bionic hydrogels with oriented structures, with great potential in TE. They are favored by researchers to regulate the growth, orientation, migration, and differentiation of various cell phenotypes in vitro and in vivo, given the involvement of endogenous electric fields in the growth and repair of cells, tissues, and organs [139]. Future research can explore the potential of electric field induction to create oriented structural hydrogels and direct the alignment of cell growth within these hydrogels for TE.

However, it should not be ignored that electric fields are more reliant on the electrochemical stability of the hydrogel substrate material when filling the oriented hydrogel with nanomaterials or its own polymer network, compared with magnetic fields. Moreover, direct contact with the precursor solution during gel synthesis may result in unforeseen electrochemical reactions and/or electrophoresis. Consequently, optimization of voltage and current based on the electrochemical stability of various materials is necessary. These limitations greatly restrict the use of electric field-induced oriented hydrogels.

2.1.3. Mechanical Force-Induced Highly Oriented Nanofiller Hydrogels

Mechanical force-induced alignment involves arranging disordered polymer chains or filler materials in hydrogels in response to external stress, like stretching or shearing. The mechanical force or strain can be applied during or after partial or complete gelation, resulting in the alignment of the nanofiller material and/or hydrogel polymer network in the direction of the applied strain. Compared to other methods, this technique is simple, fast, and straightforward, making it widely used in the preparation of highly oriented nanocomposite hydrogels.
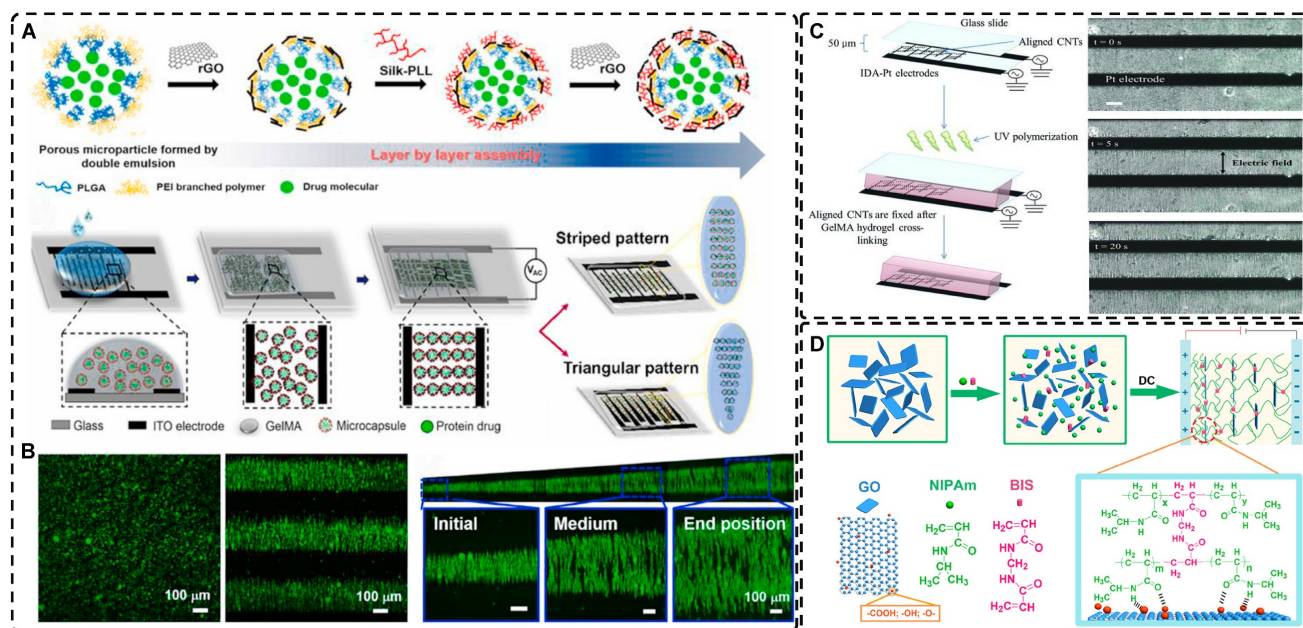
Figure 5. A) a) Synthesis of 0D microcapsule assembly. b) The fabrication process of orienting 0D microcapsule alignment by DEP manipulation. B) Random distribution of 0D microcapsule and subsequent orientation alignment within the hydrogel after DEP. Adapted with permission from [128], copyright 2021, Elsevier. C) Schematic representation of the fabrication process for CNT alignment within the GelMA hydrogel and phase contrast images of the CNT alignment over time. CNTs were aligned after 20 seconds. Adapted with permission from [129], copyright 2013, Wiley-VCH. D) Scheme of preparation of 2D PNIPAm/GO oriented hydrogel. Adapted with permission from [131], copyright 2018, American Chemical Society.

Among the mechanical induction methods, the preferred method for preparing highly oriented nanofiller hydrogels is using shear forces [21, 140-151], which induce larger and more well-ordered alignments compared to magnetic and electric fields, and cover larger areas. However, as with magnetic and electric fields, the metastable state of the induced highly oriented alignment structure may be changed or destroyed when the external field is removed or altered. To prevent loss of the oriented structure, the hydrogel can act as an external matrix to fix the highly oriented structure during the transition from the sol to the gel state. In recent years, 3D printing has led to tremendous growth in the application of bionic hydrogel scaffolds in TE. Shear force-induced directional alignment of polymer chains and/or filler materials within hydrogels is widely used during the printing process when the bioink passes through the nozzle and generates shear forces. Zhao et al. [21] utilized shear force to align and distribute CNTs within hydroxyethyl methacrylate (HEMA) gels, resulting in composite hydrogels with varying CNTs orientations that exhibited distinct mechanical properties. Kumacheva et al. [141-143] published a series of studies on the preparation of highly oriented hydrogels by shear induction **(Figure 6B)**. They recently used a 3D printed microfluidic print head to extrude a hydrogel consisting of CNCs and GelMA through 16 microchannels with varying shear forces [143]. Due to the different shear forces, the CNCs were oriented differently and subsequently photo-crosslinked to lock the oriented CNCs within the hydrogel matrix. This uniaxially oriented hydrogel could be applied in TE and regenerative medicine of e.g., artificial muscles.

In addition to orienting filler material, 3D printing can also align cells within hydrogels using shear force has become a popular topic in hydrogel development. When hydrogels contain both filler and cells, this aligned structure allows cells to grow along it, more effectively replicating the anisotropic nature of human tissues. Prendergast et al. [152] created fiber-aligned hydrogels by mixing hydrogel fiber suspensions, derived from mechanically fragmented electrospun scaffolds of norbornene-modified hyaluronic acid (NorHA), with GelMA. They used shear forces during extrusion printing to achieve high orientation **(Figure 6A)**. After optimizing the suspension properties and printing flow rate, meniscal fibroblasts, mesenchymal stromal cells, or cardiac fibroblasts immobilized in composite-oriented hydrogels were induced to align by the highly oriented fibers, in contrast to random cell growth in non-oriented hydrogels. This provided the possibility to construct meniscus, cartilage, heart, and other tissues in vitro for TE repair and the development of physiological tissue models.

Stretch induction, the other common method for orienting hydrogel polymer chains, can also induce the alignment of filler materials within the hydrogel. Wang et al. [153] elastically stretched a composite hydrogel of sodium alginate, acrylamide, and polypyrrole (PPy), and found that PPy nanotubes tended to align parallel to the stretching direction and slide relative to the hydrogel network, resulting in the successful preparation of highly oriented PPy nanocomposite hydrogels after repeated stretching **(Figure 6C)**. The highly oriented hydrogel induced by stretching can promote the formation of an elongated cellular morphology in cardiomyocytes, and its highly biocompatible, electrically conductive, and stretchable properties make it a promising candidate for cardiac TE **(Figure 6D)**. Hu et al. [154] developed stretchable supramolecular hydrogels through host-guest interactions between β-cyclodextrin-modified tunicate cellulose nanocrystals (TCNCs) and damantane-containing polymers. Pre-stretching of the hydrogels caused the polymer chains and TCNCs in the network to move and align in the direction of the stretching force, and the highly oriented TCNC structures were then locked in the hydrogel network through the ionic coordination between Fe^{3+} and -COO on acrylic acid, by immersion in a $FeCl_3$ solution. Additionally, the group utilized TCNC fillers to pre-stretch the oriented structure within a semi-rigid sodium alginate network and subsequently locked it via Ca^{2+}/-COO ion coordination. These hydrogels exhibited superior mechanical properties compared to isotropic hydrogels due to their highly oriented filler structures, making them promising candidates for TE applications such as ligaments and tendons.

The preparation of highly oriented nanofiller hydrogels by mechanical induction is a simpler and more feasible method compared to other techniques. Mechanical tensile induction is more commonly used to achieve the highly oriented orientation of hydrogel polymer chains. While the development of 3D printing has led to an increased application of shear force induction in preparing highly oriented hydrogels, producing thicker highly oriented filled structure hydrogels is challenging due to the uneven distribution of shear force [37]. In addition, the orientation of the filler material by shear force is influenced by various factors, such as the rheological properties of the ink, the properties of the filler material, and the specifications of the nozzle. If the ink viscosity is low, the orientation structure may be lost before the hydrogel gels, whereas high viscosity can result in higher flow resistance leading to clogging of

the extruder and inconsistent ink deposition [123]. Moreover, when hydrogels are used with cells, the impact of shear force on the cells should be considered, as excessive shear force can reduce the activity and function of the cells and even cause apoptosis [155]. Therefore, in the field of TE, optimizing the relationship between shear force, nanomaterial orientation, hydrogel rheology, and viability of the loaded cells is a major challenge that needs to be addressed in producing highly oriented biomimetic hydrogels.

2.1.4. Other Strategies for Preparing Highly Oriented Nanofillers Hydrogels

In addition to using magnetic fields, electric fields, and mechanical forces, methods like directed freezing and self-assembly are also utilized to prepare highly oriented nanofiller hydrogels.
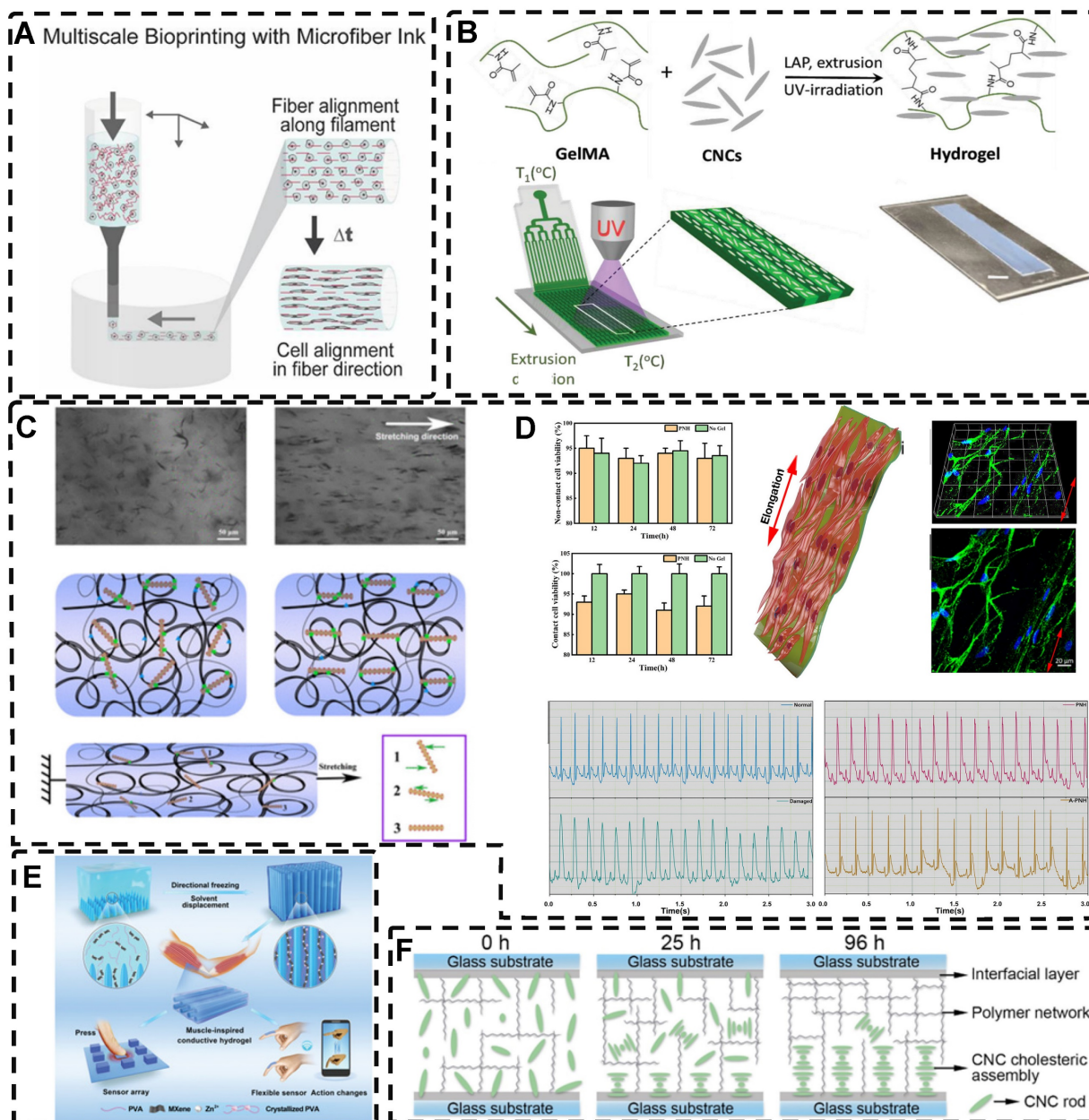
Figure 6. A) Schematic of prepared highly oriented, fiber-aligned hydrogels using shear forces during extrusion printing. Adapted with permission from [152], copyright 2021, IOP Publishing. B) (a,b)Schematic of shear-mediated extrusion of highly oriented hydrogel from the mixture of CNCs, GelMA, and LAP using a microfluidic printhead, and (c) photograph of the hydrogel sheet. Adapted with permission from [143], copyright 2021, Wiley-VCH. C) Confocal microscopy images of random aligned hydrogels and highly oriented hydrogels, and schematic of preparation of highly oriented PPy nanocomposite hydrogels after repeated stretching. D) They have good biocompatibility, induce targeted growth of cardiomyocytes and promote restoration of electrical conductivity. Adapted with permission from [153], copyright 2021, American Chemical Society. E) Schematic representation of the synthesis procedures of oriented void channels hydrogels with an ordered internal orientation structure and further applications in wearable flexible sensors and 3D sensor arrays. Adapted with permission from [162], copyright 2021, Wiley-VCH. F) Schematic of self-assembled oriented structures of CNC arrangement in the polymer network after UV curing with different standing times Adapted with permission from [168], copyright 2021, Elsevier.

Directed freezing is a common method used to prepare directed macroporous hydrogels, as will be further discussed in Section 2.3. During the formation of ice crystals caused by a temperature gradient, the hydrogel network and/or filler material can be separated and confined to the interstitial region between the ice crystals, which allows the filler material to be oriented in the hydrogel while preparing the macroporous structure [156-161]. Drawing inspiration from muscles, Feng et al. [162] developed oriented void channels hydrogels with an ordered internal orientation structure, by repeatedly freezing MXene nanosheets processed with Ti_3AlC_2, mixed with polyvinyl alcohol (PVA), and $ZnSO_4$ in Polytetrafluoroethylene (PTFE) molds. The MXene nanosheets were connected to the PVA main chain through hydrogen bonding, and the addition of Zn^{2+} ions disrupted the electrostatic repulsion between the MXene sheets, generating high binding energy with the -OH groups on the MXene surface, forming an ion-chelated cross-linked network that was crucial in improving the mechanical properties of the hydrogels. During the freezing process, ice crystals created occupancy, while PVA chain segments and MXene nanosheets were squeezed at the water-ice interface to form a highly ordered arrangement in the hydrogel. This reduced the distance between nanosheets, thus enhancing the electrical conductivity of the hydrogel. Moreover, the formation of small microcrystals after repeated freeze-thawing of PVA strengthened the network structure of the hydrogel, resulting in excellent shape recovery properties. These outstanding properties make this muscle-inspired, highly oriented macroporous hydrogel a promising material for sensor applications **(Figure 6E)**.

Self-assembly is a widespread phenomenon that plays a crucial role in biological growth and development. Examples include the hybridization of the DNA double helix, protein folding, and the self-assembly of troprocollagen into highly ordered and tightly arranged collagen fibers in tissues like tendons [163, 164]. Drawing inspiration from these natural processes, self-assembly has become prominent in TE. This method, where the basic structural units within a hydrogel spontaneously assemble into an ordered structure through non-covalent bonds, such as hydrogen bonds, van der Waals forces, and hydrophobic forces [165, 166], has been researched for the construction of tissues and organs. The lack of need for external forces enhances cell-material interactions in TE, expanding the potential applications of self-assembly methods [167]. Liu et al. [168] embedded self-assembled oriented structures of CNCs into polyethylene glycol derivatives/polyacrylamide hydrogel precursors. The

arrangement of CNCs in suspension or pre-polymerization solution was influenced by time and self-assembly angle **(Figure 6F)**; over time, the CNC rods sank due to gravity, and as the self-assembly angle increased from 0° to 90°, the arrangement of CNC rods transitioned from a chiral nematic structure to a symmetrical nematic structure. These hydrogels thus exhibited great potential as mechanical stress and temperature multi-stimulation sensors. Furthermore, the high transparency of hydrogels in visible light makes them suitable for anti-counterfeiting applications.

Self-assembly is a highly organized process at the molecular level, but achieving highly oriented spatial structures in hydrogels solely by using self-assembling filler material can be challenging. External forces are often needed to control the mesoscopic order of self-assembly and create highly ordered hydrogel-filled structures [169]. For instance, Akhil Patel et al. [170] self-assembled graphene-doped chitosan (CHT) with gellan gum (GG) in a microfluidic chamber and aligned them with the aid of long needles (shear force) to form self-assembled hydrogels with a unidirectional fiber structure. These hydrogels were then manually collected to form films with graphene sheets evenly dispersed within them. The inclusion of graphene enhanced the mechanical strength and electrical conductivity of the hydrogels, promoted cell adhesion, and induced the initial orientation of myogenic cells, leading to the formation of multinucleated myotubes. As a result, these hydrogels may have potential applications in skeletal muscle TE.

In addition to shear, magnetism-induced and directional ultrasound can also be applied in conjunction with self-assembly [171-175]. Despite the significant progress made in self-assembly strategies in recent decades, the preparation of highly oriented hydrogels through self-assembly still poses challenges, such as the development of simple and feasible strategies, and the need for more precise control of self-assembled modules.

In general, although most of the nanofillers materials themselves have excellent biocompatibility and thus influence the hydrogel performance, such as MNPs, CNTs, MXene and other materials, they can enhance the biocompatibility, mechanical properties and other characteristics of the composite hydrogel in different degrees and fulfill the function of the material itself. More importantly, when endowed with a highly oriented structure, the hydrogel nanofiller material more closely resembles the bionic structure of highly oriented tissues, thereby regulating tissue repair and regeneration. Although the study of how highly oriented hydrogels affect the

mechanism of cell behavior is not clear so far, highly oriented nanofillers hydrogels occupy an important position in the field of TE.

2.2. Highly Oriented Polymer-Chain Network Hydrogels

In addition to manipulating the orientation of nanofiller materials, utilizing polymer-chain networks is another strategy for preparing highly oriented hydrogels. Highly oriented polymer-chain network hydrogel is a type of hydrogels which the polymer-chain networks of hydrogel monomers are oriented. And thevmost important preparation methods for highly oriented polymer-chains hydrogel is mechanical stretching.

2.2.1. Mechanical Stretch-Induced Highly Oriented Polymer-Chain Network Hydrogels

As previously discussed in the section on mechanical force-induced orientation of filled materials, mechanical stretching is also a widely used method for inducing the orientation of hydrogel polymer chains. This method can easily orient a network of randomly oriented hydrogel polymer chains along the stretching direction. However, due to the elastic nature of hydrogel polymer networks, it is difficult to maintain the structure as they tend to revert to their original, less ordered isotropic state once external forces are removed. For example, dual network hydrogels made of calcium alginate (ALg) and polyacrylamide (PAM), crosslinked ionically and covalently, are highly stretchable [2] . When stretched, the ionically cross-linked ALg chains in the stretched state become unlinked, break and align in the direction of the stretching force. However, the stable deformability of PAM chains makes the double network hydrogels reversible. To maintain the structure and maximize orientation retention after stretching, a strategy has been developed. Kim et al. [176] achieved an irreversible fixation state of the highly oriented structure by crosslinking alginate chains after directional stretching. This secondary ionic crosslinking largely retained the orientation after the stretching force was removed and increased the elastic modulus of the hydrogel. Additionally, by embedding mesoporous silica microrods as inorganic fillers in the double network hydrogels [177] they improved the mechanical properties of the hydrogels, creating structures that resemble ligaments or tendons.

Chen et al. [178] also prepared highly oriented ALg/PAM hydrogels using stretching and subsequent ionic cross-linking strategies. Their hydrogel, which was significantly oriented in both microstructure and ion transport, provides a

promising direction for the development of next-generation wearable electronics. In another study, Park et al. [179] replaced Ca^{2+} with Al^{3+} as the cross-linking agent **(Figure 7A-B)**. By adjusting the degree of directional stretching, the mechanical properties of the hydrogel could be controlled within a certain range. The layered combination of oriented hydrogel cables prepared by applying a braiding textile process exhibited a significant load-bearing capacity and tensile behavior similar to that of tendons. Additionally, Choi et al. [180] developed highly oriented triple network hydrogels by combining poly (2-hydroxyethyl aspartamide) modified with aminopropyl imidazole (PHEA-API), which provided strong bone adhesion through multiple hydrogen bonds, and an energy-dissipative Alg/PAM double-network **(Figure 7C-D)**. The triple network hydrogels had high tensile modulus and strength, mimicking natural ligaments, and exhibited high adhesion properties at the interface with bone. This work set the foundation for future hydrogels with high mechanical properties and adhesion to bone.

Thus, the preservation of the highly oriented structure after directional stretching can be achieved by controlling the supramolecular interactions between polymer chains. Mredha et al. [22] stretched rigid/semi-rigid alginate/cellulose chains to obtain a highly oriented single polymer network hydrogel. Subsequently, the supramolecular interactions between the highly oriented polymer chains, such as hydrogen bonds/ionic bonds, were strengthened by a specific drying method, thereby strengthening and maintaining the structure and preventing it from being destroyed upon rehydration. Li et al. [181] achieved highly oriented chitosan hydrogels using the same method, and the good biocompatibility of the hydrogel and the highly oriented structure induced the proliferation and orientation of osteoblasts and fibroblasts **(Figure 7E)**. For flexible polymer chains, Chen et al. [182] prepared highly oriented PVA hydrogels using stretch-freezing cycles. Stretching oriented the PVA chains and brought the isotropic and loose PVA chains relatively close together, while freezing further brought the chains into close contact. The PVA chains in close contact easily adopted suitable conformations for hydrogen bond formation, and therefore more hydrogen bonds were formed between the oriented PVA chains, and even the cooperativity of hydrogen bonding became possible when consecutive hydrogen bonds were formed. As a result, the hydrogels maintained high orientation even after thawing, significantly enhancing their mechanical properties. Wang et al. [183] prepared PVA/NaCl highly oriented hydrogels using a hot

stretch freezing method. These hydrogels exhibited various anisotropic ion transport behaviors, providing a new strategy for developing human sensors. Sun et al. [184] utilized the abundant hydrogen bonding between stiff aramid nanofibers (ANFs) and flexible PVA to achieve permanent alignment of the fiber network, resulting in hydrogels with robust mechanical properties, which was confirmed by SEM analysis. The excellent mechanics and functionality of these hydrogels, which mimic tendons, suggested their potential for use in advanced TE. Although the mechanical stretching method is simple and effective, its requirement for a large stretching force for the precursor hydrogel polymer network imposes some limitations.

2.2.2. Other Strategies for Preparing Highly Oriented Polymer-Chain Network Hydrogels

The polymer network of hydrogels can also be directed by ion diffusion, shear induction, and electric field induction.

In directional ion diffusion, a cationic aqueous solution is brought into contact with an anionic polymer aqueous solution to drive directional cation diffusion. As diffusion proceeds, the anionic polymer chains are cross-linked, forming a hydrogel with a network of directional polymer chains [23, 185-187]. Yang et al. [23] physically formed poly(2,2'-disulfonyl-4,4'-benzidine terephthalamide) (PBDT) gels with a highly ordered structure by uniaxially controlling the diffusion of Ca^{2+} as a cross-linking agent in the solution of PBDT in the reaction mold. The highly oriented PBDT gels were then immersed in an acrylamide (AAM) solution containing the chemical cross-linker to chemically form the PAAm gel as a second network, resulting in highly oriented double network hydrogels with excellent mechanical properties. Qiao et al. [185] designed masks with holes to guide the diffusion of multivalent metal ions into the bottom solution of anionic PBDT, allowing for the
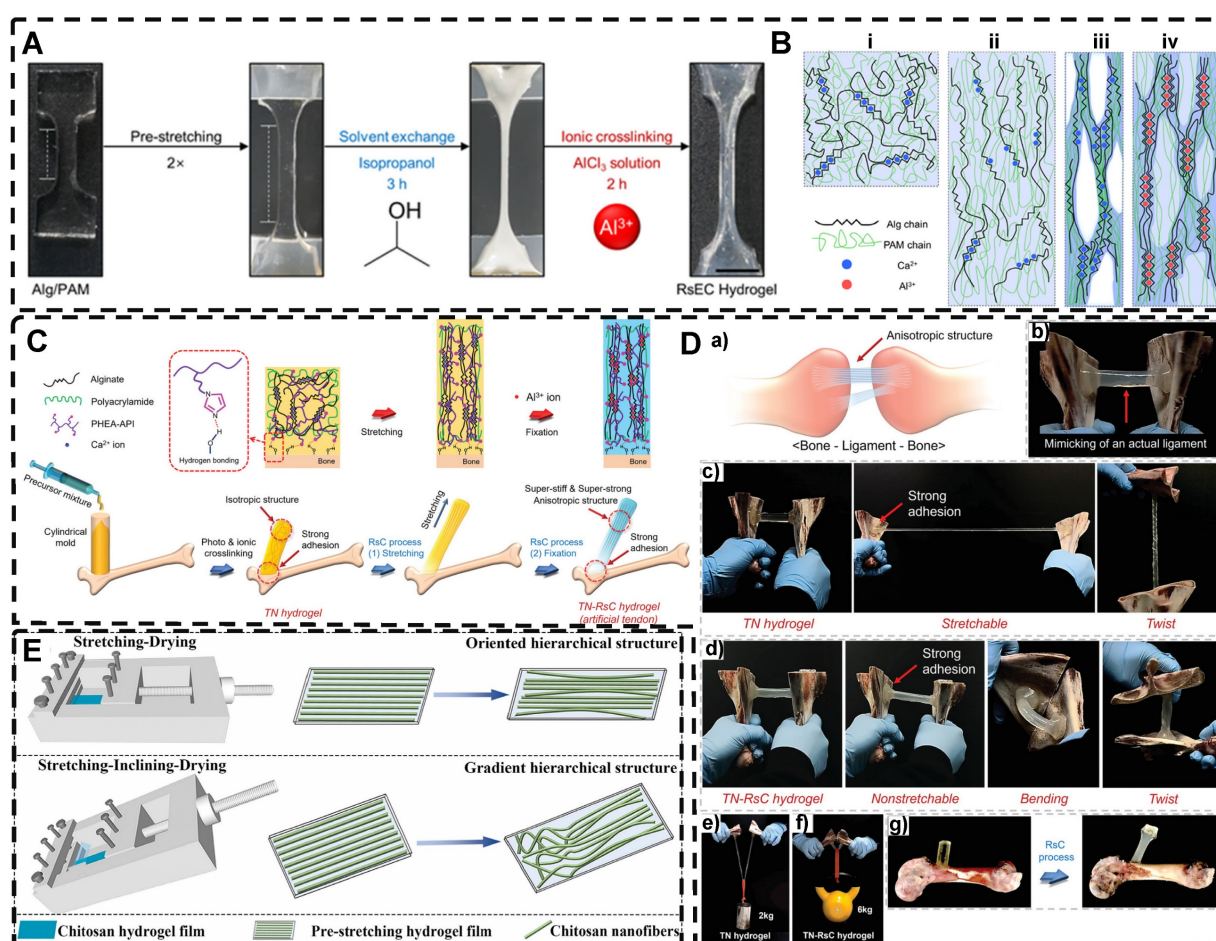
Figure 7. A) Photographs of the highly oriented Alg/PAM hydrogels during the RsEC process; remodeling (pre-stretching) and subsequent solvent exchange followed by ionic crosslinking (RsEC). B) Illustrations of the changes in the molecular structure during the RsEC process: (i) as-prepared Ca^{2+}-crosslinked Alg/PAM hydrogel, (ii) pre-stretched hydrogel, (iii) solvent-exchanged hydrogel, and (iv) Al^{3+} crosslinked hydrogel. Adapted with permission from [179], copyright 2022, American Chemical Society. C) Design of the strong, stiff adhesive highly oriented TN hydrogel. The final TN-RsC highly oriented hydrogel subjected to the RsC process was cross-linked by Al^{3+} ions and exhibited strong mechanical and adhesion properties. D) a) Schematic of the real ligament and anisotropic structure of the ligament, and b) photographs of TN-RsC hydrogel mimic the real ligament. Adapted with permission from [180], copyright 2022, Wiley-VCH. E) Graphical illustrations for the production of oriented and gradient chitosan hydrogel films with hierarchical structure via the self-made mold. Adapted with permission from [181], copyright 2022, Elsevier.

preparation of hydrogels with complex ordered structures **(Figure 8A)**. By programming the diffusion field and adjusting the pattern and position of the mask containing holes, such highly oriented hydrogels with high mechano-optical sensitivity have potential for use in e.g., optical devices and sensors, and provide new ideas for preparing hydrogels without bionic complex tissues. In addition to polysaccharides and alginates, which have been used as anionic polymers in aqueous solutions, Ca^{2+}, Zn^{2+}, and Cu^{2+} have been used as the corresponding cations. Mredha et al. [186] formed an anisotropically oriented structured hydrogel on the surface of a core hydrogel by the controlled diffusion of cations in a pre-designed core hydrogel through a biopolymer storage solution, resulting in an oriented tubular alginate hydrogel with mechanical properties comparable to those of natural blood vessels. By controlling the concentration, diffusion time, and flow direction of ions and the size and shape of the core hydrogel, complex ordered tubular hydrogels with different 3D structures can be prepared, and even live cells can be carried. While this synthesis process is relatively simple, the relationship between the diffusion direction and polymer chain orientation has

not been elucidated, and the resulting hydrogels had a non-homogeneous crosslink density gradient along the diffusion direction.

Shear forces can also be applied to orient a polymer chain network of a hydrogel. Nazhat et al. [188, 189] developed the gel aspiration-ejection (GAE) method, which uses shear stress to prepare injectable dense collagen (I-DC) hydrogels with highly oriented collagen fibers. The shear stress reshaped the geometry of the gel and aligned the collagen nanofibers along the long-axis direction. In addition to its ability to guide the orientation and alignment of inoculated cells, this highly oriented hydrogel mediated osteoblast differentiation of murine mesenchymal stem cells (MSCs) and supported and accelerated neuronal transdifferentiation. Additionally, a high strain mechanical stimulation of this highly aligned dense collagen fibril hydrogel induced tenogenic commitment of MSCs [190]. Shao et al. [191] produced a highly oriented, porous, cell-laden GelMA hydrogel by mixing PEO, different types of cells, and GelMA **(Figure 8B)**. The oriented hydrogel chains were sheared through a coaxial nozzle, followed by photo-crosslinking, fixation, and washing off polyethylene glycol PEG in PBS. The cells
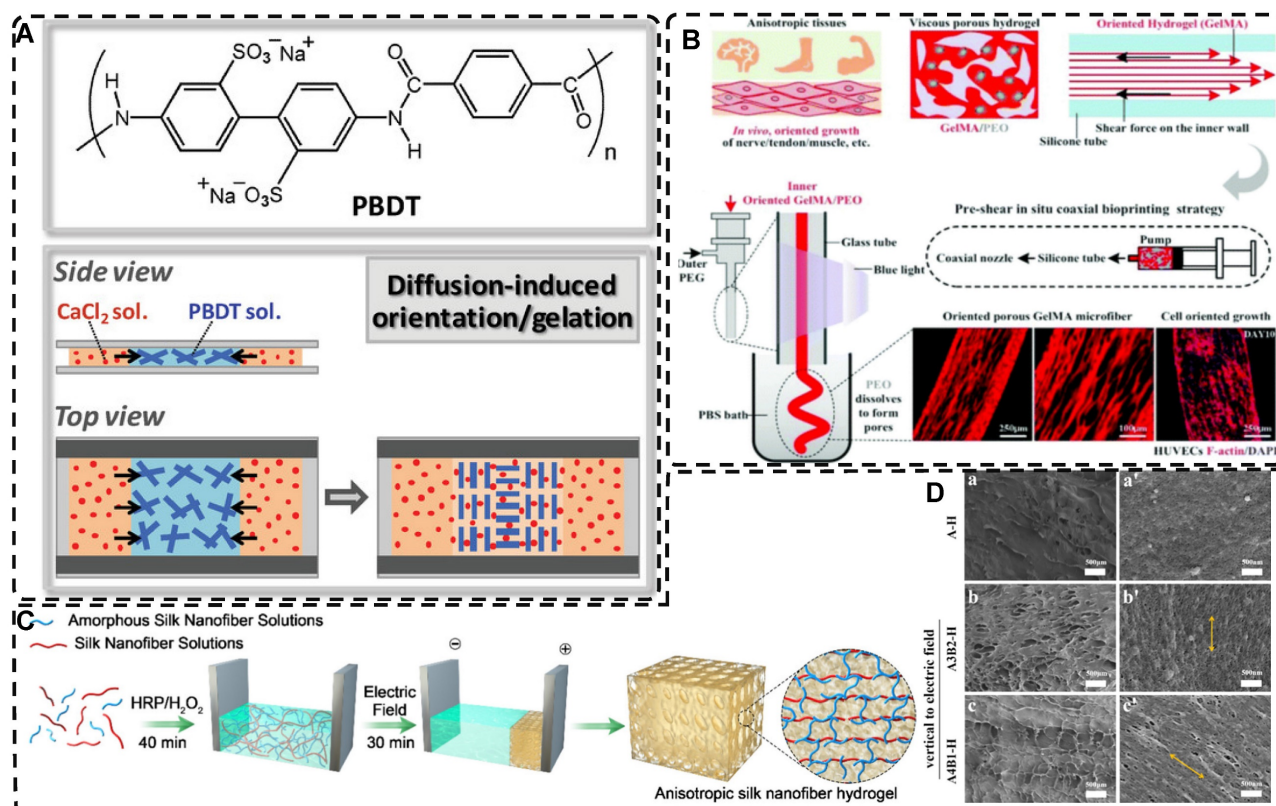
Figure 8. A) Chemical structure of the rigid polyanion, PBDT, and schematic for the formation of anisotropic hydrogel by unidirectional diffusion of Ca^{2+} ions into PBDT solution from two opposite lateral sides. The diffusion induced the alignment of PBDT perpendicular to the diffusion direction near the entrance yet parallel to the diffusion direction at the middle region where the two fluxes met. Adapted with permission from [185], copyright 2019, WILEY-VCH. B) Schematic illustration and effect of pre-shear bioprinting of highly oriented hydrogel microfiber-enabled oriented growth of cells. Adapted with permission from [191], copyright 2021, Royal Society of Chemistry. C) Process to Form Tough Silk Nanofiber Hydrogels with highly oriented Architectures. D) Characterization of SF hydrogels with highly oriented structures. Adapted with permission from [195], copyright 2020, American Chemical Society.

encapsulated in this hydrogel showed highly oriented growth behavior similar to that in vivo, offering more biomimetic options for TE. Chen et al. [14] developed an alginate-assisted microfluidic system that can be fine-tuned with a combination of methacrylate hyaluronan (HA-MA) and fibrin (Fb) as well as microfluidic shear and stretch parameters to optimize the homogeneous orientation of bionic nerve fibers. The highly oriented hydrogel was guided by nano-topography in a focal adhesion kinase-associated manner, promoting aligned neurite growth, directional extension of axons, and myelin maturation of Schwann cells. This bionic neural composite hydrogel has significant potential in neural regeneration as well as other bionic TE applications. Kim et al. [192] utilized the shear stress of 3D printing nozzles to prepare highly oriented collagen hydrogels that contained various types of cells. The physical and biochemical cues provided by the collagen induced attachment, growth, and alignment of cardiomyocytes (H9C2), preosteoblasts (MC3T3-E1), and human adipose stem cells (hASCs) in a synergistic manner. Additionally, the shear force-induced cell alignment was achieved without losing cell viability.

Electric fields can also orient hydrogel polymer chains in addition to inducing the orientation of the filler material within the hydrogel, as described in the previous section [193]. Tong et al. [194] developed highly oriented chitosan hydrogels with complex layering by exposing chitosan solutions to electrical signals of varying intensities; chitosan chains assembled and aligned at the cathode and reacted with OH- ions to create an ordered structure. By regulating the electrical signal, a direct equilibrium between OH- diffusion rate and chitosan electrophoretic rate was established, allowing for precise and continuous control of the internal structure of the hydrogel. This novel approach for multilayered, orderly assembly of polysaccharides facilitates the replication of complex structures. It serves as a valuable tool in TE for creating for example bionic, multi-layered blood vessel structures. Ding et al. [195] used horseradish peroxidase (HRP) cross-linked with amorphous silk nanofibers (ASNFs) in an electric field to form the native hydrogel, and at the same time, β-sheet-rich silk nanofibers (BSNFs) were aligned and oriented as reinforcing chains during cross-linking, resulting in a structured composite with enhanced mechanical properties **(Figure 8C-D)**. The highly oriented structure can provide various physical cues for cells, such as better stiffness and alignment aggregation, promoting stem cell proliferation and osteodifferentiation induction in vitro, with potential applications in bone TE. Moreover, Abu-Rub et al. [196] used an electric field

to prepare highly oriented collagen fiber hydrogels, which supported directional orientation, growth, and guidance of nerve protrusions, overcoming the inhibitory aspect of myelin-associated glycoprotein on nerve protrusion growth. This work provides a reference for preparing nerve-guided catheters for spinal cord injury.

Compared to hydrogels filled with highly oriented materials, orienting the polymer chains is relatively straightforward, requires less equipment, and is more reproducible. Moreover, the oriented polymer chains within the hydrogel provide a continuous physical topographic cue to the cells, facilitating cell adhesion, migration, and growth, which is crucial for TE regeneration. Nonetheless, several preparation strategies have limitations. Mechanical stretching necessitates a specific polymer chain tolerance, ion orientation yields non-homogeneous hydrogels, and electric field induction may produce unexpected electrochemical reactions or electrophoresis of the polymer solution. Additionally, accurately replicating complex and intricate tissue structures while maintaining highly oriented structures and mechanical properties similar to human tissues remains challenging. However, as further investigations proceed, hydrogels with highly oriented polymer chains have a bright future in TE.

2.3. Highly Oriented Void Channel Hydrogels

The primary role of hydrogels in most applications is to regulate transport through pores, which is done by varying size and pore distribution; the porous structure of hydrogels plays a crucial role in regulating the transport of nutrients, gases, and waste and providing physical space for cell diffusion and communication, facilitating the formation of the final tissues. Conventional hydrogels are limited to a pore size of 100 nm, which hinders the potential for TE applications requiring micrometer-scale cell permeation. While some template-sacrificing methods, such as salt/porogen templating and gas foaming, can create hydrogels with micron-scale pores, they lack control over the interconnectivity and directionality of the pore network. Creating highly oriented continuous void channel hydrogels, makes it possible to better mimic natural biological tissues and more efficiently direct solute diffusion or transport.

2.3.1. Directional Freeze-Casting for Preparing Highly Oriented Void Channel Hydrogels

Directional freezing, also known as ice templating, freeze casting, or ice separation-induced self-assembly, involves freezing a pre-reaction solution in a cold bath along a unidirectional temperature gradient to form ordered ice crystals that

grow in the freezing direction. As one of the sacrificial template methods, the solute material repels from the ice and separates into the interstitial region defined by the curing solvent during ice crystal formation, while the ice crystals sublimate and then form highly oriented 3D pore channels along the freezing direction without disturbing the interstitial region. The orientation, number, morphology, and size of the porous or channel structure can be controlled by several factors, including solvent content, freezing temperature, freezing rate, and ice template support. Nucleation theory is the fundamental principle used to control pore size and the number of pores; lower freezing temperatures and faster freezing rates result in an increase in hydrogel nucleation sites and the formation of a large number of smaller ice crystals, while at higher freezing temperatures, the distribution of nucleation sites becomes looser, and the ice crystals increase in size. Lowering the polymer/solute concentration can also produce larger pore sizes. This method is environmentally beneficial compared to other methods for preparing highly oriented hydrogels, and since most hydrogels are made from aqueous precursor solutions, it is relatively easy to control highly oriented ice crystallization. Therefore, this simple, effective, and controllable method is commonly used to prepare hydrogels with highly oriented pore channels by templates and has been widely used recently to design highly oriented void channel hydrogels with various functions.

Since the initial report by Wu et al. [24] on preparing aligned porous hydrogels through unidirectional freezing, an increasing number of researchers have been using this method to develop highly oriented void channel hydrogels [162, 197-205]. Liang et al. [198] used an ice-template freeze casting process to create highly oriented aligned micro/nanostructures in PVA hydrogels, followed by crystal growth initiated by thermal annealing **(Figure 9A-B)**. The resulting hydrogels exhibited excellent mechanical properties, high fatigue threshold, anti-crack sensitivity, and anisotropy, with a 100-fold increase in fatigue threshold compared to normal PVA hydrogels after swelling to equilibrium in deionized water. These properties make it a promising material for use in low-cost, high-performance, and durable soft applications such as robotics and artificial muscles. Additionally, this strategy is applicable to various hydrogel materials, including polysaccharides, proteins, synthetic polymers, and corresponding polymer composites. Hua et al. [199] synergistically created highly oriented void channel hydrogels at different length scales across multiple levels, from millimeter to molecular,

by using directional freeze-casting, resulting in the Hofmeister effect and subsequent salting-out treatment. The researchers used PVA as the model material, and the solution was directly soaked in a kosmotropic salt solution after directional freezing. Directional freezing caused the PVA hydrogel to form highly directional honeycomb microchannels with arranged pore walls, and the polymer was concentrated and accumulated in the gap area between the channels, which was then ready for the subsequent strong aggregation and crystallization of polymer chains through salting-out. The preconcentrated PVA chains strongly self-coalesced and phase-separated from the original homogeneous phase under the influence of kosmotropic ions, which in turn formed a mesh-like nanofiber network on the surface of the micron-sized aligned pore walls. The hydrogels developed by this method exhibited high strength, toughness, tensile properties, and fatigue resistance. Since the Hofmeister effect is present in various polymer and solvent systems, this method may offer some assistance for other originally weak hydrogel applications in TE.

The subzero temperature environment during the fabrication of directed freeze casting may impair cell viability and limit the application of hydrogels intended to encapsulate functional cells in TE [206, 207], as the formation of ice crystals in the extracellular matrix results in an osmotic gradient in the cell membrane, leading to cellular dehydration and damage [208]. Although cryoprotectants such as dimethyl sulfoxide and glycerol can be used, their concentration at low temperatures may cause osmotic shock or toxic damage to cells and lead to adverse effects in humans, such as clonic seizures and cardiac arrest [208, 209]. Therefore, the development and exploration of advanced cell cryopreservation agents, such as vitrification agents, ice recrystallization inhibitors, macromolecular cryoprotectants, ice nucleating agents, and regulation of biochemical pathways, will contribute to expanding the applications of targeted cryogels in TE.

2.3.2. Other Strategies for Preparing Highly Oriented Void Channels Hydrogels

Similar to the directional freeze-casting method, He et al. [210] developed highly oriented pore hydrogels using a crystal template technique called "hot ice", the principle of which is that needle-like and micrometer-sized aligned $NaAc \cdot 3H_2O$ crystals can form from saturated NaAc solutions at room temperature. A saturated NaAc and agarose mixture solution was prepared at a high temperature of 90°C, which was then cooled to room temperature to create an agarose gel in the supersaturated solution. Next,

NaAc $3H_2O$ crystals were placed on the surface of the supersaturated mixture solution to induce the formation of oriented crystals in the hydrogel in the vertical direction. Finally, the crystals were removed by multiple washes with water to obtain oriented pore hydrogels. The highly oriented pore hydrogels prepared using this technique exhibited great potential in TE due to the resulting high survival rate of cultured NIH3T3 cells and linear alignment.

The physical template method is a common technique for preparing highly oriented void channel hydrogels. This process involves polymerizing the hydrogel precursor solution in a mold which then determines the orientation and shape of the void channels in the hydrogel. For instance, Chen et al. [211] were inspired by the preparation of oriented pore PLGA scaffolds and used a mold comprising seven uniformly distributed stainless steel rods and glass tubes to fabricate oligo(polyethylene glycol) fumarate (OPF) and positively charged OPF (OPF+) hydrogel scaffolds with oriented void channels. These hydrogels were designed to closely match the mechanical properties of rat spinal cord tissue, and animal studies showed that OPF+ hydrogel promoted a unique pattern of axonal regeneration with a large number of regenerated axons concentrated in the channel. Subsequent studies have explored the potential value of such hydrogels loaded with cells or growth factors for neurological and spinal cord injuries [212-214]. To further improve tissue integration and uniaxial tissue growth, Dumont et al. [215] utilized a two-step cross-linking process to modularly assemble hydrogel tubes prepared via templates. The multiple void channels of the hydrogel tubes promoted tissue integration while the directional void channels supported uniaxial tissue growth, which is crucial for highly structured tissue regeneration. Hydrogel tubes can be easily customized by cutting and packaging to the desired size and shape with directed regenerative void channels. This strategy has the potential for personalized repair of spinal cord, peripheral nerve, muscle, and vascular tissue defects.

Directed ion diffusion can also be used to prepare highly oriented pore channels in hydrogels. Weidner et al. [216, 217] achieved this by using electrolyte solutions containing Ba^{2+}, Sr^{2+}, Zn^{2+}, and Ni^{2+} cations to prepare highly oriented capillary pore hydrogels with capillary sizes ranging from 12-100 μm. The oriented capillary pore channels were formed through a self-organizing process driven by the unidirectional diffusion of divalent cations into
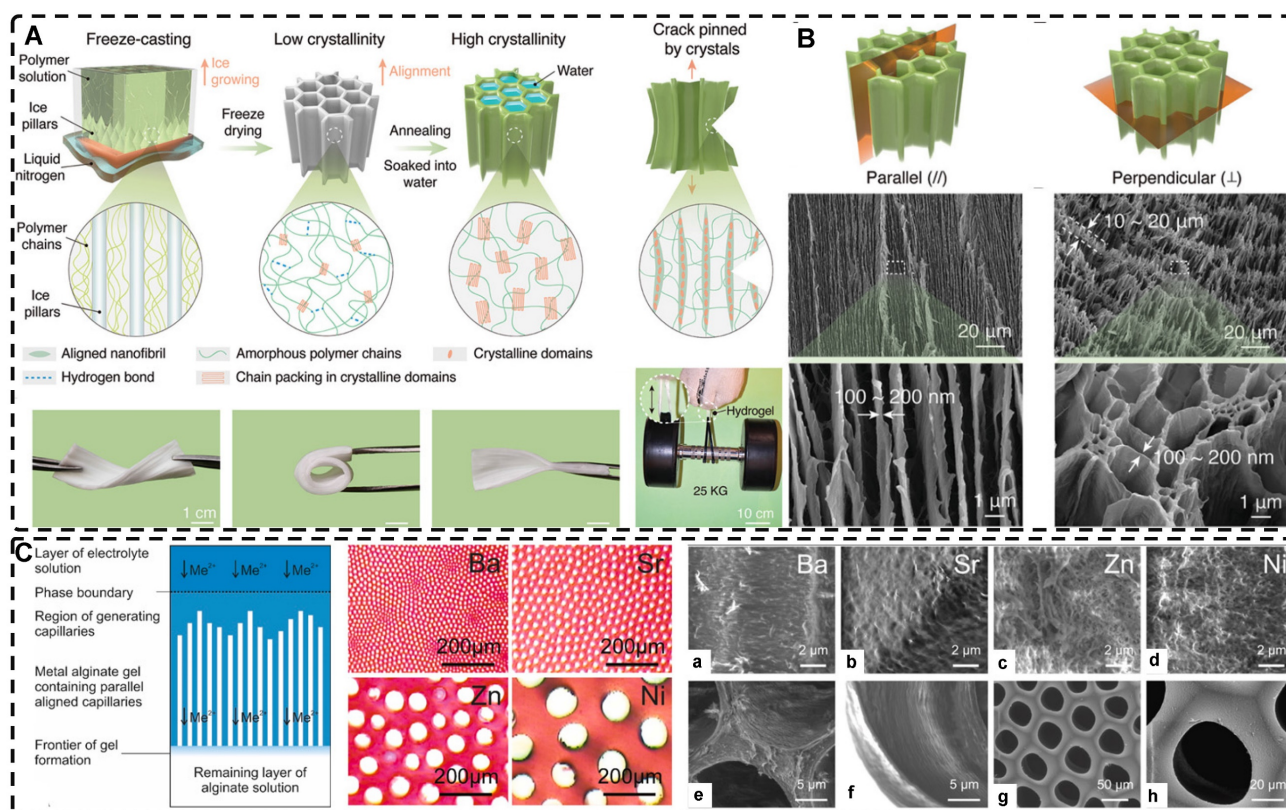
Figure 9. A) Schematic illustration for the highly oriented void channels hydrogels fabrication by using an ice-template freeze casting process. B) SEM images of the highly oriented void channels hydrogels. Adapted with permission from [198], copyright 2021, Wiley-VCH. C) Schematic drawing of the void channels formed by unidirectional diffusion of divalent metal cations (Me^{2+}) into a solution of sodium alginate, and cross-sections of the void channels in hydrogels formed by different cations. (a-h). Scanning electron microscopy images for highly oriented void channels hydrogels. Adapted with permission from [218], copyright 2022, Elsevier.

sodium alginate sols, opposite diffusion gradients, and the dissipation of the driving force of convective processes during friction of alginate chains. This led to the continuous precipitation of metal alginate, resulting in highly oriented capillary gels with honeycomb-like structures. The mechanical properties and chemical stability of this hydrogel were recently studied by Müller et al. [218], who found that the mechanical properties and degradation stability can be varied by the degree of chemical cross-linking and the formation of interpenetrating networks **(Figure 9C)**. The higher the concentration of cross-linking agent, the higher the mechanical strength. Additionally, the mechanical strength of the hydrogel generally decreased with an increase in capillary pore diameter, and the concentration of the cross-linking agent positively correlated with the resistance of the hydrogel to degradation.

3D printing enables the fabrication of hydrogel structures with highly oriented pore channels of various dimensions and directions. Li et al. [219] utilized digital light processing-based 3D printing to produce HA gelatin-based hydrogels with controlled and oriented microchannels, and they investigated the impacts of different microchannel sizes on NSC neural stem cell viability and proliferation. The outcomes demonstrated that directional micro-channels could direct the migration of NSC spheroids, and the aligned microchannels could constrain the neuronal growth of NSCs within the channels, promoting alignment and preventing disorganization. Furthermore, 3D printing could accurately match the size of the hydrogel to the size of the lesion area, offering promising potential for personalizing TE treatments, with the highly oriented channel structure facilitating directed cell growth.

Hydrogels with highly oriented void channels facilitate the transport, diffusion, and growth of macromolecules like growth factors or cells due to the presence of micrometer or larger pore channels compared to void-free channel hydrogels. However, their inherently poorer mechanical properties compared to homogeneous void-free hydrogels can limit their use in load-bearing tissues [199]. Template-sacrifice methods such as directional freeze-casting methods are simple, easy, economical, and environmentally friendly but do not provide precise geometric control of the material's dimensional characteristics compared to techniques like 3D printing. Additionally, accurately simulating natural tissue organs remains a challenge. In the future, hydrogels with highly oriented pore channels should aim to improve their mechanical strength and achieve more precise bionic direction.

2.4. Highly Oriented Hydrogels with Microfabricated Structures

2.4.1. 3D Printing for Preparing Highly Oriented Hydrogels with Microfabricated Structures

Although the fabrication strategies for highly oriented hydrogels discussed in the previous sections have a wide range of applications, many of these strategies lack precise control over the hydrogel's structure, which is crucial for TE applications of hydrogels. Therefore, 3D printing is a promising method for creating complex tissue structures with high precision and reproducibility. This technology is increasingly being explored and applied due to its ability to prepare biomimetic hydrogels efficiently and individually according to the biological tissue structure in both micro- and macro-structures. The current techniques widely used for hydrogel 3D printing are mainly classified into extrusion printing, inkjet printing, stereolithography printing, and laser-assisted printing methods [220-223]. Many reviews have examined or reviewed the details of these techniques in detail, so this paper does not discuss them in depth [223, 224]. Among these techniques, extruded 3D printing is the most widely used, with its ability to prepare highly oriented filler/polymer chain/void channel hydrogels at microscopic and macroscopic levels [225, 226]. As described in Section 2.1, the shear and tensile forces of the printing nozzle can orient the distribution of the filler material within the hydrogel. For example, Dong et al. [25] prepared an oriented CN+HAMA hydrogel using extrusion-based 3D printing. Similarly, shear forces during the printing process can cause the hydrogel polymer-chains to align in a highly directional manner **(Figure 10A-B)**. Kim et al. [192] prepared highly oriented collagen hydrogels with different cells using the shear stress of 3D printing nozzles. The physical topographical and biochemical cues carried by the highly oriented collagen hydrogels synergistically induced attachment, growth, and alignment of H9C2, MC3T3-E1, and hASC. Furthermore, shear force-induced cell alignment without any loss of cell viability was achieved, presenting a new approach to TE regeneration. The preparation of hydrogels with oriented pores by 3D printing has been discussed in Section 2.3.2 and will not be covered here.

In addition to utilizing shear forces alone, 3D printing can also be used in conjunction with other external fields to prepare highly oriented hydrogels. Pardo et al. [227] combined magnetically and matrix-assisted 3D bioprinting strategies to extrude bioinks composed of GelMA, short magnetically responsive microfibers (sMRFs), and hASCs into a

support bath based on CNCs hydrogels, under the presence of a low-intensity magnetic field **(Figure 10C-G)**. This resulted in the preparation of hydrogels filled with highly oriented alignments of sMRFs. The high magnetic response of the MNPs bound in the sMRFs allowed them to obtain orientation by remote alignment in low viscosity GelMA inks at low content of magnetic material condition by weaker magnetic field strength (14±2 mT). The structure of the hydrogel, as well as the ability of magnetomechanical stimulation to induce the oriented growth of encapsulated hASCs, and the subsequent addition of tendon dECM (decellular extracellular matrix) to the hydrogel to induce differentiation of hASCs toward tenogenic lineage, provide a new strategy for the reconstruction of natural tendon tissue and the maturation of bioengineered tendon constructs. While the hydrogel was designed with the principle of satisfying the regenerative reconstruction of tendon tissue, it also serves as a design reference for exploring the application of other oriented tissues, such as skeletal muscle, cartilage, and cardiac muscle.

Incorporating cells or stem cells into bioink is a promising research direction toward biocompatibility. Inducing cellular orientation in hydrogels through shear force by extrusion 3D printing is another important research focus. The cells within the highly oriented hydrogel can grow directionally along the
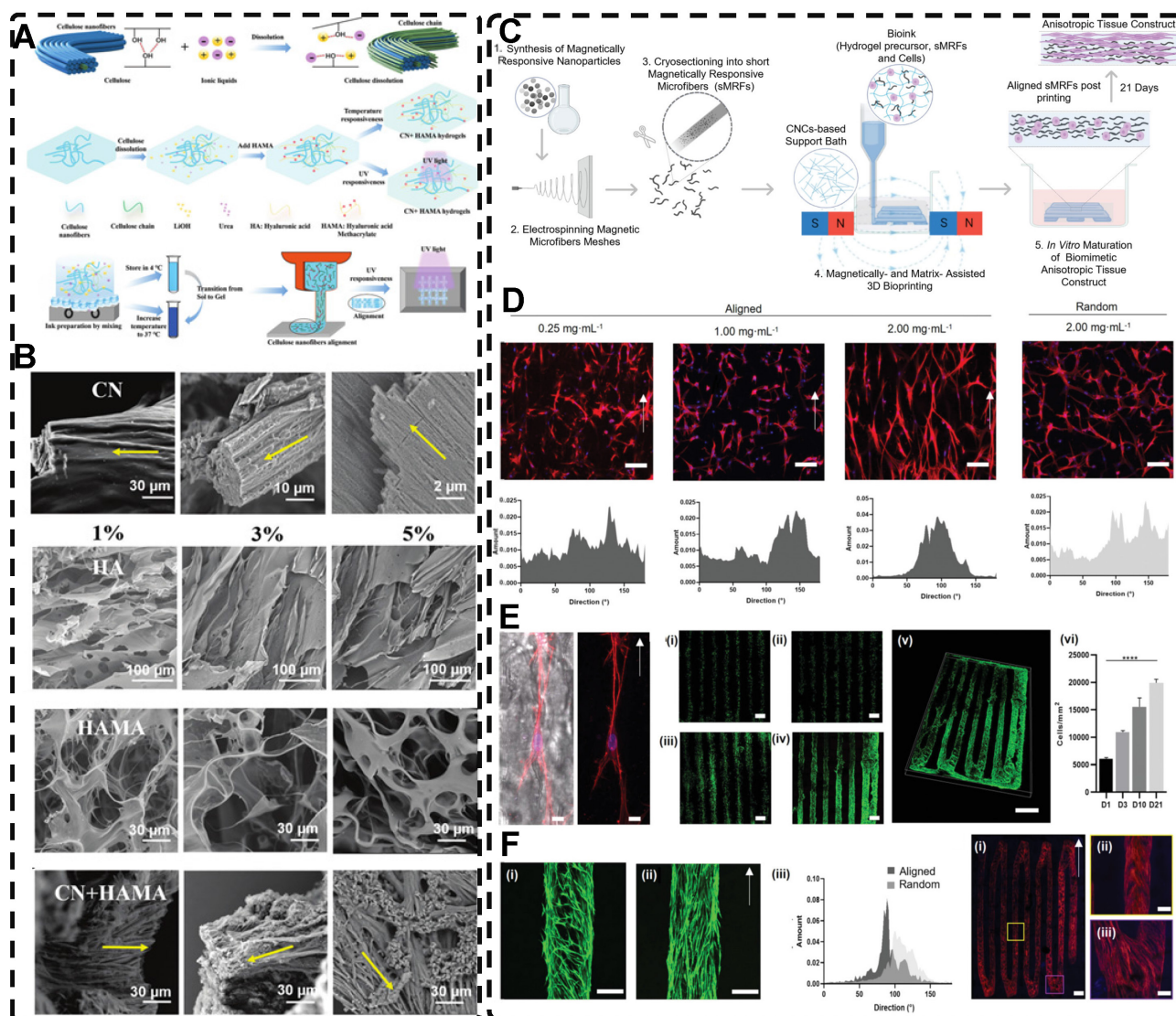
Figure 10. A) Schematic illustration of the composition and synthesis mechanism of the cellulose nanofibers + hyaluronic acid methacrylate (CN+HAMA) highly oriented hydrogels. B) SEM images of CNs, hyaluronic acid (HA), HAMA, and CN+HAMA hydrogels with different concentration ratios. Adapted with permission from [25], copyright 2022, AccScience Publishing. C) Schematic illustration of the proposed strategy to fabricate high-resolution oriented biomimetic constructs. D) The effect of short magnetically-responsive microfibers (sMRFs) orientation and concentration over the alignment and morphology of the encapsulated hASCs, along with their orientation plots. E) CLM images of hASCs adhered to sMRFs and acquiring elongated morphologies in highly oriented hydrogels, and viability and orientation of the hASCs encapsulated within oriented hydrogel after i) day 1, ii) day 3, iii) day 10 and iv/v/vi) day 21 of cell culture. F) Cell viability after 21 days in 3D bioprinted hydrogels with 2.00 mg mL^{-1} of i) randomly-oriented sMRFs and ii) aligned sMRFs. G) CLM images of hASCs cytoskeleton in GelMA, i) tile scan of fabricated construct, ii) straight line of the printed filaments, iii) curve of the printed filaments. Adapted with permission from [227], copyright 2022, Wiley-VCH.

highly oriented structure, better mimicking the aligned tissue found in the human body. However, the inevitable shear forces during the preparation process can damage or kill the cells and reduce their viability after 3D printing. Mechanosensing, mechanotransduction, and downstream mechanical response pathways are the three primary processes that occur in the cellular response to mechanical stresses, such as shear force, which integrate multiple biochemical signals from sensing and transduction events in time and space. Although shear stress can have negative effects on piggybacking cells, it plays a crucial role in controlling cell growth, motility, contraction, and differentiation into specific tissues or organs. For example, suitable shear stress can induce the differentiation of stem cells into vascular endothelial cells and osteogenic cells while controlling directional cell alignment. To achieve predefined 3D hydrogel scaffolds that mimic living tissues and organs and potentially shorten the length of organ transplant lists, scientists are exploring the balance between material properties, printing parameters, and the different cells used. This direction of research holds promise for the future of TE and 3D printing technologies. To date, there is no bioprinting technology capable of creating synthetic tissues and organs at all levels of complexity, which is the ultimate goal of 3D bioprinting in TE. Although 3D printing for TE organ transplants is still in the early stages, the ultimate goal is expected to be closer to reality with the advancement of printing technology (resolution, printing speed, consistency reproducibility, etc.) and the selection of suitable printing materials.

2.4.2. Other Strategies for Preparing Highly Oriented Hydrogels with Microfabricated Structures

Creating highly oriented topographic patterns on the surface of hydrogels is a method employed to generate microstructured, highly oriented hydrogels. Among the various methods used to shape highly oriented hydrogels, molding is a well-established and straightforward approach [228-231]. For instance, Hu et al. [230] employed a silicon master to fabricate a Polydimethylsiloxane (PDMS) mold, which was then used to create a highly oriented surface morphology pattern on a poly(2-hydroxyethyl methacrylate) (pHEMA) hydrogel **(Figure 11A)**. This highly oriented morphology pattern can promote the adhesion, spreading, and elongation of human MSCs cultured on the hydrogel, serving as a foundation for the future development of highly oriented hydrogels for TE applications.

Wrinkling can give rise to highly oriented surface morphologies in hydrogels [232-234].

Professor Rodríguez-Hernández introduced the wrinkling model and proposed a comprehensive mechanism [235]. The Allen model [236] established the theoretical foundation for orientational wrinkling, and Bowden et al. [237] developed an anisotropic wrinkling model that correlates spatially inhomogeneous stress distributions with wrinkling patterns to analyze the characteristics of wrinkles accurately, including their wavelength and direction [238]. Kashihara et al. [239] employed electrophoresis to create a polyion complex (PIC) layer on the hydrogel surface **(Figure 11B-C)**. The resulting stress mismatch between the two layers led to the formation of wrinkles as the PICs deformed on the hydrogel surface. Applying uniaxial compression to the hydrogel in the planar direction enabled control over the direction of wrinkle motion during the formation process, resulting in a highly oriented wrinkled morphology. Ye et al. [240] immersed pre-stretched cellulose alkaline gels into acidic solutions for varying durations, resulting in the formation of a dense nanofiber structure and a robust dual-crosslinked hydrogel after the removal of external forces **(Figure 11D)**. In this process, the physical cross-linking of the pre-stretched aligned cellulose chains within the acidic solution induced mechanical instability in the hydrogel. The removal of the stretching led to the formation of a highly oriented self-wrinkling surface structure due to this mechanical instability. The highly oriented wrinkled structure of the hydrogel enhanced the adhesion and alignment of MC3T3 cells. The programmability and biocompatibility of this hydrogel, along with its design concept, make it a valuable material for application and exploration in TE. The wrinkling method offers a simple, rapid, and cost-effective approach for producing large-area hydrogels with oriented surface morphologies, thereby effectively generating multi-scale, highly oriented hydrogels.

2.5. Highly Oriented Hydrogels Prepared by Special Methods

Many natural organic materials have a highly oriented extracellular matrix with excellent mechanical properties, making them ideal templates for developing highly oriented hydrogels with improved mechanical properties. Hu et al. [241] utilized natural wood as a biomold to fabricate hydrogels that mimic muscle tissue. They removed lignin from white wood by a delignification process in a $NaClO_2$ solution at pH=4.6 to release the tight connections between fibers while maintaining the inherent structure of oriented aligned cellulose nanofibers (CNFs). The acrylamide (AM) monomer effectively formed strong hydrogen bonds with the

CNF backbone in the presence of an initiator and cross-linker to develop layered highly oriented composite wood hydrogels. The high tensile strength of 36 MPa in the longitudinal growth direction was attributed to the wood backbone, and the strong interfacial bonding provided favorable mechanical properties **(Figure 12A-B)**. Furthermore, the hydrogel's anisotropic optical properties and excellent ionic conductivity make it attractive for various applications, including TE. Xu et al. [242] utilized natural sugarcane as a biotemplate to create three highly oriented sugarcane composite hydrogels that form hydrogen bonds with different materials: pHEMA, poly(acrylamide) (pAM), and poly(acrylamide-co-acrylic acid) (p[AM-co-AA]) **(Figure 12C)**. These hydrogels exhibited good flexibility, elastic recovery, and anisotropic lubrication behavior, making them promising

candidates for the development of artificial skin and cartilage-lubricating materials. Similarly, Yan et al. [243] developed highly oriented all-wood tough hydrogels through dynamic bonding between natural wood biotemplates, PAM chains, and iron ions, by exploiting the reversible crosslinking of catechol groups of lignin in natural wood with Fe^{3+} ions under the influence of Ammonium peroxydisulfate (APS), which also acted as a crosslinker to link the cellulose fibers in the highly oriented wood skeleton to the PAM chains **(Figure 12D)**. The resulting hydrogel exhibited a wide range of strain, high sensitivity, and good flexibility due to the reversible hydrogen bonding and metal coordination bonding, making it an excellent candidate for compressive sensing. It is believed that the technique of using natural biological templates to create highly oriented hydrogels has a promising future in TE applications [238].
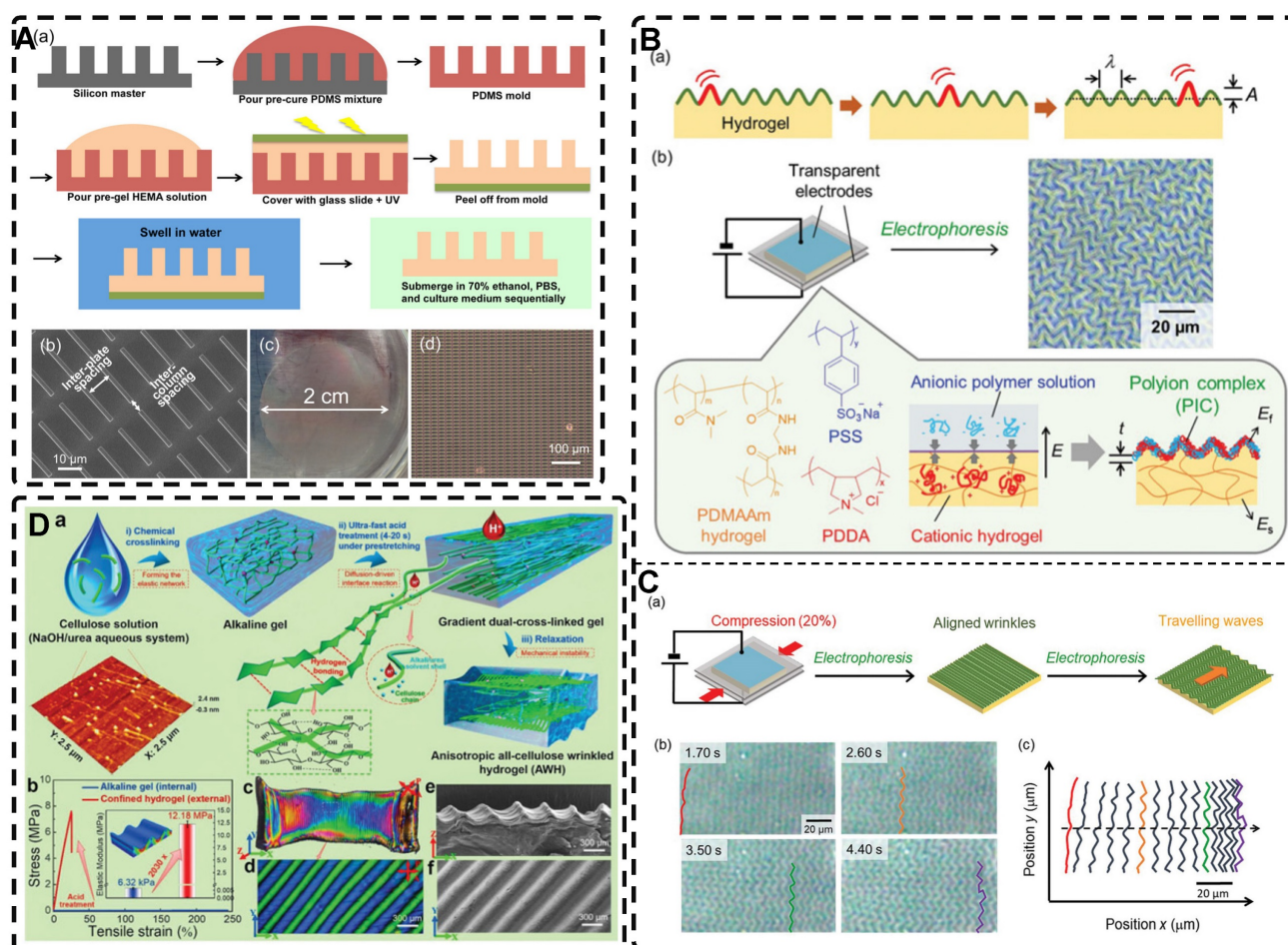
Figure 11. A) (a) Schematic illustration of the procedure for the fabrication of the microstructured highly oriented hydrogel substrate. Scanning electron microscopic image (b), picture (c) and microscopic image (d) of hydrogel. Adapted with permission from [230], copyright 2016, American Chemical Society. B) a) Schematic of Travelling wave generation of PIC wrinkles on the hydrogel surface. b) Fabrication of wrinkles on a hydrogel surface by electrophoretic. C) a) Experimental electrophoretic formation of aligned wrinkles under the lateral compression of gels. b) Time-course images of aligned wrinkle formation during electrophoresis. c) Trajectories of aligned wrinkle as a function of time. Adapted with permission from [239], copyright 2022, Wiley-VCH. D) a) Schematic image of highly oriented hydrogels fabrication. b) Differences in mechanical properties between the outside and inside of hydrogels. c,d) Birefringence patterns and magnified POM images of an hydrogels sample. e,f) Cross-section and surface SEM images of hydrogels showing a long-range and highly oriented self-wrinkling configuration. Adapted with permission from [240], copyright 2019, Wiley-VCH.
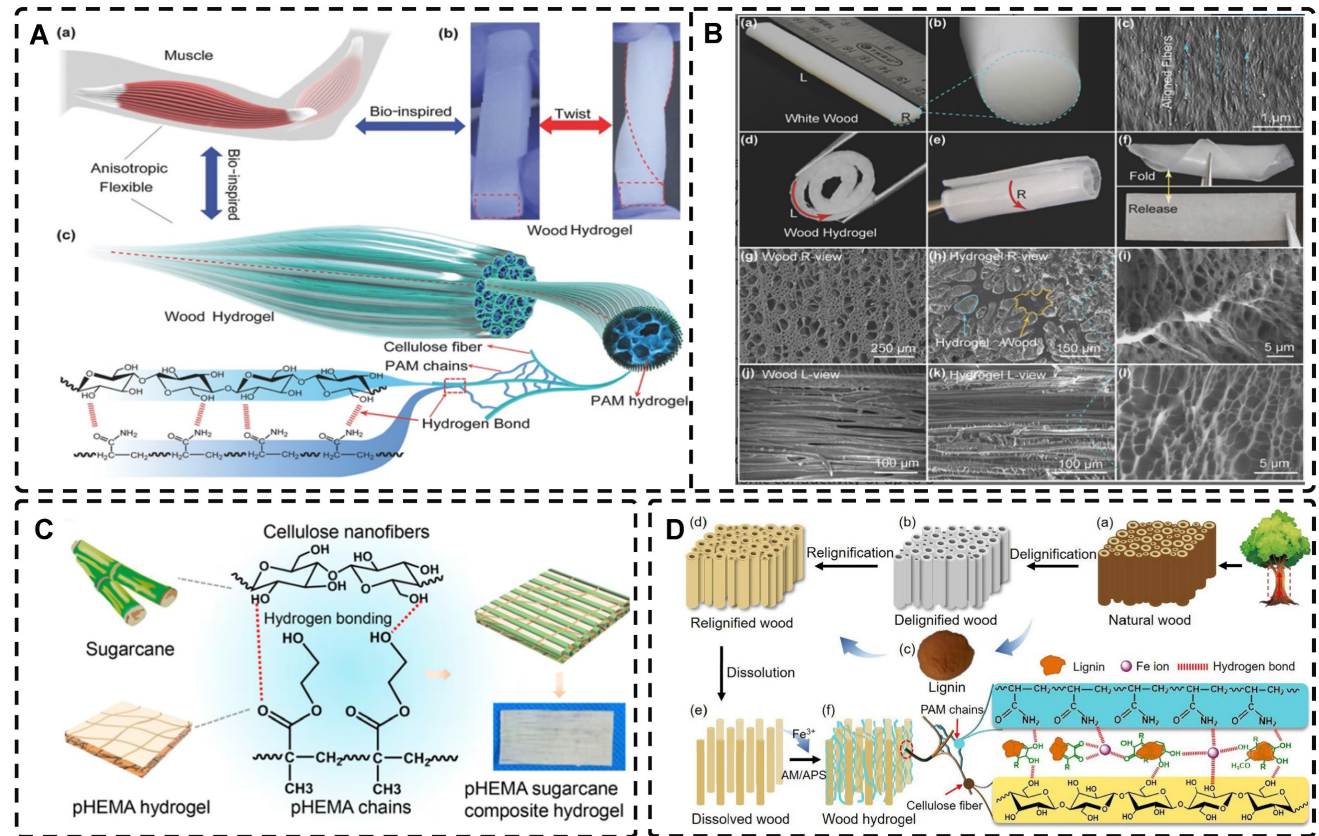
Figure 12. A) a) Schematic of a conventional flexible and striated skeletal muscle tissue to be emulated by the wood hydrogel. b) Images of a 7 cm long wood hydrogel sample being twisted 180°. c) Depiction of the wood hydrogel hydrogen bonding and covalent cross-linking between PAM chains. B) Optical (a-f) and SEM images (g-i) of the wood hydrogel and white wood. Adapted with permission from [241], copyright 2018, Wiley-VCH. C) Schematic illustration of hydrogen bonding formed between white sugarcane and pHEMA chains. Adapted with permission from [242], copyright 2021, Wiley-VCH. D) Schematics illustrating the all-wood hydrogel preparation (a-f). Adapted with permission from [243], copyright 2021, Eleseur.

Liu et al. [30] introduced the biofabrication technique "Filamented Light" (FLight) to produce hydrogels. They utilized optical modulation instability (OMI) to induce highly aligned hydrogel microfilaments through the interaction of spatially coherent light beams with various photoresin compositions **(Figure 13A-B)**. After removing the uncrosslinked photoresin, the voids between the microfilaments appear as microchannels with ultra-high aspect ratios, which can be used to guide cell alignment and migration **(Figure 13C)**. The diameter and spacing of hydrogel microfilaments could be adjusted by changing the coherence length of the beam from 2 to 30 μm. In less than 10 seconds, cells were safely and rapidly encapsulated in a highly oriented hydrogel microfilament network. Furthermore, other FLight biomanufacturing strategies such as Cross-Flight and Multi-Flight can been used to construct layered complex tissue constructs with different orientations, such as cardiac muscle tissue, by implementing multi-directional hydrogel microfilaments **(Figure 13D)**. This study was the first to apply this technique to the field of TE, and it offers promising prospects for future applications in highly oriented tissue regeneration, avoiding cellular shear stresses compared to extrusion-based 3D printing.

The incorporation of highly oriented structures from electrostatic spinning products into hydrogels can bestow the hydrogels with desired structures [244, 245]. For example, Wu et al. [246] devised a weaving technique to prepare a conductive nanofiber yarns network (NFYs-NET) structure using electrostatic spinning and a combination of polycaprolactone, silk fibroin, and carbon nanotubes. This structure was further encapsulated in a photocross-linked GelMA hydrogel to closely mimic the natural structure of heart tissue while imparting an oriented architecture to the hydrogel. The NFYs-NET demonstrated the ability to guide cell alignment and elongation, as well as enhance the maturation and function of cardiomyocytes (CMs). The GelMA hydrogel shells provided a favorable three-dimensional environment for mechanical protection and endothelialization by facilitating co-culture with endothelial cells (ECs). These three-dimensional hybrid scaffolds hold immense potential for applications in cardiac TE **(Figure 14)**.
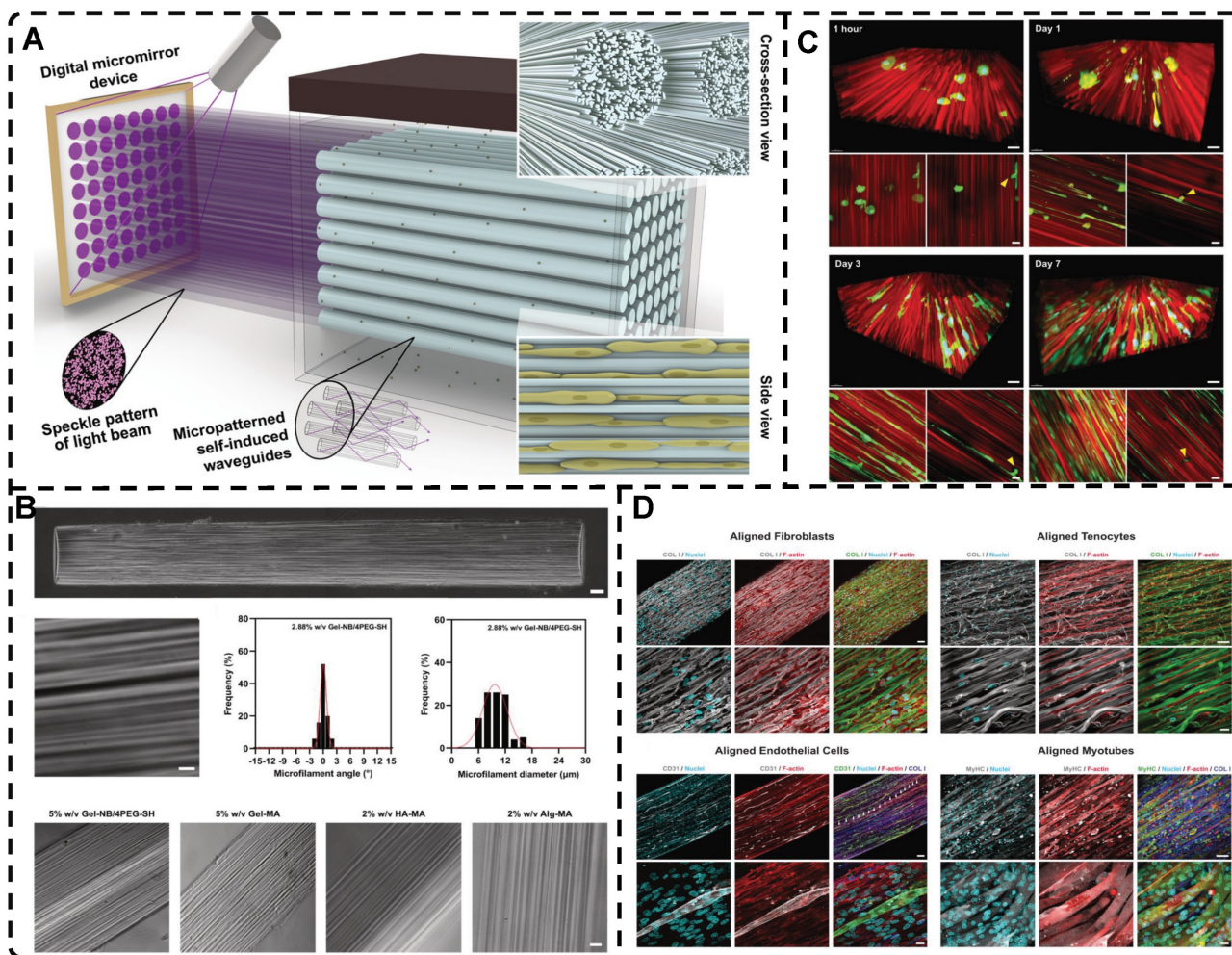
Figure 13. A) Schematic illustration of FLight strategy for fabricating highly oriented microfilaments and their cell guidance properties. B) Bright-field image of FLight hydrogel construct, magnified image of microfilaments structuring of oriented hydrogel, distribution of the microfilament diameter, and the distribution of angles' difference between the orientation of microfilament and direction of projection. C) Fluorescence images of cell-laden hydrogel matrix. D) Cell guidance properties of microfilaments and maturation of highly aligned tissue-engineered constructs. Evidence of highly oriented fibroblasts, tenocytes, endothelial cells, and myotubes by immunofluorescence staining. Adapted with permission from [30], copyright 2022, Wiley-VCH.

3. Effect of Highly Oriented Structures on Cell Behaviors

Cells within natural physiological niches experience a multitude of cues, including physical stimuli such as mechanical, electrical, and topographical factors, as well as biochemical cues such as specific drugs, proteins, growth factors, and combined insoluble particles [247-249]. These cues effectively direct cell behavior and function by regulating cell adhesion, migration, proliferation, and differentiation, thereby promoting tissue repair and regeneration [250-252]. Highly oriented hydrogels can endow ordinary hydrogels with highly oriented structural cues, which may be analogous to physical cues being integrated and converted into intracellular signals through mechanical transduction that microcells can recognize in the microniche, ultimately influencing cellular behavior [26]. The purpose of this part is mainly to analyze the crude cellular behaviors of highly oriented structures in highly oriented hydrogels affecting cell adhesion, migration, proliferation, and differentiation, and provide a brief review of the relevant literature. Despite their significance, the underlying biological mechanisms by which cells perceive and respond to these cues have so far remained incompletely understood and require further investigation. Limited research has explored cell behavior within 3D hydrogel systems with highly oriented structures. Consequently, discussions on the impact of the highly oriented structure of 3D hydrogels on cell behavior draw largely from insights derived from anisotropic materials, particularly micropatterned surfaces.
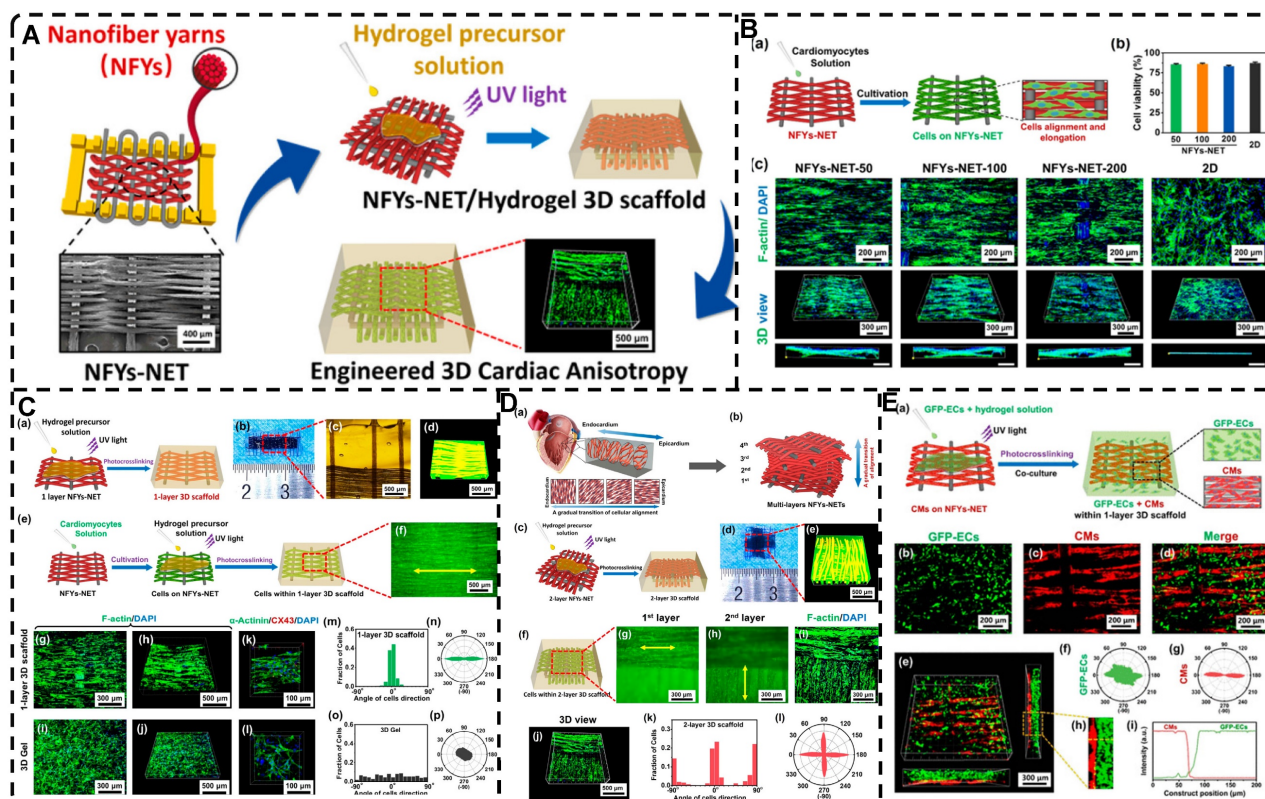
Figure 14. A) Schematic illustration of NFYs-NET hydrogel preparation. B) (a) Cardiomyocytes seeded and cultured on NFYs-NET hydrogels. (b) Relative cells viability percentages of cardiomyocytes on NFYs-NET hydrogels evaluated by live/dead assay. (c) The top views and 3D views of fluorescent images of cardiomyocytes on NFYs-NET hydrogels. C) (a-d) Fabrication process of 1-layer oriented hydrogels, and their gross image, optical image, and the 3D view of confocal image. (e, f) Scheme of cardiomyocytes seeded and cultured within hydrogels and the fluorescent image of cardiomyocytes. (g, h, k) The confocal images showed the cellular alignment and elongation within oriented hydrogels while (i, j, l) the random morphology of cells within GelMA hydrogel, and (m-p) the quantitative analysis of cellular orientation distribution. D) (a-c) Schematic of myocardium oriented structure, multilayers orientation of NFYs-NETs assemble, and 2-layer oriented hydrogels fabrication. (d, e) The gross image and 3D view of confocal image of 2-layer 3D scaffolds. (f-h) The scheme of culturing cells within oriented hydrogels and fluorescent images of cardiomyocytes with horizontal direction and vertical direction. (i-l) The top view and 3D view of confocal images of cells and the quantitative analysis of cellular orientation distribution. E) (a) CMs were cultured on the NFYs-NET layer, ECs were encapsulated within hydrogel shell. (b-d) The fluorescent images of ECs, CMs and their merge image. (e-g) The 3D view of confocal images of ECs and CMs within scaffolds, and the quantitative analysis of cellular orientation distribution. (h, i) The distribution of ECs in hydrogel and CMs on NFYs-NET. Adapted with permission from [246], copyright 2017, American Chemical Society.

Cells cultured on highly oriented hydrogels or scaffolds exhibit robust adhesion, potentially attributed to specific topographical cues embedded within these structures, such as oriented ridges, grooves, or pores. At the macroscopic scale, topographical features influence cellular arrangement at the colony level [253], and at the microscale, topographies correspond to the size range of individual cells, thereby impacting cell behavior at the cellular level. The alignment and orientation of cells on microtopographical features are known as "contact guidance," a concept first proposed in 1964 [254, 255]. Moreover, at the nanoscale, topographical features manifest at a similar magnitude as cellular receptors, including integrins, influencing the adsorption of adhesion-related proteins [256].

The initial step in cell behavior is adhesion formation, which enables the cell to perceive and respond to the physical and functional properties of its external topographic environment, thus influencing cellular decision making [257]. At the molecular level, cells detect topographical cues through integrins, which are transmembrane receptors located on thin protrusions of the cell membrane. Integrins consist of unique combinations of at least 24 α-subunits (18 types) and β-subunits (8 types) that interact non-covalently. These integrins form adhesion complexes and bind to ECM ligands, including RGD peptides [258]. Integrins play a vital role in cell adhesion, serving as the primary family of cellular receptors responsible for interactions between cells and the ECM. Aside from anchoring cells to their surroundings, integrins also establish connections with the cytoskeleton within the cell, making integrin binding a crucial step in various intracellular signaling pathways [259]. Integrins do not possess enzymatic activity; nevertheless, they have the capacity to recruit and accumulate multiple intracellular proteins at integrin clusters, forming integrin adhesion complexes (IACs) [260]. These complexes serve as mechanical linkages between integrins and the actin cytoskeleton, playing a crucial role in directing cell spreading and fate. Focal complexes emerge as a result of IAC aggregation and

subsequently mature into larger, elongated supramolecular complexes known as focal adhesions (FAs) [261]. Within these complexes, certain proteins such as talin and vinculin participate in mechano-sensitive events, crucial for adhesion maturation [262, 263]. Other proteins, including paxillin, tensin, and p130cas, act as articulation proteins [264]. Signaling molecules such as focal adhesion kinase (FAK) and Src family kinases are also present. Integrins and their complexes play a pivotal role in driving cellular functions and behaviors, encompassing cell adhesion, morphology, migration, proliferation, and differentiation. Topographical cues regulate these processes by modulating cell adhesion, migration, proliferation, and differentiation through integrin-mediated focal adhesions, which contribute significantly to mechanotransduction and the activation of intracellular signaling pathways.

The dynamic actin and microtubule cytoskeleton are key regulators of cellular morphology, undergoing reorganization via signaling pathways associated with guidance cue receptors [265]. Initially, filamentous pseudopods respond to aligned topographic cues, and subsequently, adhesion is directed in the same orientation, leading to cytoskeleton alignment and cell rearrangement along the nanoscale guidance cue [266]. Consequently, a highly oriented topography can influence filopodia orientation through spatially restricted adhesion sites, exerting anisotropic migratory forces on cytoskeletal arrangement. This results in cell elongation parallel to the hydrogel orientation and overall cytosol alignment. In neuronal cells, for instance, FAs play a crucial role in controlling axon initiation by orchestrating cell polarization, cytoskeletal organization, and axon pathfinding/motility [267]. The contractile machinery of cells, mediated by Rho-associated protein kinase (ROCK), significantly influences their morphological responses to surface topography and substrate mechanics [268]. Sun et al. [184] conducted an experiment where the addition of the ROCK inhibitor Y-27632 resulted in a reduced alignment of fibroblasts cultured on highly oriented hydrogels, demonstrating the impact of highly oriented structures on cell morphology. Ryosuke Ozasa et al. [269] further demonstrated a parallel relationship between cell orientation and FAs extending along oriented collagen scaffolds. Importantly, the cellular response to anisotropic topographic cues is dependent on cell type and can be influenced by cell-cell interactions and pattern density [270, 271].

Cell migration plays a crucial role in various physiological and pathological processes, and its induction is a vital aspect of TE and regeneration.

Cells exhibit both individual and collective migration modes [272, 273]. Individual migration can be categorized into two modes: mesenchymal and amoeboid. Mesenchymal migration, observed in fibroblasts, stem cells, and certain cancer cells, relies heavily on ECM adhesion, actin-based protrusions (lamellipodia or filopodia) at the leading edge, contraction of the actin network, and an elongated cell shape, resulting in slower migration [274]. On the other hand, amoeboid migration, employed by various cells like primitive germ cells and immune cells such as leukocytes, features weak ECM adhesion and a transition of cell protrusions from lamellar and filamentous pseudopods to actin polymerization-driven rounded cell shapes and transient actin-free globular membrane protrusions known as blebs [275]. Amoeboid migration relies on myosin-based contraction and pressure-driven cytoplasmic flow, enabling fast migration. In collective migration, signals from external cues are transmitted to the entire cell population through intracellular and intercellular signaling cascades, and mechanical transduction at cell-cell junctions and cell-ECM interfaces [276]. Notably, cells can switch between individual and collective migration patterns, influenced by multiple factors, such as topographic features, ECM composition, adhesion strength, and biochemical signals [277, 278]. However, the understanding of how highly oriented structures drive cell migration is still in its nascent stages.

Numerous studies have examined alterations in cell shape, protrusion shape, actin cytoskeleton, and motility when exposed to artificially created simulations of various topologies found in human-oriented tissues, including specific patterns or 3D aligned channels [279-281]. However, there is a paucity of research investigating how the perception of these landscapes is integrated into cellular dynamics through downstream intracellular events. Several studies have reported that cells such as fibroblasts and neurons sense nano- to micrometer-scale oriented structures topographically through frontier protrusions to drive subsequent cell migration [282, 283]. Recently, it has been discovered that local deformation or curvature of the plasma membrane at the cell-substrate junction serves as a sensor for nanomorphology. Bar family proteins, particularly FBP17, are considered pivotal in bridging the connection between nanomorphology and intracellular actin reorganization [284]. This revelation of membrane curvature as a topological sensor fills a critical gap in understanding how surface topological signals trigger intracellular actin fiber reorganization. Moreover, topological cues also elicit changes in cell nuclear location and

morphology, which can significantly impact cell migration [285]. Kim et al. [286] investigated the effect of oriented structures on cells and found that NIH-3T3 cells cultured with oriented nanotopographic cues exhibited varying migration rates depending on topographic densities and orientations, demonstrated by the absence of growth factors during wound healing. Another study by Ray et al. [270] revealed that orientation-aligned structures, which provide contact-guided cues, physically restrict the maturation and orientation of FA, leading to directional traction, anisotropy, and orientation of actin fibers that drive cell orientation and directional migration.

The significance of cell proliferation in tissue regeneration is well-established, and the topographical cues provided by materials play a crucial role in regulating cell proliferation and differentiation. Previous studies have demonstrated that microtopography can effectively control the growth of neural cells and tissues, promoting enhanced cell proliferation and differentiation [287]. Additionally, microtopography patterns have been shown to stimulate the proliferation of adherent cells. For instance, Seunghan Oh et al. [288] found that oriented titanium nanotubes significantly increased osteoblast proliferation by 300-400% compared to titanium metal surfaces. At the molecular level, inhibition of FA formation through modulation of the FAK/RhoA-regulated mTORC1 and AMPK pathway leads to reduced cell proliferation and metastasis [289]. Consequently, integrins and their complexes are essential for cell proliferation; the adhesion of cells to the ECM through integrin receptors serves as an important checkpoint for entry into the cell cycle. Without proper integrin signaling, cells are unable to transition from the G1 phase to the S phase, preventing proliferation. The integrin adhesion complex activates multiple signaling cascades that facilitate cell progression to the S phase, including the Mek/Erk, PI3K/Akt, and the small GTPase Rac pathways [290]. Scaffold proteins like talin can also play a role in proliferation by bridging mechanistic signals and nuclear responses. However, the mechanisms underlying the connection between actin polymerization and cytoskeletal changes during proliferation remain incompletely understood.

Controlling the nanomorphology of substrates presents an effective approach to modulating cell differentiation. For instance, Izadpanahi et al. [291] demonstrated that highly oriented aligned PLLA scaffolds could promote the expression of osteogenic marker genes in adipose MSCs (hMSCs), which randomly oriented scaffolds could not. At the molecular level, it was discovered that nanotopo-

graphical cues possess the ability to influence the osteogenic differentiation process of hMSCs. This influence is achieved through the modulation of lncRNAs and miR-125b, which serve as negative regulators of osteogenesis, as well as the H19 modulator BMP signaling pathway that functions as an miRNA sponge. In a similar vein, Lee et al. [292] prepared PLGA patches with highly oriented aligned nanogrooves, which exhibited enhanced migration and differentiation of osteoblasts in comparison to planar patches. In vivo studies conducted on rats further demonstrated the improved bone regeneration capabilities of the aligned nanogrooved patches. Furthermore, Xiao et al. [293] investigated the impact of distinct surface morphologies on the osteogenic differentiation of rat bone marrow-derived MSCs (rBMSCs) in the absence of osteogenic induction mediators. Their findings revealed that surfaces with oriented nano-grating-like films exhibited higher levels of osteogenic gene expression and distinctive activation of MAPK and Smad signaling pathways compared to flat and nanoporous films, which promoted the osteogenic differentiation of rBMSCs.

Previous studies have provided evidence linking FAs to the FA kinase and ERK pathways, both of which have the potential to influence cell differentiation [294]. This suggests an effect of topography on cell differentiation through the mechanotransduction of extracellular biophysical signals to cells [265]. Cells perceive topographical cues through integrins and transmit them to the nucleus via FA signaling and the actin cytoskeleton, thereby eliciting differential gene expression and promoting differentiation along specific lineages. For instance, anisotropic topologies can stimulate the osteogenic differentiation of cells by promoting the polymerization of FAs and actin. FAs have the ability to modulate cellular contractility and cytoskeletal organization, and an increased formation of FAs facilitates the osteogenic differentiation of cells [268, 295-297]. The synergistic effects of cellular contractility, FAs, and YAP-TAZ signaling further enhance the osteogenic differentiation of cells [298, 299].

Indeed, the effect of highly oriented structures on cell behavior is a complex process involving multiple signaling pathways and the cytoskeleton. Understanding the mechanisms by which highly oriented structures affect cell behavior is essential for the development of novel biomaterials and therapeutic approaches in various research areas such as TE, regenerative medicine and cancer research. Further research is needed to fully understand the underlying mechanisms and to develop new

approaches to improve cellular arrangement and function on highly oriented structures.

4. Application of Highly Oriented Hydrogels in Tissue Engineering

Biological soft tissues composed of highly oriented composite structures demonstrate pronounced anisotropic mechanical strength and functionality. Tissues and organs, such as the cornea, skin, skeletal muscle, tendons, ligaments, cartilage, bone, blood vessels, and heart, are composed of fibers and/or cells that possess a high degree of orientation, resulting in their distinctive structural orientation. While highly oriented tissues and organs share general orientation characteristics, each of them possesses unique composition, structure-related properties, and mechanical and biological functions. Therefore, the application of highly oriented hydrogels should be tailored to the specific properties of individual tissues or organs, and the corresponding hydrogels should be customized accordingly.

This section provides a comprehensive review of the existing research on highly oriented hydrogels in the field of TE. Furthermore, it offers a concise overview of the primary orientation characteristics exhibited by different tissues and organs, setting the stage for further discussion.

4.1. Highly Oriented Hydrogels for Cartilage Tissue Engineering Applications

Cartilage, a vital connective tissue in the body, is composed of 10-15% chondrocytes and ECM. The ECM of mature articular cartilage primarily comprises type II collagen (90%), with smaller proportions of type XI (3%) and type IX (1%) collagen. Cartilage serves as a crucial contributor to joint function by providing a frictionless and lubricated surface [44, 300]. Cartilage exhibits a hierarchical structure characterized by distinct orientations of collagen fibers: a superficial layer with parallel orientation to the cartilage surface, a middle layer with randomly arranged fibers, and a deep layer with fibers oriented perpendicular to the surface [301, 302] Each layer's specific orientation corresponds to distinct functional roles: the superficial layer bears shear forces generated by joint motion, the middle layer serves as the primary cushion against resistance, and the deep layer provides exceptional compression resistance [44]. These three layers collaborate synergistically to enable cartilage to effectively dissipate compressive loads and absorb impact forces, thereby safeguarding and facilitating bone movement [303].

Healing cartilage defects larger than 2 mm in diameter pose a significant clinical challenge due to the lack of blood vessels and nerves within natural cartilage tissue [304]. Numerous tissue-engineered scaffolds have been employed to fill defects and promote cartilage regeneration [303, 305-308]. By replicating the orientation of natural cartilage, highly oriented hydrogels can effectively emulate the anisotropy of the native tissue. Bas et al. [245] utilized a network of highly oriented polycaprolactone (mPCL) fibers prepared via melt electrospinning to reinforce a star-shaped poly(ethylene glycol)/heparin hydrogel (sPEG/Hep) **(Figure 15A)**. This approach aimed to replicate the biomechanical characteristics of human articular cartilage, encompassing mechanical anisotropy, nonlinearity, viscoelasticity, and morphology. Furthermore, it provided an appropriate microenvironment for chondrocyte culture and facilitated the in vitro formation of new cartilage tissue. Liu et al. [32] fabricated CNC/collagen nanocomposite hydrogels with hierarchically oriented pores, including horizontally aligned, randomly aligned, and vertically aligned orientations, which replicated the structural characteristics of natural articular cartilage through the process of directional freezing. Dai et al. [201] developed a highly oriented hydrogel using Silk fibroin (SF), poly(ethylene glycol) (PEG), and CNCs through the process of directional freezing. The resulting hydrogel exhibited a Young's modulus of 709 kPa and 160 kPa, which is comparable to the range (0.4-0.8 MPa) observed in natural cartilage. Chen et al. [309] fabricated bionic cartilage hydrogels with hierarchical orientation using magnetic field orientation technology, the freeze-thaw method, and the annealing process. The hydrogels consisted of a horizontally oriented surface layer made of PVA/3 wt % $PDA-Fe_3O_4-MMT/PAA$ hydrogels and vertically oriented deep layer made of PVA/3 wt % $PDA-Fe_3O_4-CF/PAA$ hydrogels **(Figure 15B)**. The materials employed include PVA, montmorillonite (MMT), Polyacrylic acid (PAA), and Carbon fiber (CF). The layered, oriented hydrogels demonstrated excellent frictional properties in the surface layer and high load-bearing capacity in the bottom layer, closely resembling natural cartilage. This innovative approach offers a novel strategy for the design of cartilage-like hydrogels. Furthermore, these highly oriented hydrogels hold significant clinical translational value as they can induce the aligned alignment of cultured cells while maintaining their natural mechanical properties. Wu et al. [310] developed a composite oriented hydrogel by incorporating a radially oriented poly(lactide-co-glycolide) (PLGA) scaffold into an oxygen species (ROS)-scavenging hydrogel (RS Gel). Upon implantation, the oriented hydrogel exhibited excellent biocompatibility, anti-inflammatory properties, and natural cartilage-like tidemarks. Moreover, the

abundant chondrocytes within the hydrogel were arranged in a well-ordered manner, closely resembling the orientation observed in natural cartilage tissue. However, during the initial stage, the composite hydrogel somewhat influenced cell infiltration into the hydrogel; adding bioinductive factors, such as growth factors, may enhance the optimization of the scaffold. Gossla et al. [311] fabricated composite highly oriented hydrogels by combining oriented chitosan scaffolds with alginate hydrogels. This combination resulted in improved compressive strength and elasticity, specifically in the direction of the oriented fibers, offering superior mechanical stability when compared to chitosan scaffolds or pure alginate hydrogels. Moreover, the oriented hydrogels promoted chondrogenic different-iation of primary human chondrocytes, upregulated the expression of chondrogenic markers at both the RNA and protein levels, and effectively reduced the synthesis of type I collagen. Wang et al. [312] utilized cellulose fabric, cellulose nanofiber, and wood cellulose fiber in combination with a poly(ethylene glycol) diacrylate (PEGDA) polymer matrix. These components were polymerized using UV radiation to fabricate hierarchically oriented hydrogels that mimic the structure of cartilage **(Figure 15C)**. The composite layered, oriented hydrogel exhibited a shallow fiber morphology parallel to the hydrogel surface, a randomly distributed fiber morphology in the middle region, and deep reinforcing fibers oriented perpendicular to the hydrogel surface **(Figure 15D)**. The hierarchical orientation structure imparted distinct nonlinear and viscoelastic mechanical properties to the composite hydrogel across different regions. The highly oriented superficial and deep regions promoted the alignment of mouse bone-derived mesenchymal stem cells (BMSCs), resulting in predominantly hyaline cartilage differentiation across all regions after 14 days **(Figure 15E)**, which exhibited comparable morphology and collagen II content distribution to natural cartilage. Furthermore, the presence of channel-like wood cellulose fiber frames in the deeper regions created capillaries, enhancing nutrient and cell transport within the hydrogel, which played a crucial role in facilitating cartilage recovery and regeneration. These findings highlight the potential of bionic highly oriented hydrogels for various applications in cartilage TE.

4.2. Highly Oriented Hydrogels for Bone Tissue Engineering Applications

Bone is a widely distributed, large, and structurally complex mineralized connective tissue that serves crucial roles in providing mechanical support, protecting the body, and facilitating essential metabolic processes including mineral transfer and hematopoiesis [313]. Bone primarily comprises organic matter, minerals, and water organized in specific structural arrangements. It consists of approximately 65% minerals by weight, mainly carbonate apatite, and 20-25% type I collagen, which serves as the predominant organic component [314]. Notably, the hierarchical composite structure of bone encompasses highly oriented, interlaced cross-linked collagen protofibrils embedded within plate-like hydroxyapatite (HAp) nanocrystals. This composite structure spans multiple scales, ranging from the nano to macroscopic level, and contributes to the remarkable mechanical properties and diverse biological functions exhibited by bone [10, 315].

While bone possesses remarkable inherent self-healing abilities, the challenge of repairing extensive bone defects persists in the absence of external interventions [316, 317]. Given the high toughness and stiffness of bone tissue, bone scaffolds represent the preferred option for filling and providing support to bone defect sites. Despite hydrogels not being the primary choice for bone TE, recent studies utilizing highly oriented hydrogels in this field have demonstrated promising applications, leading to a growing interest in bone TE [318-320]. Lin et al. [321] employed a non-covalent assembly approach combined with mechanical deformation to produce highly oriented hydrogels composed of chitin and 2D materials such as molybdenum disulfide and brushite **(Figure 16A-B)**. Furthermore, apart from excellent cytocompatibility, the oriented structure's higher modulus led to superior osteogenic differentiation of BMSCs compared to isotropic hydrogels. This was supported by the increased YAP nuclear/cytoplasmic (n/c) ratios, enhanced expression of phosphorylated myosin light chains (pMLCs), upregulated expression of osteoblast-specific transcription factor runt-related transcription factor 2 (RUNX2), significant elevation in alkaline phosphatase (ALP) expression, and enhanced matrix mineralization. Immunofluorescence imaging revealed that BMSCs on the oriented hydrogel exhibited diffused and aligned distribution in the direction of orientation, indicating the guidance provided by the oriented nanofiber structure in the adhesion and migration of BMSCs **(Figure 16C)**. In vivo experiments showcased that the oriented hydrogel facilitated the migration of BMSCs towards the defect area in the rat skull, promoted osteogenic differentiation, and stimulated bone regeneration. Over time, the new bone progressively replaced the hydrogel, resulting in the simultaneous integrated lamellar bone formation and hydrogel degradation.

He et al. [322] developed chitin composite highly oriented hydrogels comprising chitin chains and maleated chitin whiskers (mCHWs) using a dual chemical and physical crosslinking strategy along with a stretch-drying process. Moreover, they employed bioactive desferrioxamine (DFO) functionalization to augment the osteogenic and angiogenic properties of the oriented hydrogels. The release of DFO from hydrogels can chelate with iron ions in cells, and the activity of prolyl hydroxylases (PHDs) and the degradation of hypoxia inducible factor-1α (HIF-1α) by PHDs are inhibited without the assistance of iron ions. Upon reaching a certain threshold, the elevated expression of HIF-1α facilitated the upregulation of vascular endothelial growth factor (VEGF) as well as osteogenic differentiation-related genes (RUNX-2, OCN, OPN, etc.) **(Figure 16D)**. Consequently, this promoted the differentiation of BMSCs into osteoblasts while inhibiting the differentiation of osteoclasts from osteoblastic precursor cells. The highly oriented hydrogel structure facilitates cell adhesion, orientation, and elongation. Combined with its

osteogenic and angiogenic effects, this hydrogel holds significant potential for applications in artificial bone membranes.

Although these findings that highly oriented hydrogels promote osteogenic differentiation and regeneration are exciting, the applications of highly oriented hydrogels in bone tissue engineering still has some shortcomings, such as insufficient mechanical properties and too single biological function. Therefore, to enhance the mechanical properties, such as toughness and strength, of hydrogels, Wang et al. [33] drew inspiration from wood and developed highly oriented composite hydrogels **(Figure 16E-F)**. They achieved this by impregnating sodium alginate hydrogels into delignified wood, followed by in situ mineralization of HAp nanocrystals. The in situ mineralized HAp nanocrystals promoted MC3T3-E1 cell adhesion, spreading, and alignment with cellulose protofibrils, facilitated osteogenic differentiation, and further stimulated bone formation in a rabbit femoral defect model. This composite hydrogel combines an oriented structure, excellent mechanical properties, high water absorption, and osteoconductivity,
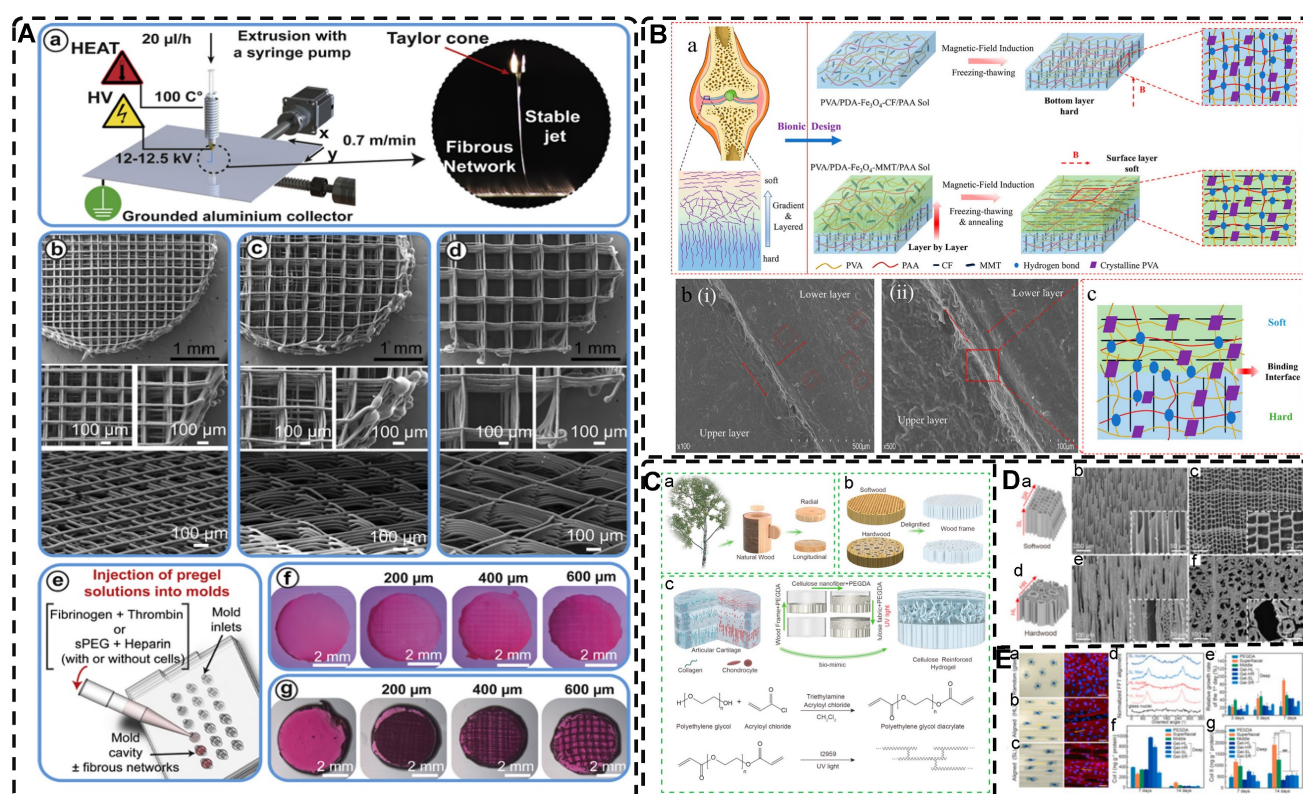
Figure 15. A) (a) Schematic of preparation of highly oriented mPCL fibers. (b-d) Different fiber spacing of the printed fibrous networks. (e) Schematic of preparation of highly oriented hydrogels, and their stereomicroscopy images. Adapted with permission from [245], copyright 2017, IOP Publishing. B) (a) Schematic illustration of the bilayer oriented heterogeneous hydrogel (BH-CF/MMT hydrogel). (b) SEM images of the BH-CF/MMT hydrogel. (c) Schematic illustration of the binding interface of the BH-CF/MMT hydrogel. Adapted with permission from [309], copyright 2022, American Chemical Society. C) (a) Schematic illustrates two types of wood frames that can be cut from a natural tree trunk. (b) The process of delignification. (c) The fabrication process of the bio-inspired three-zone highly oriented composite hydrogel. D) (a, d) Schemes of softwood and hardwood structure. (b, e) Longitudinal direction cross-sectional and (c, f) radial direction cross-sectional SEM images of the softwood and hardwood with aligned channels. E) (a-c) Schemes and cell morphologies of actin filaments and nuclei on the surface of glass slide, HL and SL. (d) 2D-FFT curves of the fluorescent images cultured on different material surfaces. (e-g) BMSCs relative proliferation rate and the relative content of collagen I and collagen II of different zone hydrogels. Adapted with permission from [312], copyright 2020, Elsevier.

offering a promising approach for bone tissue repair. Similarly inspired by wood, Chen et al. [323] infused the delignified wood (white wood, WW) with a porous and highly oriented cellulose fiber skeleton. This scaffold was combined with a PVA hydrogel loaded with curcumin (Cur) and phytic acid (PA) to create a composite hydrogel with a highly oriented structure. The inclusion of Cur and PA in the hydrogel resulted in a synergistic increase in ALP activity and calcium nodule formation in BMSCs. Moreover, it upregulated the expression of OPN, Runx-2, and BMP-2, thereby promoting osteogenic differentiation of BMSCs. The composite oriented hydrogel exhibited a synergistic effect by inhibiting bacterial growth and inflammatory response, promoting osteogenic differentiation, and holds the potential to serve as an artificial bone membrane. As the preparation strategy for highly oriented hydrogels continues to mature, there is a growing belief that the utilization of hydrogels in bone TE will expand in the future.

4.3. Highly Oriented Hydrogels for Tendon Tissue Engineering Applications

Tendons are connective tissues characterized by a high degree of orientation, primarily consisting of collagen and elastin embedded within an extracellular matrix that includes water and proteoglycans, among other components. Tendons play a crucial role in linking skeletal muscle to bone, enabling the transmission of forces generated by muscle contraction for movement and postural maintenance. This unique function and their remarkable mechanical properties, characterized by high tensile strength and resistance to compressive forces, are intricately linked to their structural composition [324]. Tendons possess a hierarchical orientation, wherein highly aligned collagen fibers are enveloped by membranes or sheaths of varying structures, resulting in the formation of microfibrils, subfibrils, fibers, bundles,
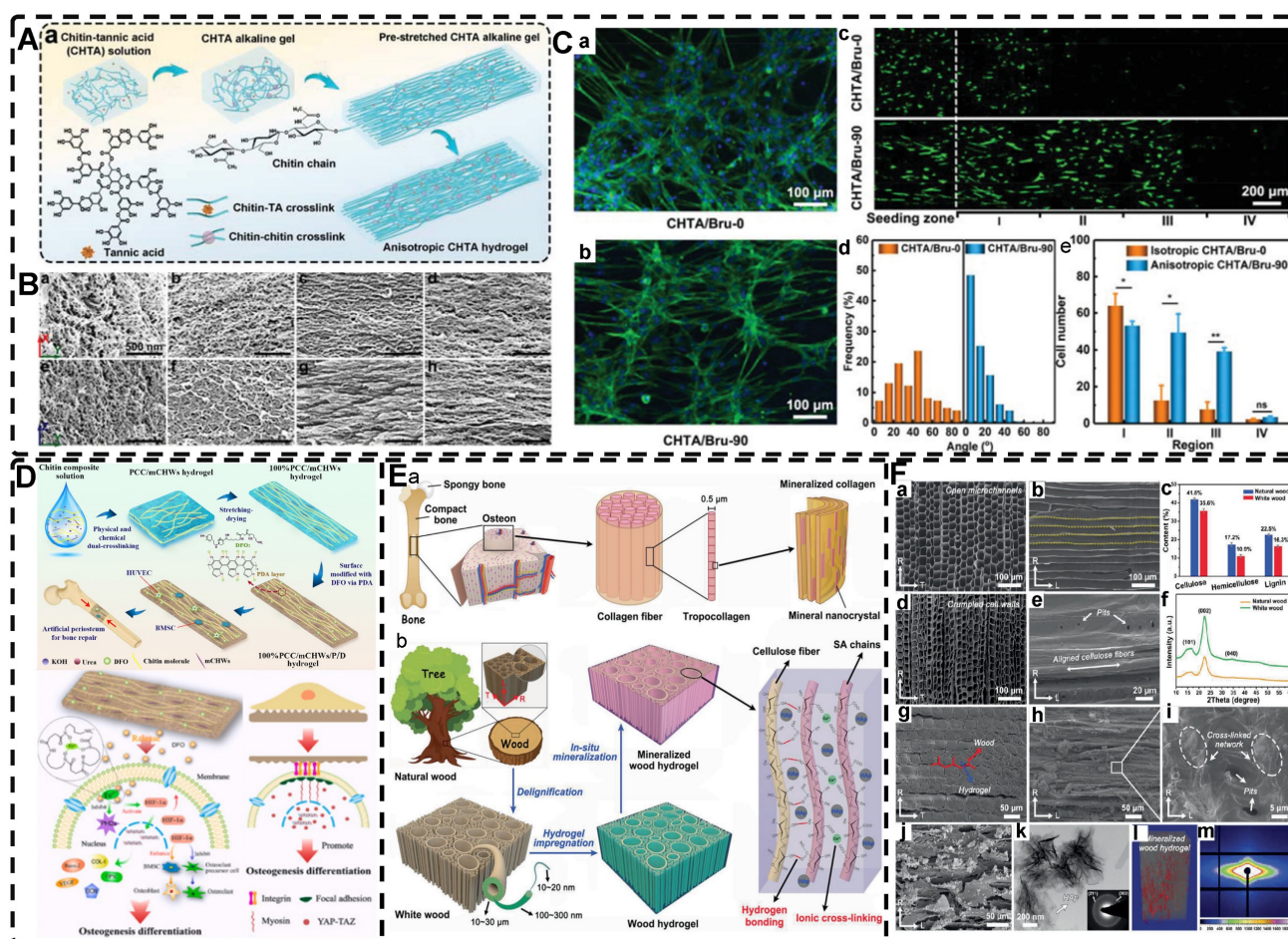
Figure 16. A) Processing principles of the highly oriented chitin–tannic acid hydrogel. B) Field emission SEM images of a,e) CHTA-0; b,f) CHTA-30; c,g) CHTA-60; and d,h) CHTA-90 hydrogels. C) a-c) Fluorescence microscopy images of BMSCs on isotropic CHTA/Bru-0, oriented CHTA/Bru-90 hydrogels and their migration. d, e) Angle distribution histograms and the number of the BMSCs cultured on isotropic CHTA/Bru-0 and anisotropic CHTA/Bru-90 hydrogels. Adapted with permission from [321], copyright 2022, Wiley-VCH. D) The flowchart of the experimental process, and the mechanism diagram of DFO promoting angiogenesis. Adapted with permission from [322], copyright 2022, Elsevier. E) a) Schematic of the hierarchical structure of natural bone. b) Schematic illustration of the fabrication approach and the structure of the MWH. F) a-m) Structural and compositional characterization of highly oriented MWH. Adapted with permission from [33], copyright 2021, Wiley-VCH.

and ultimately multiple bundles arranged in a highly ordered manner, constituting the tendon [325, 326]. The ECM of tendons, along with the layered membranes or sheaths, facilitates the frictionless sliding of these highly oriented fibers, imparting them with distinctive mechanical properties. It is worth noting that the highly oriented structure of tendons, in conjunction with the ECM and the tendon cell population, achieves distinctive mechanical properties, along with viscoelastic and nonlinear elasticity beyond anisotropy [327]. However, these aspects are not extensively discussed within the scope of this paper.

Tendon injuries, known as tendinopathies, significantly impact the lives, occupational activities, and overall well-being of athletes, active individuals, and older adults worldwide. Common examples include rotator cuff injuries and Achilles tendon injuries [328]. Due to the limited cellularity, vascularity, and metabolic activity of tendon tissue, the recovery process after injury is notably inadequate, often resulting in matrix disorders, scar formation, and compromised mechanical properties. Restoring the mechanical properties of the original tendon after healing the damaged tissue is challenging due to two primary reasons: the regenerated tendon may lack native tendon cells, and the composition or arrangement of the ECM differs from that of the natural tendon. Consequently, these factors can result in weakness, pain, adhesions, retears, or even complete tendon rupture [324, 328, 329]. The current conservative and surgical treatments available in clinical practice are limited in their effectiveness [330, 331]. TE presents a promising avenue for achieving comprehensive and effective treatment of tendon injuries, with the incorporation of highly oriented structures providing improved mimicking of native tendon tissue. An illustrative example is the ANF/PVA highly oriented hydrogel developed by Sun et al. [184], which features bundled and curled highly oriented fibers that closely resemble the natural tendon's structure. Notably, when subjected to 80% elongation during stretching, the hydrogel demonstrated an impressive elastic modulus of 1.1 GPa and a strength of 72.1 MPa, effectively matching those of natural tendons. Kim et al. [177] successfully developed alginate and polyacrylamide double-network (DN) hydrogels incorporated with silica microrod inorganic fillers. These hydrogels exhibited excellent mechanical properties and featured a highly oriented anisotropic structure reminiscent of natural tendons. The hydrogel holds promising potential for application in artificial tendon engineering. However, a comprehensive evaluation of the composite's biological behavior necessitates cell encapsulation.

Furthermore, highly oriented structures, such as electrostatically spun nanomicrofiber scaffolds, can serve as valuable cues for directing cell differentiation towards tendon formation [27]. However, these scaffolds are deficient in an ECM-like 3D environment, which can be effectively supplemented by hydrogels. Liu et al. [30] employed Flight biomanufacturing technology to prepare highly oriented microfilament hydrogels, which facilitated the oriented alignment of human tenocytes (HTs). After two weeks of co-culture with the highly oriented hydrogel, HTs exhibited a remarkable presence of highly aligned filamentous actin (F-actin) **(Figure 13C)**. Furthermore, immunofluorescence analysis revealed that the highly oriented microfilaments effectively guided the oriented deposition of cells and ECM, as evidenced by the expression of type I collagen. Rinoldi et al. [332] successfully fabricated 3D oriented cell-laden hydrogel yarns using the wet-spinning technique, which closely mimic the structural characteristics of natural tendon bundles **(Figure 17A)**. The highly oriented structure, combined with mechanical stimulation through stretch and biochemical stimulation via the growth factor BMP-12, effectively facilitated hBM-MSC attachment, spreading, elongation, and oriented alignment, resulting in the formation of dense and highly oriented 3D cell constructs **(Figure 17B)**. Moreover, this approach holds the potential to promote collagen orientation and deposition, ultimately leading to the development of an oriented matrix. Furthermore, the observed significant expression of tendon-related genes, such as scleraxis (SCX), tenomodulin (TNMD), collagen I, and collagen III, strongly suggested the successful tengenic differentiation of hBM-MSCs, thus highlighting the potential of this method for tendon TE. Park et al. [190] employed the gel GAE method to efficiently densify and remodel collagen, yielding a highly oriented aligned dense collagen (ADC) system **(Figure 17E)**. The casting solution removal enhances collagen fiber density (CFD) or collagen content, while the applied pressure difference facilitates the orientation and alignment of the resulting hydrogel. Short-term, high-strain mechanical stimulation of highly oriented ADC hydrogels significantly enhanced the expression of tendon-related genes, including Tenascin-C and tenomodulin **(Figure 17F)**. This stimulation led to substantial remodeling of the matrix, resulting in the formation of a mature tendon-like matrix. These findings exemplify the significant potential for employing highly oriented ADC hydrogels in conjunction with mechanical stimulation for tendon TE.
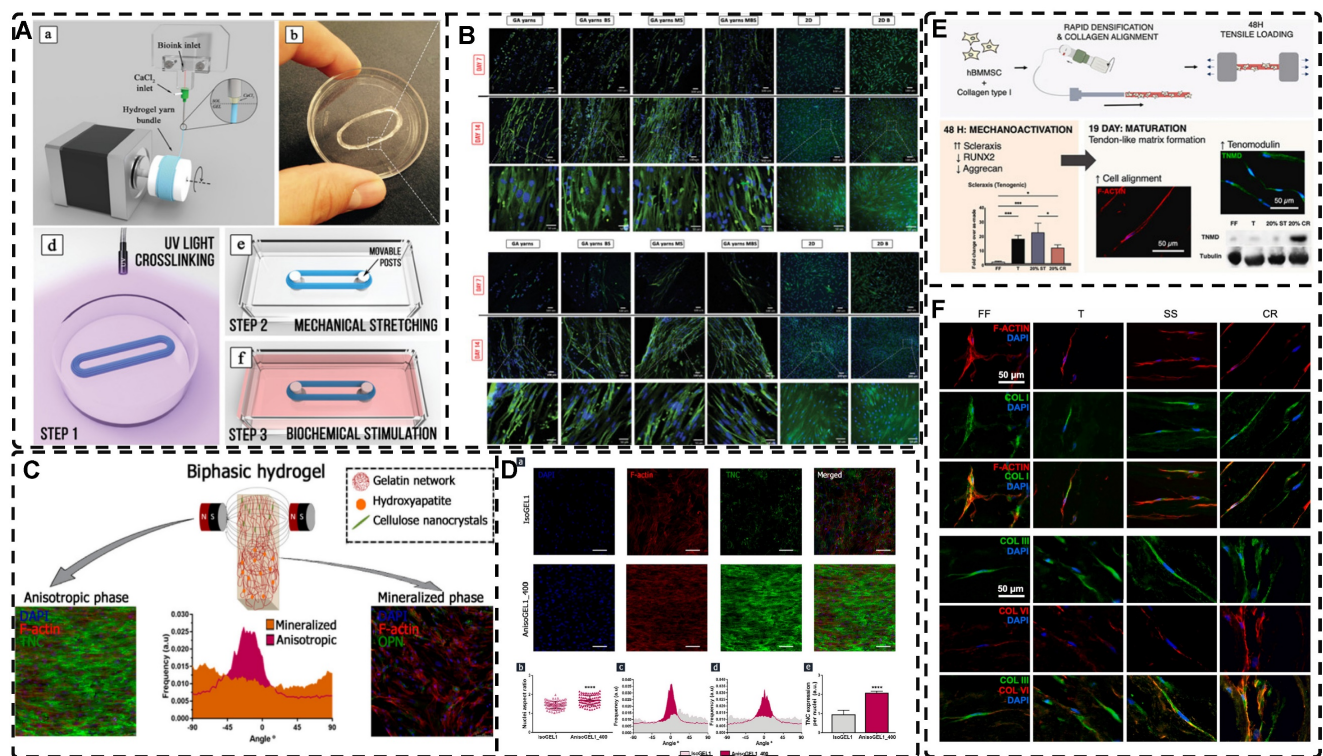
Figure 17. A) a-f) Schematic of biofabrication and stimulation of 3D oriented cell-laden hydrogel yarns using the wet-spinning technique. B). Collagen I expressed by hBM-MSCs encapsulated into different hydrogels. Adapted with permission from [332], copyright 2019, Wiley-VCH. C) Schematic of biofabrication of cellulose nanocrystals (CNC) and hydroxyapatite (HA) oriented and aligned under a magnetic field. D) a-f) The nuclei aspect ratio, directionality of cell distribution, and tendon-related ECM protein TNC secretion were assessed by confocal immunofluorescence. Adapted with permission from [31], copyright 2019, American Chemical Society. E) Schematic of biofabrication of highly oriented ADC hydrogel scaffolds and the ability to tenogenic differentiation. F) Cellular morphology and collagen formation of hBM-MSC-seeded ADCs of 20% static strain (SS) and 20% cyclic rest (CR) and their controls, free-floating (FF) and tethered (T). Adapted with permission from [190], copyright 2022, Elsevier.

Tendon-to-bone integration, also known as the point of attachment called enthesis, is another characteristic of tendons. The enthesis comprises four distinct zones with remarkable adhesive and mechanical properties: pure dense fibrous connective tissue, uncalcified fibrocartilage, calcified fibrocartilage, and bone [333, 334]. Currently, TE approaches for the tendon-bone interface predominantly focus on fibrous scaffold development [335-338]. Kim et al. [180] developed a triple-network hydrogel comprising imidazole-containing polyaspartamide and an energy-dissipative alginate–polyacrylamide double-network. This hydrogel demonstrated an exceptional tensile modulus (3.0 MPa) and strength (0.8 MPa), as well as strong adhesion to bone (2.73 kJ m^{-2} and 725 kPa), effectively mimicking the native tendon-to-bone attachment interface. Furthermore, the hydrogel's excellent biocompatibility suggests its considerable potential for advancing TE research and fostering future developments in the field. Hierarchically highly oriented hydrogels were prepared by Echave et al. [31] through the incorporation of CNCs and HAp into gelatin networks that were oriented and aligned under a magnetic field **(Figure 17C)**. During the tendon-mimicking phase, hASCs encapsulated within highly oriented hydrogels exhibited a spindle-shaped morphology characterized by elongated nucleus length diameter, aligned cytoskeleton, and enhanced expression of the tendon-associated ECM protein TNC **(Figure 17D)**. These observations indicate the potential of the hydrogels to effectively mimic tendon tissue when compared to the isotropic system. During the bone-like phase, the inclusion of HA particles in the hydrogel enhanced its rigidity and promoted the differentiation of hASCs toward the osteogenic lineage. This differentiation process resulted in an upregulation of bone markers, including the bone bridge protein OPN. The hierarchical structure of these hydrogels closely mimicked the composition, structure, and cellular organization found in natural tendon-bone attachment sites, thereby offering significant potential for various applications.

4.4. Highly Oriented Hydrogels for Skeletal Muscle Tissue Engineering Applications

Skeletal muscle constitutes approximately 45% of the total body weight and serves crucial functions such as protecting and supporting internal organs, facilitating body movement, and regulating body temperature and basal energy metabolism [339]. Skeletal muscle comprises numerous myofibrils, the

fundamental functional units of muscle fibers. These myofibrils are arranged in series, giving rise to highly oriented myogenic fibers that are tightly packed within the endomysium. Subsequently, these myofibrils are enveloped by fascicles, which form bundles, and ultimately, the bundles are encased by the epimysium, thereby forming the muscle tissue [340, 341]. The oriented structure of skeletal muscle contributes to its notable mechanical strength along the direction of fiber accumulation and high elasticity coefficient in the direction of alignment, thereby ensuring stability during a wide range of postures and movements [38, 40].

Skeletal muscle possesses intrinsic regenerative capabilities to repair minor injuries. However, its capacity to heal is hindered when the damage or loss exceeds a critical threshold, resulting in scar tissue formation and functional impairments, such as volumetric muscle loss following trauma or surgical interventions [342-344]. Surgical transplantation of autologous healthy muscle tissue/flaps is a commonly employed strategy to mitigate scar tissue formation and preserve functionality. However, this approach is associated with limitations, including inadequate availability of donor tissue, compromised donor function, and heightened morbidity at the donor site [341, 345]. Muscle TE has emerged as a means to replace damaged or absent muscle tissue, aiming to facilitate tissue regeneration and restore functional capacity in areas affected by muscle deficiency. Bionic materials with high orientation offer a promising approach as they guide the alignment of muscle cells and facilitate myoblast regeneration, resulting in the formation of densely packed muscle fibers that align closely with aesthetic requirements [40, 346]. Additionally, these materials promote tissue regeneration and functional recovery. Highly oriented hydrogels play a crucial role in muscle TE and have garnered considerable attention in current research endeavors. A graphene–polysaccharide nanocomposite hydrogel film, meticulously designed by Patel et al. [170], exhibited a highly oriented structure and elicited an initial alignment of mouse myoblast cells (C2C12) upon inoculation. Furthermore, the hydrogel promotes the differentiation of these cells into multinucleated myotubes. Highly oriented MSNF/GelMA hydrogels, as developed by Wang et al. [29], demonstrated superior capability in promoting the elongation and alignment of C2C12 cells when compared to random MSNF/GelMA and pure GelMA hydrogels **(Figure 4H, Figure 18A)**. This effect can be attributed to the affinity of the cells for the MSNF, leading to their alignment and elongation along the highly oriented

structure of the hydrogel **(Figure 18B)**. Furthermore, mice treated with the highly oriented MSNF/GelMA hydrogel exhibited an increased number of longer myotubes formed by fused C2C12 cells compared to mice in other groups. This observation highlighted the capacity of the highly oriented MSNF structure within the hydrogel to enhance the three-dimensional myogenic differentiation of C2C12 cells. Additionally, mouse satellite cells encapsulated within the highly oriented hydrogel group demonstrated spontaneous beating and synchronous contraction, aligning with the highly oriented direction of the MSNF. This observation further supports the notion that highly oriented structural hydrogels hold significant promise as a TE strategy for skeletal muscle regeneration. Liu et al. prepared highly oriented microfilament hydrogels using Flight biomanufacturing technology, in which C2C12 myofibroblasts were encapsulated. The fusion of myofibroblasts and alignment of myotubes in these hydrogels were observed through immunofluorescence staining, using anti-mouse myosin heavy chain (MyHC) antibody and ghost pen cyclic peptide **(Figure 13C)** [30]. The highly oriented microfilament hydrogels exhibited a remarkable contrast to bulk hydrogels, with 95% of myotubes aligning parallel to the microfilaments, and over 76% of myotubes containing more than six nuclei per myotube, a feature absent in bulk hydrogels. These findings highlight the potential of highly oriented microfilament hydrogels in muscle TE and their role in advancing the biofabrication of muscle tissue-engineered constructs. Highly oriented aligned hydrogels containing polydopamine-Fe_3O_4-CNTs were prepared by Liu et al. [85] to mimic muscle tissue **(Figure 18C)**. These highly oriented hydrogels exhibited superior orientation conductivity and mechanical properties compared to randomly aligned hydrogels, and when combined with oriented electrical stimulation, they promoted the directed growth and elongation of C2C12 mouse myogenic cells, as evidenced by immunofluorescent staining of the cell adhesion protein Vinculin (green) **(Figure 18D)**. Furthermore, the highly oriented hydrogel, when subjected to electrical stimulation, exhibited cortical and homogeneous cytosolic staining of oriented vinculin, along with ellipsoidal cell nuclei and the formation of clustered cell protrusions at the cell periphery. These observations confirmed that the highly oriented hydrogel, in synergy with electrical stimulation, effectively guided the directional growth of C2C12 cells. These studies provide compelling evidence for the potential applications of highly oriented hydrogels in skeletal muscle TE.
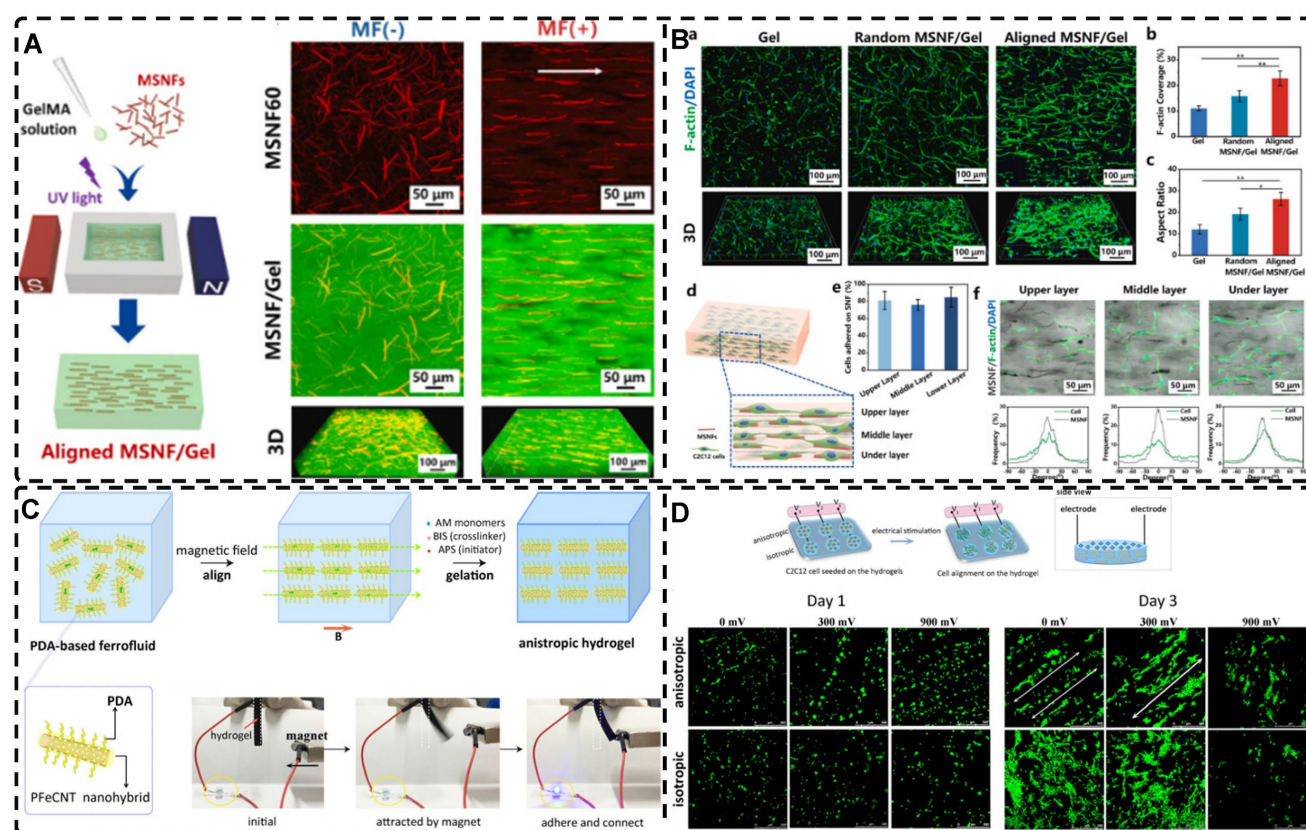
Figure 18. A) Schematic illustration of the fabrication of aligned MSNF/Gel scaffold in situ under magnetic field, and the fluorescence images showed that MSNF was oriented encapsulated within GelMA hydrogels. B) (a-c) Cytoskeleton morphology of C2C12 cells encapsulated within Gel, random MSNF/Gel scaffold and oriented MSNF/Gel scaffold after culturing for 3 days, and their F-actin coverage and aspect ratio. (d-f) C2C12 cells adhered to MSNFs and showed oriented aligned morphology in each layer within the aligned MSNF/Gel scaffold. Adapted with permission from [29], copyright 2022, Elsevier. C) Schematics of preparation of an anisotropic hydrogel based on a mussel-inspired conductive ferrofluid. D) Schematic representation of C2C12 cells seeded on the hydrogels and cells being electrically stimulated under different voltages, and CLSM micrographs of C2C12 cells on the anisotropic and isotropic hydrogels after 1 and 3 days of culturing under different electrical stimulation voltages. Adapted with permission from [85], copyright 2019, American Chemical Society.

4.5. Highly Oriented Hydrogels for Cardiac Muscle Tissue Engineering Applications

Cardiovascular disease is the leading cause of global mortality, resulting in approximately 18.6 million deaths in 2019, marking a 17.1% increase since 2010 [347]. Notably, myocardial infarction or ischemic heart disease stands out as the primary contributor to the elevated morbidity and mortality associated with cardiovascular diseases. During this pathological process, there is a significant reduction in blood supply to the infarcted area, leading to the demise of myocardial cells. Presently, available therapeutic and preventive strategies encompass pharmaceutical interventions involving catecholamines, angiotensin, aldosterone, surgical interventions, and the implantation of pacemaker devices. However, given their limited effectiveness in halting disease progression, heart transplantation stands as the definitive treatment option [348]. In light of the challenges posed by immunosuppression and the scarcity of cardiac donors, the development of artificial cardiac tissue-engineered hydrogels, stents, and patches has gained substantial attention over the last twenty years [349, 350].

The cardiac muscle is composed of numerous highly oriented cardiomyocytes, each containing an abundance of myofibrils aligned parallel to the long axis of the cells [13]. Consequently, the development of cardiac TE necessitates highly oriented manufacturing strategies capable of emulating the natural myocardial structure and facilitating the elongated morphology and functionality of the cells [351-355]. Wang et al. [153] fabricated highly oriented PPy nanocomposite hydrogels through mechanical stretching, inducing a cardiomyocyte alignment resembling that of the natural myocardium, along with an elongated cell morphology **(Figure 6D)**. The hydrogels exhibited excellent electrical conductivity and enabled stable and directional transmission of electrical signals, potentially reducing the occurrence of myocardial infarction. Ye et al. [35] developed nanoscale highly oriented cellulose hydrogels through pre-stretching and leveraging of cellulose's inherent robust self-aggregation forces within an alkali/urea aqueous solution **(Figure 11C)**. The subsequent acid treatment and release of the pre-stretched highly oriented hydrogels in a dilute

acid solution resulted in the formation of microgroove-like structures that promoted the alignment and adhesion of neonatal rat ventricular myocytes (NRVM) along the orientation of the stretch force. Furthermore, the cultured NRVM exhibited enhanced mitochondrial content, well-defined myonodular structures, and spontaneous beating. Navaei et al. [356] synthesized gold nanorods (GNRs) and GelMA hydrogel with surface-concave microgrooves with a width and depth of 50 µm, using PDMS molds to emulate the electrical functionality and histomorphology of natural cardiac muscle **(Figure 19A)**. Compared with pure GelMA hydrogels, the F-Actin-stained images and data on the area of fluorescence demonstrated the development of uniformly dense and highly aligned cardiac tissue in GelMA-GNR hydrogels **(Figure 19B-C)**. Neonatal rat cardiomyocytes cultured on both hydrogels for 4-7 days displayed spontaneous contractility. However, only the cardiac tissue formed on the electrically conductive GelMA-GNR hydrogels exhibited responsiveness to external stimuli at various frequencies (0.5, 1, and 2 Hz) at low voltages **(Figure 19D)**. These findings highlight the potential of the microgroove GelMA-GNR hydrogel for constructing natural cardiac tissue with the capability to function as a cardiac patch after myocardial infarction.

The establishment of vascularized myocardial tissue is important for the exchange of nutrients and oxygen with cardiomyocytes, and poses a significant challenge for TE. Mehrotrad et al. [357] presented a novel silk-based biomaterial ink for fabricating well-aligned cardiac structures with favorable elasticity and stiffness (≈40 kPa). The anisotropic hydrogel scaffold, fabricated using the double cross-linking method, facilitated the organization of aligned sarcomeres, promoted the upregulation of gap junction proteins like connexin-43, and sustained the coordinated contraction of cardiomyocytes. Furthermore, they endeavored to generate vascularized myocardial tissue by encapsulating human, induced pluripotent stem cell-derived cardiac spheroids (hiPSC-CSs) in silk-based inks for viability. They employed embedded bioprinting techniques to create perfusable and well-aligned vascular channels. The endothelial cells enclosed within the bioink of these aligned channels could gradually migrate toward the channel edges, establishing an endothelial vascular network. As the culture matured, the vascularized myocardial tissue exhibited maturity-
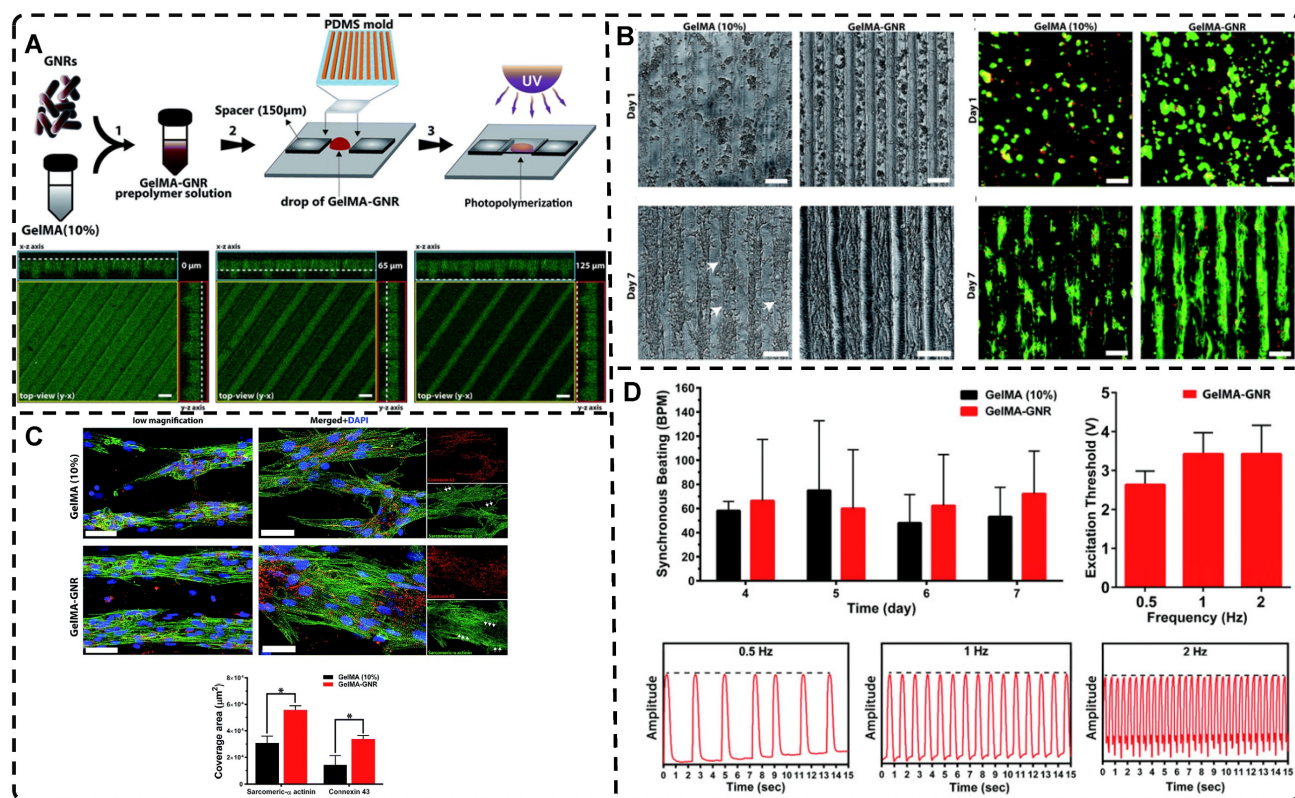
Figure 19. A) Schematic illustration of the fabrication procedure of GelMA–GNR microgrooved tissues, and z-Stack images showing the 3D structure of the microgrooved patterns. B) Phase-contrast images of cardiac cells seeded on GelMA and GelMA–GNR microgrooved hydrogel, and fluorescent viability images of GelMA and GelMA–GNR microgrooved cardiac tissues on day 1 and day 7 of culture. C) Immunostained images of SATN (green) and Cx43 gap junctions (red) within GelMA and GelMA–GNR microgrooved cardiac tissues on day 7 of culture, and quantified area coverage of cardiac specific markers on day 7. D) Synchronous spontaneous beating behavior (beats per minute; BPM) of cardiac tissues on GelMA and GelMA–GNR constructs, voltage excitation thresholds, and extracted beating signals of GelMA–GNR cardiac tissue at different frequencies. Adapted with permission from [356], copyright 2017, Royal Society of Chemistry.

dependent protein expression in both cardiomyocytes and human umbilical vein endothelial cells (HUVECs). Establishing vascularized in vitro tissues is an important step in advancing TE, and this approach warrants continued investigation and refinement.

The above study was performed on a single directionally oriented hydrogel applied to cardiac TE, whereas the actual native cardiac tissue showed a multilayered, oriented arrangement and a gradual transition in the orientation of the arrangement between the layers of the myocardium [358, 359]. Therefore, a design of highly oriented hydrogels with distinct orientations between layers would offer greater potential for mimicking the structure of natural myocardial tissue. Wu et al. [246] prepared a GelMA hydrogel incorporating a highly oriented NFYs-NET structure, effectively emulating the architecture of the native heart **(Figure 14A)**. The presence of NFYs-NET within the hydrogel scaffold facilitated cellular alignment, elongation, and promoted the maturation and functionality of CMs **(Figure 14B-C)**. Simultaneously, the hydrogel provided a three-dimensional environment that supported nutrient exchange and offered mechanical protection. The incorporation of layered NFYs-NET structures within the GelMA hydrogel enabled the creation of a biomimetic multilayer orientation akin to the native heart **(Figure 14D)**; each layer's orientation independently influenced the arrangement of cells, closely resembling the multiple cell layers found in natural cardiac tissue. Moreover, a hybridization approach was employed to construct endothelialized myocardium by co-culturing cardiomyocytes on the NFYs-NET layer and encapsulating endothelial cells within hydrogels **(Figure 14E)**. These findings underscore the significant potential for developing and applying this three-dimensional, highly oriented hydrogel scaffold in cardiac TE.

4.6. Highly Oriented Hydrogels for Nerve Tissue Engineering Applications

Nervous tissue plays a crucial role in transmitting information and signals within the body. It is divided into two main components: the central nervous system (CNS) and the peripheral nervous system (PNS) [360]. The PNS facilitates the transmission of information and signals between the CNS and the body via its extensive network of neurons, whereas the CNS processes and coordinates these signals [361]. Neurons, which are the fundamental structural and functional units of the nervous system, consist of a cell body, highly branched dendrites that extend from the cell body, and a single axon per neuron. Dendrites receive impulses from the axons of other neurons and relay them to the cell body, which in turn transmits these impulses in a unidirectional manner through its axon to other neurons, ensuring the directionality of nerve impulses [362]. Anatomically, nerve tissue exhibits a hierarchical organization, with nerve fibers arranged and oriented to form fiber bundles. Nerve fibers possess distinctive features, such as a nano-oriented fibrous ECM and a core-shell structure composed of a tubular myelin sheath that envelops elongated axons [14]. These structural attributes contribute to the pronounced orientation observed in neural organization.

4.6.1. Peripheral Nerve

The PNS possesses inherent regenerative capabilities but faces challenges in self-healing when the defect length exceeds 5 mm, and becomes incapable of self-healing beyond 10 mm [363-365]. Short-gap injuries are typically treated with direct clinical suturing, which is considered the gold standard approach [366]. Conversely, repair of long-gap peripheral nerve injuries (PNI) often requires autografts [365]. Nonetheless, autografts are beset by limitations, including size mismatch, limited availability of suitable donor tissue, the need for secondary surgical procedures, and permanent damage to the donor site. Neural TE aims to facilitate nerve regeneration through the development of tissue-engineered bioactive nerve substitutes, which then serve as optimal scaffolds or channels for axonal regeneration, leading to the reconstruction of nerve circuits and restoration of tissue function [367-369]. Several scaffolds have received FDA approval, substantiating the potential of these alternatives in PNI repair [370, 371]. Natural neural tissue exhibits a low elastic modulus, typically below 1 kPa, and hydrogels can serve as effective mimics of this mechanical property [372]. Particular attention should be given to the fabrication of biomimetic neural tissue using hydrogels as the primary framework. Incorporating highly oriented structures into these hydrogels can provide biophysical and biological cues that promote and guide the growth of neural tissues, facilitating the reconstruction of neural circuits. Babu et al. [373] developed oriented hydrogels by incorporating a low concentration of SPION (400 µg/ml) microgel into synthetic polyethylene glycol hydrogels, aligning them using low magnetic fields (≈100 mT). The hydrogel facilitated axonal growth and orientation during in vitro culture. However, the microgel's ability to direct cells in an oriented manner was compromised by the presence of local cell binding sites on the microgel. Intriguingly, coupling the microgel covalently to a matrix PEG hydrogel

resulted in diminished orientation and growth of neuronal cells. This effect may be attributed to the modification of anisotropic force transmission due to covalent coupling, thereby attenuating the influence of mechanical signals that facilitate directional cell growth. Ghaderinejad et al. [374] fabricated magnetic hydrogels filled with short fibers oriented using unidirectional freeze-drying in a sodium alginate matrix. Olfactory ecto-mesenchymal stem cells (OE-MSCs) cultured in highly oriented hydrogels demonstrated significantly improved proliferation rates and a more elongated and flattened morphology compared to those cultured on pure hydrogels. Moreover, the heightened expression of mature neuronal markers β-tubulin III and Glial fibrillary acidic protein (GFAP) confirmed the neural differentiation of OE-MSCs. Lu et al. [375] fabricated micro-nano hierarchical hydrogels with aligned orientation as fillers for nerve conduits subjected to electric field treatment. Oriented aligned filled nerve conduits (ASFN), in comparison to randomly oriented filled nerve conduits (RSFN), effectively guided the orientation of Schwann cells and exhibited enhanced cell proliferation. Additionally, the axons of PC12 cells exhibited elongation and alignment along the oriented structure to a greater extent. Upon implantation in a rat sciatic nerve defect model, ASFN demonstrated comparable outcomes to autografted nerves, outperforming RSFN and unfilled nerve conduits, highlighting it as a viable alternative for bionic nerve tissue. Chen et al. [14] utilized a microfluidic system to fabricate core-shell structured biomimetic tubular hydrogels with an oriented ECM **(Figure 20A)**. The highly oriented hydrogels facilitated the elongation and oriented alignment of PC12 cells and RT4-D6P2T cells, i.e., myelinating Schwann cells, to a greater extent compared to a bulk composite hydrogel with random orientation **(Figure 20B)**. They effectively guided the orientation and extension of neurons while enhancing the elongation alignment of neurons and the maturation of myelin sheaths in Schwann cells. The core-shell structure of the biomimetic tubular hydrogel constructs, comprised of nano-oriented fiber ECM, core elongated neurons, and shell myelinating Schwann cells resembling tubular myelin sheaths, showcases the successful fabrication of bionic nerve fibers with significant potential in neuroregenerative TE.
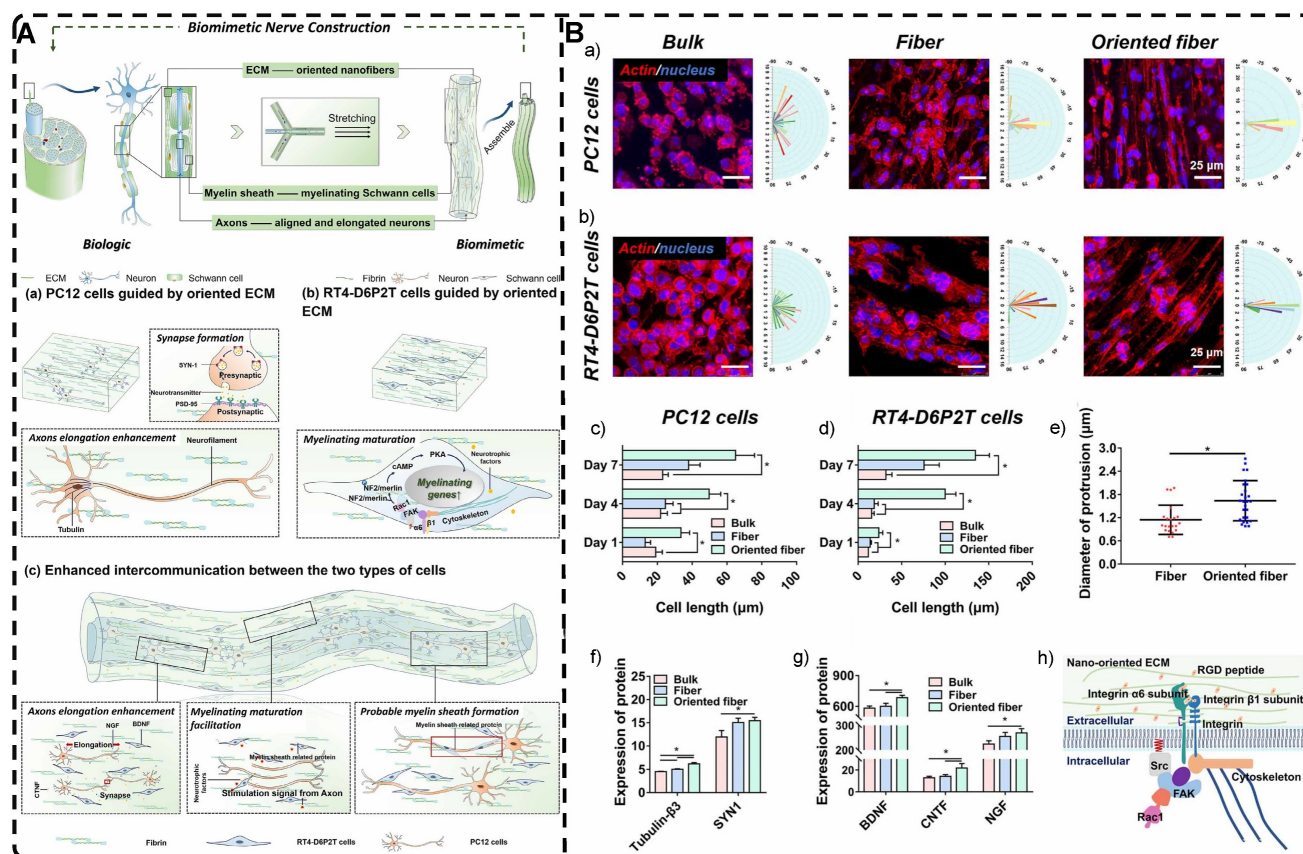
Figure 20. A) Schematic illustration of constructing biomimetic nerve fibers and their neural performances. (a) PC12 cells guided by oriented ECM; (b) RT4-D6P2T cells guided by oriented ECM; (c) Enhanced intercommunication between the two types of cells. B) (a, b) Morphology of PC12 and RT4-D6P2T cells cultured for 7 d. (c, d) Histograms of PC12 and RT4-D6P2T cells length. (e) Axons diameters of PC12 cells counted from immunofluorescence images marked by Tubulin-*β3*. (f, g) Elisa assays of Tubulin-*β3* and SYN1 expressed by PC12 cells and neurotrophic factors including BDNF, CNTF and NGF expressed by RT4-D6P2T cells. (h) Schematic illustration of possible extracellular topographic signaling transduction mechanism. Adapted with permission from [14], copyright 2020, IOP Publishing.

4.6.2. Spinal Cord

Spinal cord injury (SCI) initiates a complex, multifactorial cascade of responses, wherein primary injury, such as neuronal and glial cell death and vascular rupture, is typically succeeded by secondary injury, including secondary ischemia, edema, hypoxia, inflammatory response, and calcium overload [376]. In response, the body employs inherent protective mechanisms, such as the formation of a glial scar, to prevent further harm [377]. However, the glial scar ECM contains inhibitors of axonal growth, such as chondroitin sulfate and proteoglycan, which hinder neuronal regeneration and significantly impede the restoration of neurogenic function in SCI [377]. Clinical interventions, including medication and decompression surgery, primarily focus on safeguarding the spinal cord against further damage, yet they yield limited gains in terms of functional recovery in the reconstructed spinal cord [378, 379]. The implantation of tissue-engineered scaffolds, which can induce cellular targeting and promote spinal cord regeneration, is a burgeoning area of research, with highly oriented hydrogels assuming a crucial role [380]. For instance, Kim et al. [381] utilized microfluidic technology to encapsulate astrocytes in alginate hydrogel incorporated with the tripeptide arg-gly-asp (RGD), thus producing oriented micron-scale hydrogel fibers **(Figure 21A)**. Their experimental findings indicated that hydrogel microfibers loaded with astrocytes expedite neurite outgrowth and guide neurite elongation directionality during the early stages **(Figure 21B)**. Furthermore, they facilitate synapse formation and the establishment of well-organized neural circuits during later stages of development. Despite the relatively low viability of the encapsulated astrocytes, this method holds potential for further exploration in neural TE. Chen et al. [382] developed a stretchable and adherent, highly oriented hydrogel through electrostatic spinning and in situ sequential cross-linking. This hydrogel exhibited the ability to achieve spatiotemporal delivery of stromal cell-derived factor-1α (SDF1α) and paclitaxel while being orientation-aligned with collagen fibronectin. In vitro and in vivo experiments revealed that the oriented hydrogels stimulated the migration of exogenous or endogenous neural stem/progenitor cells (NSPCs) to intermediate/lesion sites and facilitated their neuronal differentiation. Ultimately, this process led to the reconstruction of neural networks and the restoration of function. Gao et al. [383] developed a silk fibroin nanofiber hydrogel with a hierarchically oriented microstructure and incorporated nerve growth factor (NGF), which enabled the scarless repair of the spinal cord in a rat model of spinal cord hemisection. This NGF-enriched oriented hydrogel improved Schwann cell alignment and spreading, and also enhanced axonal growth and length in PC12 cells, highlighting its ability to stimulate nerve cell proliferation, alignment, spreading, and migration. When implanted in a rat spinal cord hemisection model, the hydrogel promoted migration and differentiation of neural stem cells (NSCs) and stimulated angiogenesis, leading to scar-free regeneration of the spinal cord and functional recovery comparable to that of the intact spinal cord. This approach, combining biological and physical cues for tissue regeneration, demonstrates the feasibility of utilizing multiple cues to construct bionic neural tissue. Chen et al. [28] fabricated biomimetic oriented hydrogels with nano-alignment and viscoelastic properties using a static-dynamic strategy and microfluidic techniques **(Figure 21C)**. In vitro, the oriented hydrogel effectively guided the orientation of neuronal cells (PC12), while the nano-alignment and viscoelasticity positively influenced neuronal polarization and axonal elongation **(Figure 21D)**. Moreover, the combined influence of the nano-oriented structure and viscoelasticity resulted in enhanced neural differentiation, as evidenced by a significant upregulation of neurogenic genes, while no enhancement in glial differentiation of BMSCs was observed. In a SD rat spinal cord hemisection model, the implantation of the oriented hydrogel graft promoted neuronal differentiation and facilitated functional axon regeneration, while inhibiting cystic and glial formation, ultimately, positively impacting the functional recovery following spinal cord injury. The combination of orientation and viscoelasticity in this hydrogel serves as a valuable reference for the development of neural grafts with multiple guidance cues, significantly contributing to the field of neural TE.

4.6.3. Brain

The brain is the most intricate and sophisticated component of the nervous system, and brain injuries often result in enduring neurological impairments [384, 385] due to the limited regenerative capacity of brain tissue and the lack of sufficient nerve growth factors [386]. While numerous therapeutic approaches have been investigated in laboratory settings, current clinical treatments struggle to rebuild brain structures and restore their functions effectively [387]. The potential of aligned oriented in TE for brain injury repair has received limited attention, possibly due to the subtle nature of structural alignments in the brain at the tissue level. At the cellular level, cortical tissue

does exhibit spatially oriented aligned structures, such as neurons with elongated axons capable of unidirectional pulse signaling and radial glial (RG) cells that extend aligned fibers from the soma to the meninges [388, 389]. Hence, the utilization of highly oriented hydrogels that replicate the structural orientation found in natural tissues holds significant value in brain TE investigations. Chai et al. [390] implanted electrostatically spun and molecularly self-assembled highly oriented fibronectin hydrogels into the subventricular zones (SVZ) to facilitate the migration of endogenous NSCs towards the lesioned area, aiming to replicate the orientation and functionality of natural RG fibers. In vitro experiments demonstrated that the cytoskeleton of NSCs elongated along the long axis of the oriented hydrogel, resulting in oriented and extended axons. When implanted into a rat brain injury model, this hydrogel led to the development of regenerated tissue with an oriented morphology, unlike the results with randomly oriented hydrogel. Additionally, the implantation facilitated the differentiation and maturation of NSCs and the recovery of neurological function following brain injury in rats. RNA transcriptome analysis conducted on regenerated tissues 14 days after the operation revealed upregulation of neurogenic transcripts, including Sema3A and Sema6A, which are linked to neuronal migration, as well as Plexin2, Plxna4, and Plxnb4, associated with axonogenesis. Moreover, the oriented hydrogel facilitates neural regeneration by engaging multiple signaling pathways, including those of Notch, Wnt, axon guidance, MAPK, and neurotrophin. This study highlights the clinical translation potential of the oriented hydrogel in brain TE, while also offering novel insights for future investigations into highly oriented hydrogels for the repair of brain injuries.
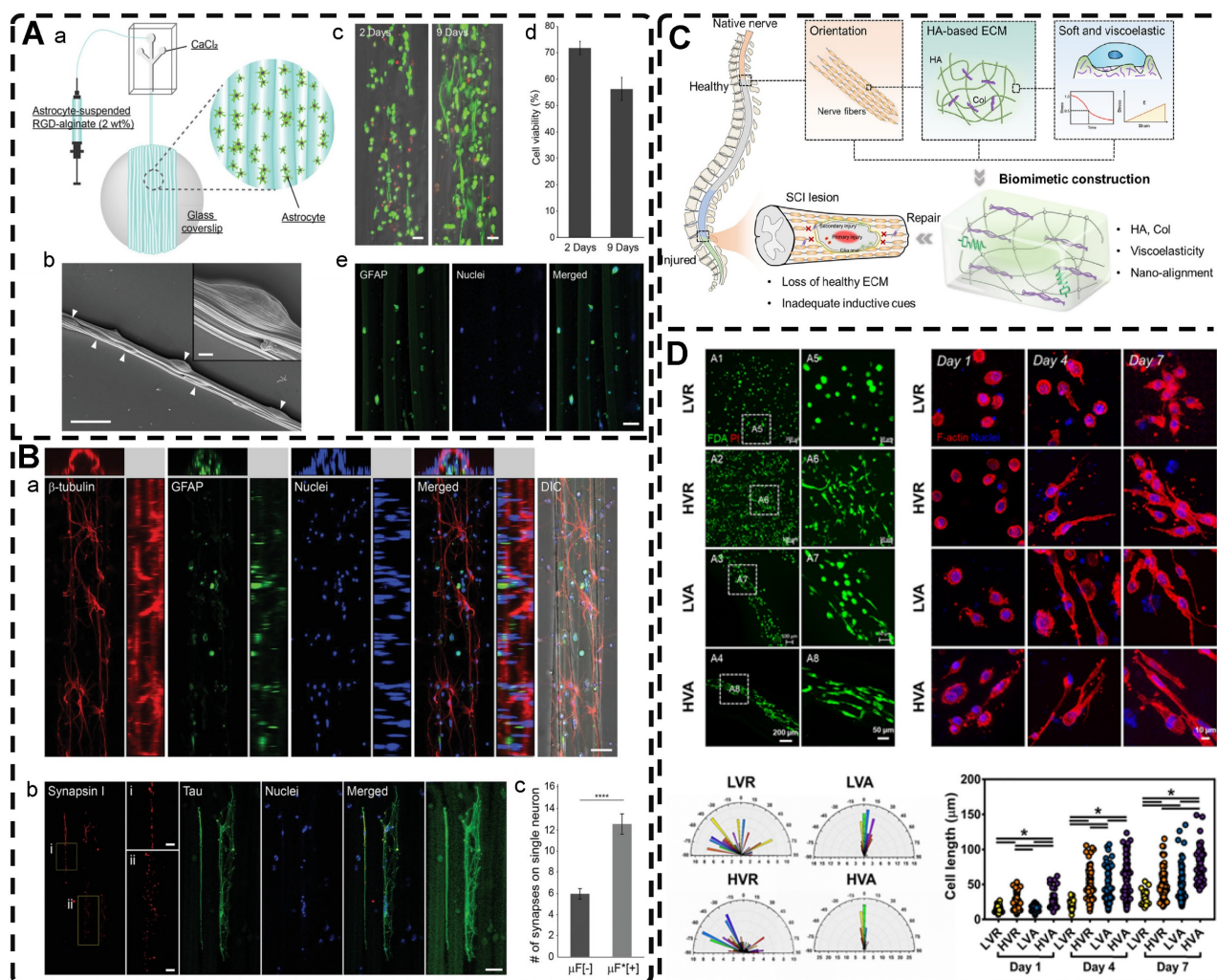
Figure 21. A) a) Schematic illustration for astrocyte-laden microfibers. b) SEM image of astrocyte-laden microfibers after drying and dehydrating. c) CLSM images of astrocytes encapsulated in the fibers. d) Viabilities of astrocytes encapsulated in the fibers on 2 and 9 days after fabrication. e) CLSM images of astrocytes stained for GFAP and nucleus on 9 days after fabrication. B) a, b) Maximum-intensity-projected CLSM z-stack images of hippocampal neurons on astrocyte-laden microfibers. c) Number of presynapses of a single hippocampal neuron. Adapted with permission from [381], copyright 2022, Wiley-VCH. C) Schematic illustration for biomimetic construction of HA/Col hydrogel incorporated with viscoelasticity and nano-alignment, as well as the exploration for co-effects of extracellular viscoelasticity and nano-orientation on neuronal cell/tissue behaviors. D) Viability and morphology of PC12 cells. Adapted with permission from [28], copyright 2021, Elsevier.

4.7. Highly Oriented Hydrogels for Corneal Tissue Engineering Applications

The cornea, which serves as the outermost layer of transparent and protective soft tissue in the eye, possesses a hierarchically oriented structure that facilitates the transmission and refraction of light to the retina [17, 391]. Comprised mainly of type I collagen, the cornea is divided into three components: the epithelium, stroma, and endothelium [392]. Each component consists of oriented collagen fibers embedded within a hydrated proteoglycan rich gel matrix, which provides support for the fibrillar collagen structure. Bektas et al. [393] fabricated 3D printed GelMA hydrogels with an oriented structure that closely replicate the biological and physical characteristics of the corneal stroma **(Figure 22A)**. By optimizing printing conditions, including the nozzle speed in the x-y direction and the spindle speed, they achieved a biomimetic structure comprising parallel fibers within each layer, with adjacent layers arranged perpendicular to one another, mirroring the natural structure of the stroma. Kim et al. [394] utilized the shear forces during the 3D printing process to prepare orientation-aligned collagen hydrogels using a bioink derived from decellularized ECM of the corneal stroma **(Figure 22B)**. The spatial orientation of collagen fibers was manipulated by adjusting parameters like nozzle diameter and flow rate **(Figure 22C)**. In vitro cell cultures demonstrated the expression of keratocyte-specific genes, including keratocan (KERA) and aldehyde dehydrogenase (ALDH). Additionally, the in vivo corneal injury model cultures conducted on New Zealand white rabbits exhibited a homogeneous cell alignment that resembled the natural structure of the human cornea. He et al. [395] employed DLP technology to fabricate a cell-laden bi-layer construct that encompassed an epithelium layer loaded with rabbit corneal epithelial cells and an orthogonally aligned fibrous stroma layer loaded with rabbit adipose-derived mesenchymal stem cells (rASCs). The intention was to mimic the microstructure and microenvironment of the natural cornea. In vivo experiments utilizing a rabbit anterior lamellar keratoplasty (ALK) model effectively facilitated corneal regeneration by promoting efficient re-epithelialization and stromal regeneration. This approach established a favorable topographical and biological microenvironment for corneal regeneration.

4.8. Highly Oriented Hydrogels for Vascular Tissue Engineering Applications

The vascular network plays crucial biological roles in the human body, including facilitating nutrient and gas exchange, removing metabolic waste, and maintaining internal environmental homeostasis [396]. Furthermore, the formation of the vascular network is accompanied by cellular behaviors that contribute to the growth and development of tissues and organs, as well as various biological events [397]. Blood vessels comprise an inner layer of endothelial cells aligned along the long axis of the vessel that is surrounded by smooth muscle cells aligned circumferentially relative to the long axis of the vessel [34]. This specific orientation is crucial for preserving the vessel's constant tone and elasticity [38].

Vascular diseases, particularly those affecting vessels with a diameter less than 6 mm, have a high global prevalence [398]. While autologous vessel transplantation is the preferred option for revascularization, over 30% of patients do not have an available vessel for use, highlighting the need for tissue-engineered artificial vessels as an alternative graft source in vascular replacement [399]. Despite the progress in this field, numerous bionic hollow duct hydrogels have been developed using 3D printing or template-sacrificing techniques [400-407]. However, there is a need for more precise strategies to replicate the natural vascular morphology for effective TE applications. Replicating the circumferentially oriented alignment of vascular smooth muscle cells remains a crucial challenge in vascular TE. Sun et al. [408] introduced a GelMA hydrogel-based circumferentially oriented spring structure formed through semi-automated coiling of microscale nucleus-shell microfibrils **(Figure 23A)**. This structure was subsequently utilized as a perfusion culture device to induce the differentiation of human MSCs into contractile vascular smooth muscle cell (SMC) -like cells **(Figure 23B)**. McClendon et al. [409] devised liquid crystalline solutions containing peptide amphiphile nanofibers to create gel ducts with fibers arranged in a circular orientation **(Figure 23C)**. The SMCs were successfully encapsulated during the preparation process, preserving their viability, and exhibited parallel alignment with the fibers, effectively mimicking the circumferential arrangement observed in natural arterial vasculature **(Figure 23D)**.

Replicating the multilayered oriented structure of blood vessels is a key objective in vascular TE research. Bosch-Rué et al. [34] utilized a triple coaxial nozzle to fabricate a bilayer hydrogel that mimics the native vascular structure. The inner hydrogel layer was loaded with HUVECs, while the outer hydrogel layer was loaded with human aortic smooth muscle cells (HASMCs). The injection speed was adjusted to control the size of the simulated vessels. The HUVECs and HASMCs were aligned parallel and perpendicular to the orientation of the bilayer

hydrogel, mirroring the natural arrangement of vascular endothelial cells and smooth muscle cells, respectively. This approach presents a novel strategy for creating artificial blood vessels; however, additional experiments involving perfused cultures are necessary to ensure optimal cell alignment and promote the maturation and functionality of the constructs. The implementation of this multichannel coaxial extrusion system (MCCES) holds significant promise for fabricating multilayered tubular

biological tissues, including blood vessels [410].

4.9. Highly Oriented Hydrogels for Skin and Disc Tissue Engineering Applications

The skin, being the body's largest organ, serves as the outermost layer that provides a physical barrier and regulates body temperature [411, 412]. Skin injuries can self-heal, but this depends on the severity or thickness of the wound [413]. Managing chronic and full-thickness wounds remains a significant

Figure 22. A) Schematic representation of preparation of human keratocyte (HK) loaded hydrogels. (a) GelMA slabs, and (b) 3D bioprinted GelMA hydrogels. Adapted with permission from [393], copyright 2019, Royal Society of Chemistry. B) (a) Schematic illustration of the alignment of collagen fibers within the nozzle during bioink extrusion. (b) Viscosity profile of 2%-Co-dECM bioink incorporating cells. (c) Radial distribution of wall shear stress upon 3D printing for the different-sized nozzles. (d) Second harmonic generation (SHG) images of shear-aligned collagen. (e) Distributions of orientations obtained by analysis using Orientation-J of SHG images collected at different azimuthal angles. C) Cellular behavior of the differentiated keratocytes encapsulated in the bioink on the 28th day of cell culture. Adapted with permission from [394], copyright 2019, IOP Publishing.

challenge. Limited research has been conducted on reconstructing the oriented structures of the mammalian skin, such as a variety of ECM fibers, including collagen fibers and fibroblasts **(Figure 24A)** [286], and currently, one of the goals in skin TE is to induce fibroblasts to reorient structures resembling natural dermal tissue during dermal injury healing. Shi et al. [81] demonstrated that a magnetic field-oriented 1D $SiO_2@Fe_3O_4$ rod composite hydrogel could successfully guide the oriented and aligned growth of normal human dermal fibroblasts **(Figure 3B, 24B)**. In the future, the integration of oriented hydrogels with biological cues, such as stem cells or bioactive molecules, needs to be researched to advance the development of ideal tissue-engineered skin substitutes.

The natural intervertebral disc (IVD) primarily comprises two distinct structural tissues: the highly hydrated gelatinous nucleus pulposus (NP) situated at the center and the closely surrounding fibrous annulus (AF) **(Figure 24C)** [414]. The NP comprises a reticular fibrous structure and a proteoglycan matrix that exhibits properties of an elastic gel. The AF, which envelops the NP closely, primarily comprises a layered arrangement of type I collagen fibers that maintain the position and shape of the NP, transmit its stresses, and safeguard the integrity of the IVD against bending, stretching, and torsional damage [415]. Damage to the NP and AF can result in various degenerative spinal diseases and considerable morbidity [416], and current clinical treatments primarily focus on symptom management. The performance of current artificial IVDs does not align with the biomechanical properties of natural tissue, making it impossible to fully replace the degenerated IVD and restore its complete function [417]. Therefore, the development of TE natural discs is crucial, ideally using hydrogels with properties that
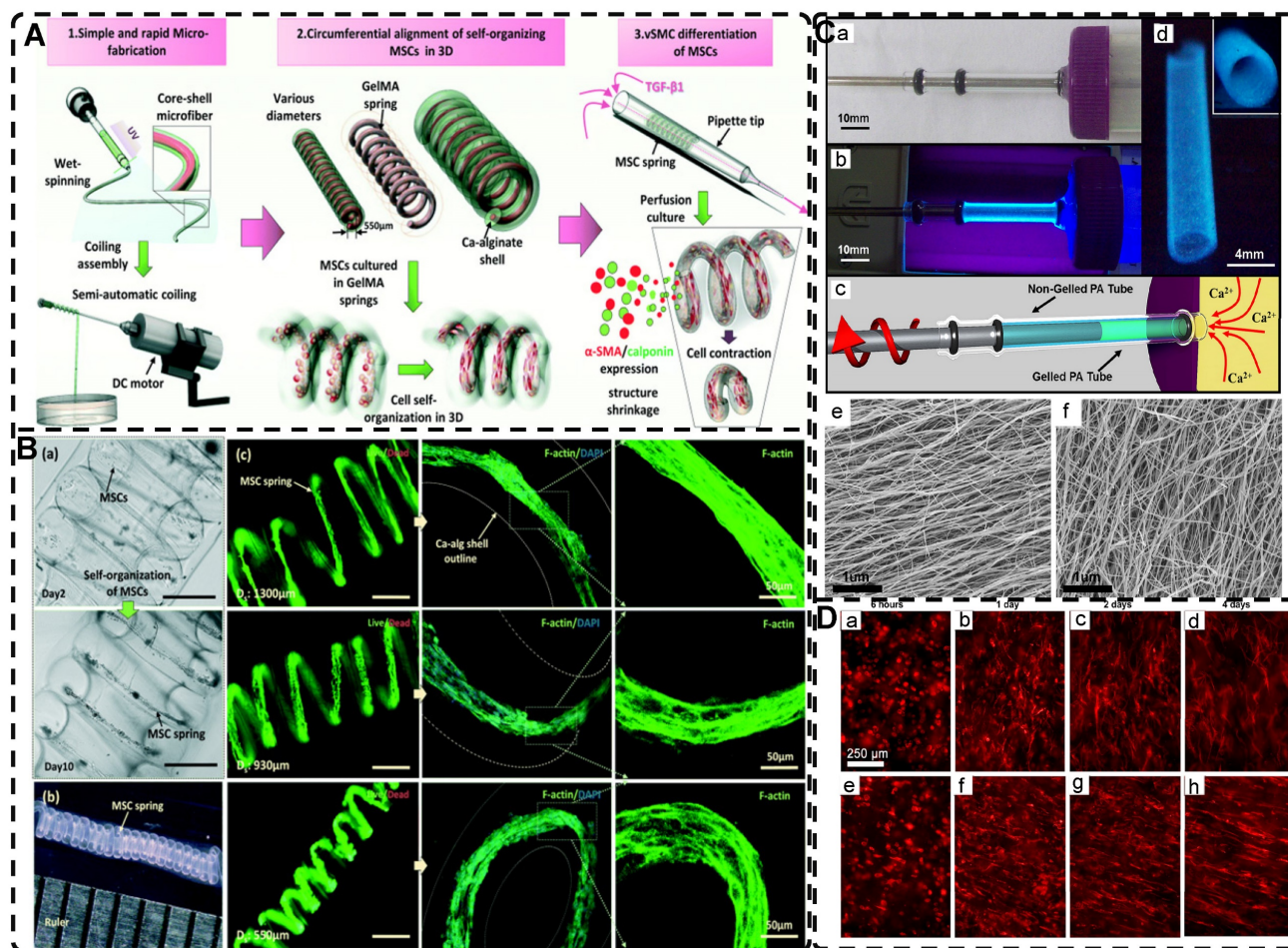
Figure 23. A) MSCs encapsulated in GelMA springs self-organized into smooth muscle-like tissues with cell alignment and contractile property similar to that of vSMCs in the media layer of blood vessels in vivo. B) Formation of MSC springs. (a) Self-organization of MSCs in a GelMA spring. (b) An MSC spring with a large length-to-diameter ratio of about 13.33. (c) Live/dead staining images showing cell viability in the resulting MSC springs encapsulated in GelMA springs with three different diameters. Adapted with permission from [408], copyright 2020, Royal Society of Chemistry. C) Schematic of fabrication device with resulting macroscopic tubular gel. (a) Empty shear chamber assembled and (b) PA solution loaded in shear chamber. (c) Fabrication procedure showing the inner rod's combined rotation and retraction movement allowing the Ca^{2+} solution to flow into the lumen of the tube. (d) Macroscopic photo of final PA tube retaining its tubular shape. The aligned sample (e) shows noticeably more aligned nanofibers than the non-aligned sample(f). D) Cellular alignment viewed from inner surface with the tube's long axis in the vertical direction; (a–d) Non-aligned samples, (e–h) Aligned samples. Adapted with permission from [409], copyright 2012, Elsevier.
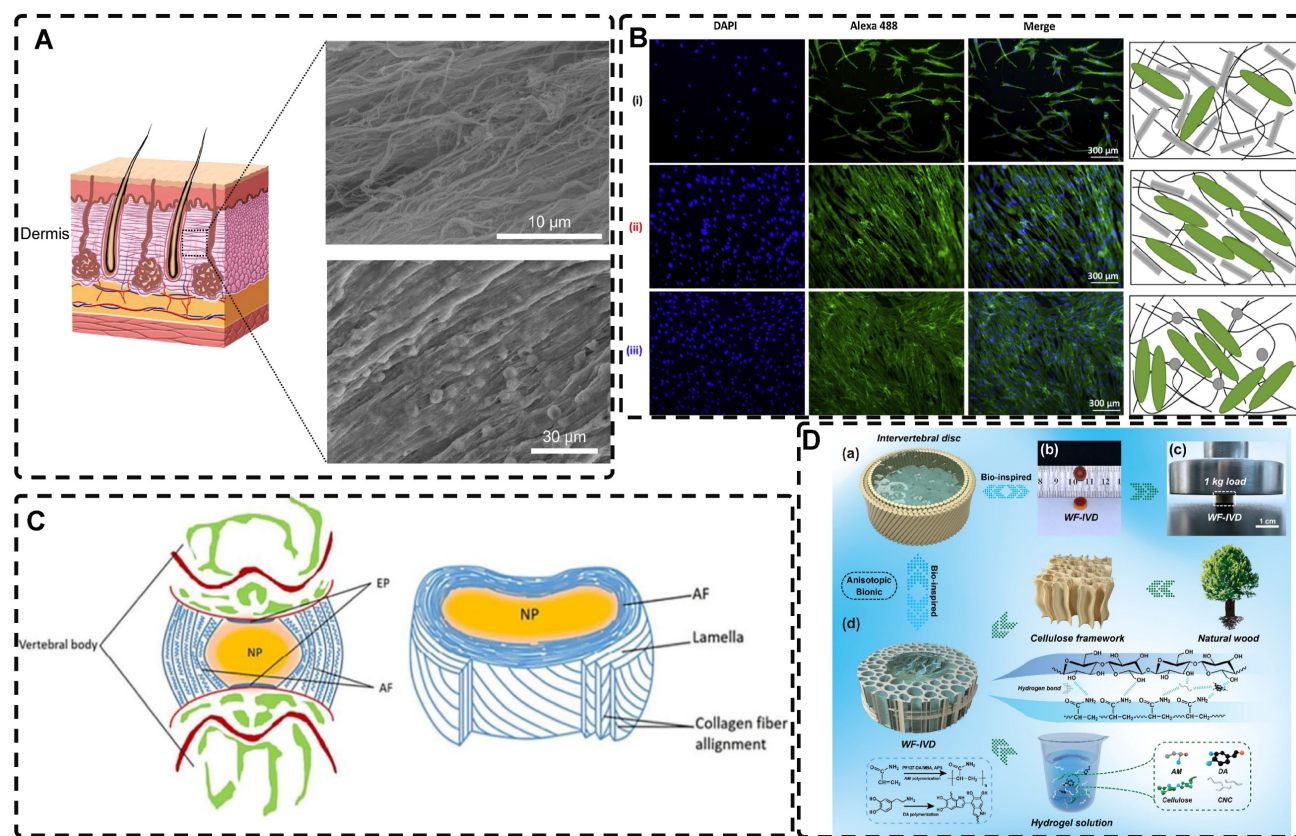
Figure 24. A) A graphical illustration of dermis in skin, and SEM image of aligned collagen fiber bundles observed in the dermis of neonatal rat skin and aligned dermal fibroblasts in the same tissue. The orientation of bundles agrees with the tension line in skin. Adapted with permission from [286], copyright 2012, Elsevier. B) Fluorescence microscopy images and schematic representation of NHDFs culture on highly oriented hydrogels after 48 h. Adapted with permission from [81], copyrights 2020, Elsevier. C) Schematic representations of the adult IVD and midsagittal cross-section showing anatomical regions. Adapted with permission from [414], copyright 2020, Frontiers Media. D) Schematic illustration and fabrication process of WF-IVD. (a) Schematic diagram of a typical intervertebral disk to be simulated by WF-IVD. Images of WF-IVD (b) in different directions and (c) under a 1 kg load. (d) Two-component composite fabrication process. Adapted with permission from [418], copyright 2021, American Chemical Society.

closely mimic the properties of the IVD. Highly oriented hydrogels present promising strategies for simulating and constructing complex IVDs. For instance, Liu et al. [418] demonstrated the development of a biomimetic IVD through the combination of a naturally oriented cellulose framework with nanocomposite hydrogels **(Figure 24D)**. These hydrogels encompassed Cellulose PAM-Polydopamine (PDA) Composite Hydrogels (CCHs) that mimic the NP, as well as Wood Framework Hydrogels (WFHs) that emulate the AF **(Figure 24D)**. The formation of robust hydrogen bonds among the multi-hydrogen bonded substances (e.g., cellulose (hydroxyl), CNC (hydroxyl), PAM (amino group), and PDA (phenolic hydroxyl)) ensures stable bonding and endows the composite structure with exceptional mechanical properties. The isotropic CCH exhibited a distinct, highly elastic behavior that promoted significant recovery (up to ~5% energy dissipation) and achieved favorable mechanical matching with the NP tissue. Additionally, the highly oriented WFH offered notable mechanical buffering and energy absorption (at a minimum of ~60% energy dissipation), akin to the characteristics observed in

natural AF tissue. Furthermore, the composite, oriented hydrogel comprised biocompatible materials. Further research is needed to explore additional applications of highly oriented hydrogels in the field of IVD TE.

5. Summary and Outlook

Highly oriented structures are crucial for the diverse functions in tissues and organs. Researchers are actively exploring TE using highly oriented hydrogels that mimic the properties of native tissues and organs to varying extents. These hydrogels exhibit characteristics such as aligned structures, anisotropic mechanical properties, and electrical conductivity. This approach is key in enhancing tissue repair, regeneration, and potential replacement, especially in addressing challenging tissue diseases and injuries. Critically, ignoring the differences in enhanced functionality of different materials, highly oriented structures are superior to randomly oriented structures for biomimetic tissue engineering in the same material, including the modulation of cellular behaviors such as adhesion, migration, proliferation, and differentiation, and the provision of a biomimetic

in vivo 3D microenvironment for cells. Significant advances in biomanufacturing technologies offer immense potential for the fields of TE and regenerative medicine. This article reviews the application of hydrogels with highly oriented structures in the field of TE and demonstrates their potential in different TE fields and their effects on cell behavior. Despite the promising application of highly oriented hydrogels in TE, there remain challenges that scientists should overcome:

i. Biocompatibility and safety are crucial considerations for hydrogels intended for TE applications. They should not only exhibit biocompatibility with cultured cells in vitro but also ensure a low risk of severe adverse effects such as direct cytotoxicity, immune reactions, or the release of toxic substances, including metabolites, upon implantation into human tissues. Consequently, researchers must prioritize the investigation of biocompatibility and the fate of highly oriented hydrogels in vivo. Additionally, strategies utilizing external stimuli like magnetic fields, electric fields, and shear forces can strongly influence cell survival, while the zero-degree environment during directional freezing can impact cell viability. These limitations present opportunities to enhance or mitigate the impact of these techniques on cell viability.

ii. Improving the mechanical properties of hydrogels is needed as currently, hydrogels are only capable of simulating the mechanical characteristics of soft tissues, and achieving a Young's modulus of up to 20 GPa, comparable to that of bone tissues, remains challenging. Furthermore, fully replicating the mechanical properties of biological tissues means also replicating the elasticity, rigidity, hardness, toughness, fracture toughness, and fatigue strength. Notably, strategies like 3D printing, which enable the fabrication of high-resolution bionic microstructures, face challenges in reconciling the mechanical properties required to ensure adequate flexibility, particularly for tendons and ligaments. A combination of multiple strategies may improve the shortcomings of individual systems. In addition, a potential challenge lies in the bio-adhesiveness of hydrogels for their in vivo implantation due to their insaturability.

iii. Simple high-orientation structures are inadequate as human tissues and organs are highly diverse and complex in their hierarchical organization. Moreover, the highly oriented structures between different layers are connected together by tissue-specific ECM to form an organic whole with a smooth transition in structure and properties, exemplified by skeletal muscle fibers wrapped by extracellular connective tissue or cornea

tissue arranged orthogonally. Certain highly oriented hydrogels successfully mimic hierarchically oriented structural tissues like articular cartilage, and this change in orientation between layers holds promise for advancing the understanding of cell behavior at interfacial boundaries. Nevertheless, fully replicating the intricate molecular-to-macroscopic scale of natural tissue structure remains a formidable challenge. Moreover, during the implantation of highly oriented hydrogels into injured tissues, it is crucial to align the tissue orientation with that of the hydrogel to prevent the formation of tissue scars resulting from conflicting orientations.

iv. The precise biological mechanisms by which cells perceive structural orientation in a 3D environment remain incompletely understood. Further investigations of the molecular mechanisms that underlie cellular behaviors, including adhesion, migration, proliferation, and differentiation in highly oriented hydrogels, are needed to enhance the efficiency of engineering manufacturing and propel advancements in TE. Currently, the majority of studies investigating the impact of oriented structures on cell behavior are focused on the 2D environment, which differs to some extent from the 3D environment within hydrogels and the human body. Consequently, the molecular biological mechanisms underlying cell responses in the 2D environment can only serve as a reference for the 3D cellular microenvironment and cannot be directly extrapolated.

v. Human tissues and organs possess not only highly oriented structures but also a diverse array of biophysical cues and biochemical signals that collectively orchestrate the development from individual cells to fully formed tissues and organs. Incorporating complex, highly oriented structures along with many other cues into hydrogels in vivo represents a promising approach in TE to mimic the natural tissue environment better. For instance, the in vitro maturation and differentiation of cardiomyocytes, nerve cells, and skeletal muscle cells can direct cell phenotypes by responding to a range of biochemical and physical cues, including growth factors immobilized in hydrogels, electrical stimulation, and mechanical forces. However, the investigation into coordinating multiple guiding cues and elucidating how cell behavior is modulated in response to diverse cues is still in the early stages.

vi. The pursuit of hydrogels that accurately replicate the structure and function of complex tissues can result in a complexity of design strategies, rendering them unsuitable for efficient industrial production. Additionally, laboratory biofabrication tools are susceptible to flaws, potentially resulting in variations between batches of hydrogels in terms of

their desired structure, mechanical properties, compositional uniformity, and so forth. Such inconsistencies can significantly impede product translation and pose challenges during the regulatory approval process. Technologies such as 3D/4D printing provide the possibility to realize simple large-scale production preparation, but the premise is to solve their own limitations.

Numerous challenges and obstacles remain to be addressed in order to attain the ultimate objective of transforming highly oriented hydrogels into finished products. Considering the remarkable progress in biomaterials science, engineering, and cell biology, we anticipate forthcoming captivating advancements in the field of TE.

Competing Interests

The authors have declared that no competing interest exists.

References

1. Langer R, Vacanti JP. Tissue engineering. Science. 1993; 260: 920-6.
2. Sun JY, Zhao X, Illeperuma WR, Chaudhuri O, Oh KH, Mooney DJ, et al. Highly stretchable and tough hydrogels. Nature. 2012; 489: 133-6.
3. Zhang YS, Khademhosseini A. Advances in engineering hydrogels. Science. 2017; 356.
4. Jiang Y, Krishnan N, Heo J, Fang RH, Zhang L. Nanoparticle-hydrogel superstructures for biomedical applications. J Control Release. 2020; 324: 505-21.
5. Gong JP, Katsuyama Y, Kurokawa T, Osada Y. Double-network hydrogels with extremely high mechanical strength. Adv Mater. 2003; 15: 1155-8.
6. Haraguchi K, Takehisa T. Nanocomposite Hydrogels: A Unique Organic–Inorganic Network Structure with Extraordinary Mechanical, Optical, and Swelling/De-swelling Properties. Adv Mater. 2002; 14.
7. Jeon I, Cui J, Illeperuma WR, Aizenberg J, Vlassak JJ. Extremely Stretchable and Fast Self-Healing Hydrogels. Adv Mater. 2016; 28: 4678-83.
8. Sun TL, Kurokawa T, Kuroda S, Ihsan AB, Akasaki T, Sato K, et al. Physical hydrogels composed of polyampholytes demonstrate high toughness and viscoelasticity. Nat Mater. 2013; 12: 932-7.
9. Sophia Fox AJ, Bedi A, Rodeo SA. The basic science of articular cartilage: structure, composition, and function. Sports Health. 2009; 1: 461-8.
10. Fratzl P, Weinkamer R. Nature's hierarchical materials. Prog Mater Sci. 2007; 52: 1263-334.
11. Lieber RL, Ward SR. Skeletal muscle design to meet functional demands. Philos Trans R Soc Lond B Biol Sci. 2011; 366: 1466-76.
12. Lynch HA, Johannessen W, Wu JP, Jawa A, Elliott DM. Effect of fiber orientation and strain rate on the nonlinear uniaxial tensile material properties of tendon. J Biomech Eng. 2003; 125: 726-31.
13. Zhang YS, Aleman J, Arneri A, Bersini S, Piraino F, Shin SR, et al. From cardiac tissue engineering to heart-on-a-chip: beating challenges. Biomed Mater. 2015; 10: 034006.
14. Chen S, Wu C, Liu A, Wei D, Xiao Y, Guo Z, et al. Biofabrication of nerve fibers with mimetic myelin sheath-like structure and aligned fibrous niche. Biofabrication. 2020; 12: 035013.
15. Serbo JV, Gerecht S. Vascular tissue engineering: biodegradable scaffold platforms to promote angiogenesis. Stem Cell Res Ther. 2013; 4: 8.
16. Landau S, Ben-Shaul S, Levenberg S. Oscillatory Strain Promotes Vessel Stabilization and Alignment through Fibroblast YAP-Mediated Mechanosensitivity. Adv Sci 2018; 5: 1800506.
17. Meek KM, Knupp C. Corneal structure and transparency. Prog Retin Eye Res. 2015; 49: 1-16.
18. Peng N, Huang D, Gong C, Wang Y, Zhou J, Chang C. Controlled Arrangement of Nanocellulose in Polymeric Matrix: From Reinforcement to Functionality. ACS Nano. 2020; 14: 16169-79.
19. Xu Y, Yin H, Chu J, Eglin D, Serra T, Docheva D. An anisotropic nanocomposite hydrogel guides aligned orientation and enhances tenogenesis of human tendon stem/progenitor cells. Biomater Sci. 2021; 9: 1237-45.
20. Zhang Y, Zheng X, Jiang W, Han J, Pu J, Wang L, et al. Formation of highly ordered micro fillers in polymeric matrix by electro-field-assisted aligning. RSC Adv. 2019; 9: 15238-45.
21. Zhao WW, Hu SM, Shi ZJ, Santaniello T, Lenardi C, Huang J. Mechanical characteristics of tunable uniaxial aligned carbon nanotubes induced by robotic extrusion technique for hydrogel nanocomposite. Compos Part A Appl Sci Manuf. 2020; 129: 105707.
22. Mredha MTI, Guo YZ, Nonoyama T, Nakajima T, Kurokawa T, Gong JP. A Facile Method to Fabricate Anisotropic Hydrogels with Perfectly Aligned Hierarchical Fibrous Structures. Adv Mater. 2018; 30: 1704937.
23. Yang W, Furukawa H, Gong JP. Highly Extensible Double-Network Gels with Self-Assembling Anisotropic Structure. Adv Mater. 2008; 20: 4499-503.
24. Wu JJ, Zhao Q, Sun JZ, Zhou QY. Preparation of poly(ethylene glycol) aligned porous cryogels using a unidirectional freezing technique. Soft Matter. 2012; 8: 3620-6.
25. Dong L, Liang M, Guo Z, Wang A, Cai G, Yuan T, et al. A Study on Dual-Response Composite Hydrogels Based on Oriented Nanocellulose. Int J Bioprint. 2022; 8: 578.
26. Eyckmans J, Boudou T, Yu X, Chen CS. A hitchhiker's guide to mechanobiology. Dev Cell. 2011; 21: 35-47.
27. Domingues RM, Chiera S, Gershovich P, Motta A, Reis RL, Gomes ME. Enhancing the Biomechanical Performance of Anisotropic Nanofibrous Scaffolds in Tendon Tissue Engineering: Reinforcement with Cellulose Nanocrystals. Adv Healthc Mater. 2016; 5: 1364-75.
28. Chen S, Wu C, Zhou T, Wu K, Xin N, Liu X, et al. Aldehyde-methacrylate-hyaluronan profited hydrogel system integrating aligned and viscoelastic cues for neurogenesis. Carbohydr Polym. 2022; 278: 118961.
29. Wang L, Li T, Wang Z, Hou J, Liu S, Yang Q, et al. Injectable remote magnetic nanofiber/hydrogel multiscale scaffold for functional anisotropic skeletal muscle regeneration. Biomaterials. 2022; 285: 121537.
30. Liu H, Chansoria P, Delrot P, Angelidakis E, Rizzo R, Rutsche D, et al. Filamented Light (FLight) Biofabrication of Highly Aligned Tissue-Engineered Constructs. Adv Mater. 2022; 34: e2204301.
31. Echave MC, Domingues RMA, Gomez-Florit M, Pedraz JL, Reis RL, Orive G, et al. Biphasic Hydrogels Integrating Mineralized and Anisotropic Features for Interfacial Tissue Engineering. ACS Appl Mater Interfaces. 2019; 11: 47771-84.
32. Liu DL, Dong XF, Liu HY, Zhao YP, Qi M. Effect of pore orientation on shear viscoelasticity of cellulose nanocrystal/collagen hydrogels. J Appl Polym Sci. 2021; 138: e49856.
33. Wang XF, Fang J, Zhu WW, Zhong CX, Ye DD, Zhu MY, et al. Bioinspired Highly Anisotropic, Ultrastrong and Stiff, and Osteoconductive Mineralized Wood Hydrogel Composites for Bone Repair. Adv Funct Mater. 2021; 31: 2010068.
34. Bosch-Rue E, Delgado LM, Gil FJ, Perez RA. Direct extrusion of individually encapsulated endothelial and smooth muscle cells mimicking blood vessel structures and vascular native cell alignment. Biofabrication. 2020; 13: 015003.
35. Ye DD, Yang PC, Lei XJ, Zhang DH, Li LB, Chang CY, et al. Robust Anisotropic Cellulose Hydrogels Fabricated via Strong Self-aggregation Forces for Cardiomyocytes Unidirectional Growth. Chem Mater. 2018; 30: 5175-83.
36. Mredha MTI, Jeon I. Biomimetic anisotropic hydrogels: Advanced fabrication strategies, extraordinary functionalities, and broad applications. Prog Mater Sci. 2022; 124: 100870.
37. Sano K, Ishida Y, Aida T. Synthesis of Anisotropic Hydrogels and Their Applications. Angew Chem Int Ed Engl. 2018; 57: 2532-43.
38. Zhao Z, Fang R, Rong Q, Liu M. Bioinspired Nanocomposite Hydrogels with Highly Ordered Structures. Adv Mater. 2017; 29: 1703045.
39. Le X, Lu W, Zhang J, Chen T. Recent Progress in Biomimetic Anisotropic Hydrogel Actuators. Adv Sci. 2019; 6: 1801584.
40. Jana S, Levengood SK, Zhang M. Anisotropic Materials for Skeletal-Muscle-Tissue Engineering. Adv Mater. 2016; 28: 10588-612.
41. Nie J, Pei B, Wang Z, Hu Q. Construction of ordered structure in polysaccharide hydrogel: A review. Carbohydr Polym. 2019; 205: 225-35.
42. Pardo A, Gomez-Florit M, Barbosa S, Taboada P, Domingues RMA, Gomes ME. Magnetic Nanocomposite Hydrogels for Tissue Engineering: Design Concepts and Remote Actuation Strategies to Control Cell Fate. ACS Nano. 2021; 15: 175-209.
43. Wu ZL, Gong JP. Hydrogels with self-assembling ordered structures and their functions. Npg Asia Mater. 2011; 3: 57-64.
44. Khuu N, Kheiri S, Kumacheva E. Structurally anisotropic hydrogels for tissue engineering. Trends Chem. 2021; 3: 1002-26.
45. Xu HY, Gu N. Magnetic responsive scaffolds and magnetic fields in bone repair and regeneration. Front Mater Sci. 2014; 8: 20-31.
46. Fernandes MM, Correia DM, da Costa A, Ribeiro S, Casal M, Lanceros-Mendez S, et al. Multifunctional magnetically responsive biocomposites based on genetically engineered silk-elastin-like protein. Compos B Eng. 2018; 153: 413-9.
47. Gil S, Mano JF. Magnetic composite biomaterials for tissue engineering. Biomater Sci. 2014; 2: 812-8.
48. Reddy LH, Arias JL, Nicolas J, Couvreur P. Magnetic nanoparticles: design and characterization, toxicity and biocompatibility, pharmaceutical and biomedical applications. Chem Rev. 2012; 112: 5818-78.
49. Subramanian M, Miaskowski A, Jenkins SI, Lim J, Dobson J. Remote manipulation of magnetic nanoparticles using magnetic field gradient to promote cancer cell death. Appl Phys A Mater Sci Process. 2019; 125: 226.
50. Hilger I, Kaiser WA. Iron oxide-based nanostructures for MRI and magnetic hyperthermia. Nanomedicine. 2012; 7: 1443-59.

51. Johnson CDL, Ganguly D, Zuidema JM, Cardinal TJ, Ziemba AM, Kearns KR, et al. Injectable, Magnetically Orienting Electrospun Fiber Conduits for Neuron Guidance. ACS Appl Mater Interfaces. 2019; 11: 356-72.

52. Sapir-Lekhovitser Y, Rotenberg MY, Jopp J, Friedman G, Polyak B, Cohen S. Magnetically actuated tissue engineered scaffold: insights into mechanism of physical stimulation. Nanoscale. 2016; 8: 3386-99.

53. Parkinson GS. Iron oxide surfaces. Surf Sci Rep. 2016; 71: 272-365.

54. Hermenegildo B, Ribeiro C, Perez-Alvarez L, Vilas JL, Learmonth DA, Sousa RA, et al. Hydrogel-based magnetoelectric microenvironments for tissue stimulation. Colloids and surfaces B, Biointerfaces. 2019; 181: 1041-7.

55. Messing R, Frickel N, Belkoura L, Strey R, Rahn H, Odenbach S, et al. Cobalt Ferrite Nanoparticles as Multifunctional Cross-Linkers in PAAm Ferrohydrogels. Macromolecules. 2011; 44: 2990-9.

56. Liu H, Wang C, Gao Q, Liu X, Tong Z. Magnetic hydrogels with supracolloidal structures prepared by suspension polymerization stabilized by Fe_2O_3 nanoparticles. Acta Biomater. 2010; 6: 275-81.

57. Sapir Y, Cohen S, Friedman G, Polyak B. The promotion of in vitro vessel-like organization of endothelial cells in magnetically responsive alginate scaffolds. Biomaterials. 2012; 33: 4100-9.

58. Wu W, Wu Z, Yu T, Jiang C, Kim WS. Recent progress on magnetic iron oxide nanoparticles: synthesis, surface functional strategies and biomedical applications. Sci Technol Adv Mater. 2015; 16: 023501.

59. Li Z, Li Y, Chen C, Cheng Y. Magnetic-responsive hydrogels: From strategic design to biomedical applications. J Control Release. 2021; 335: 541-56.

60. Gu N, Zhang ZH, Li Y. Adaptive iron-based magnetic nanomaterials of high performance for biomedical applications. Nano Research. 2022; 15: 1-17.

61. Ul-Islam M, Ullah MW, Khan S, Manan S, Khattak WA, Ahmad W, et al. Current advancements of magnetic nanoparticles in adsorption and degradation of organic pollutants. Environ Sci Pollut Res Int. 2017; 24: 12713-22.

62. Abd Elrahman AA, Mansour FR. Targeted magnetic iron oxide nanoparticles: Preparation, functionalization and biomedical application. J Drug Deliv Sci Technol. 2019; 52: 702-12.

63. Abdalla AME, Xiao L, Ullah MW, Yu M, Ouyang C, Yang G. Current Challenges of Cancer Anti-angiogenic Therapy and the Promise of Nanotherapeutics. Theranostics. 2018; 8: 533-48.

64. Wan L, Song H, Chen X, Zhang Y, Yue Q, Pan P, et al. A Magnetic-Field Guided Interface Coassembly Approach to Magnetic Mesoporous Silica Nanochains for Osteoclast-Targeted Inhibition and Heterogeneous Nanocatalysis. Adv Mater. 2018; 30: e1707515.

65. Xu J, Jia Y, Liu M, Gu X, Li P, Fan Y. Preparation of Magnetic-Luminescent Bifunctional Rapeseed Pod-Like Drug Delivery System for Sequential Release of Dual Drugs. Pharmaceutics. 2021; 13: 1116.

66. Wang JD, Guan HY, Liang QL, Ding MY. Construction of copper (II) affinity-DTPA functionalized magnetic composite for efficient adsorption and specific separation of bovine hemoglobin from bovine serum. Compos B Eng. 2020; 198: 108248.

67. Shi W, Huang J, Fang R, Liu M. Imparting Functionality to the Hydrogel by Magnetic-Field-Induced Nano-assembly and Macro-response. ACS Appl Mater Interfaces. 2020; 12: 5177-94.

68. Thoniyot P, Tan MJ, Karim AA, Young DJ, Loh XJ. Nanoparticle-Hydrogel Composites: Concept, Design, and Applications of These Promising, Multi-Functional Materials. Adv Sci 2015; 2: 1400010.

69. Majidi S, Sehrig FZ, Farkhani SM, Goloujeh MS, Akbarzadeh A. Current methods for synthesis of magnetic nanoparticles. Artif Cells Nanomed Biotechnol. 2016; 44: 722-34.

70. Friedrich RP, Cicha I, Alexiou C. Iron Oxide Nanoparticles in Regenerative Medicine and Tissue Engineering. Nanomaterials. 2021; 11: 2337.

71. Stopin A, Pineux F, Marega R, Bonifazi D. Magnetically Active Carbon Nanotubes at Work. Chemistry. 2015; 21: 9288-301.

72. Faraudo J, Andreu JS, Calero C, Camacho J. Predicting the Self-Assembly of Superparamagnetic Colloids under Magnetic Fields. Adv Funct Mater. 2016; 26: 3837-58.

73. Fan X, Walther A. 1D Colloidal chains: recent progress from formation to emergent properties and applications. Chem Soc Rev. 2022; 51: 4023-74.

74. Mehdizadeh Taheri S, Michaelis M, Friedrich T, Forster B, Drechsler M, Romer FM, et al. Self-assembly of smallest magnetic particles. Proc Natl Acad Sci U S A. 2015; 112: 14484-9.

75. Mahmoudi M, Sant S, Wang B, Laurent S, Sen T. Superparamagnetic iron oxide nanoparticles (SPIONs): development, surface modification and applications in chemotherapy. Adv Drug Deliv Rev. 2011; 63: 24-46.

76. Antman-Passig M, Shefi O. Remote Magnetic Orientation of 3D Collagen Hydrogels for Directed Neuronal Regeneration. Nano Lett. 2016; 16: 2567-73.

77. Hu K, Sun J, Guo Z, Wang P, Chen Q, Ma M, et al. A novel magnetic hydrogel with aligned magnetic colloidal assemblies showing controllable enhancement of magnetothermal effect in the presence of alternating magnetic field. Adv Mater. 2015; 27: 2507-14.

78. Wang P, Sun J, Lou Z, Fan F, Hu K, Sun Y, et al. Assembly-Induced Thermogenesis of Gold Nanoparticles in the Presence of Alternating Magnetic Field for Controllable Drug Release of Hydrogel. Adv Mater. 2016; 28: 10801-8.

79. Tognato R, Bonfrate V, Giancane G, Serra T. Fabrication of anisotropic collagen-based substrates for potential use in tissue engineering. Smart Mater Struct. 2022; 31: 074001.

80. Zhang Y, Wang Y, Wen Y, Zhong Q, Zhao Y. Self-Healable Magnetic Structural Color Hydrogels. ACS Appl Mater Interfaces. 2020; 12: 7486-93.

81. Shi Y, Li Y, Coradin T. Magnetically-oriented type I collagen-SiO_2@Fe_3O_4 rods composite hydrogels tuning skin cell growth. Colloids and surfaces B, Biointerfaces. 2020; 185: 110597.

82. Abrougui MM, Lopez-Lopez MT, Duran JDG. Mechanical properties of magnetic gels containing rod-like composite particles. Philos Trans A Math Phys Eng Sci. 2019; 377: 20180218.

83. Rincon-Iglesias M, Rodrigo I, L BB, Serea ESA, Plazaola F, Lanceros-Mendez S, et al. Core-Shell Fe_3O_4@Au Nanorod-Loaded Gels for Tunable and Anisotropic Magneto- and Photothermia. ACS Appl Mater Interfaces. 2022; 14: 7130-40.

84. Araujo-Custodio S, Gomez-Florit M, Tomas AR, Mendes BB, Babo PS, Mithieux SM, et al. Injectable and Magnetic Responsive Hydrogels with Bioinspired Ordered Structures. ACS Biomater Sci Eng. 2019; 5: 1392-404.

85. Liu K, Han L, Tang P, Yang K, Gan D, Wang X, et al. An Anisotropic Hydrogel Based on Mussel-Inspired Conductive Ferrofluid Composed of Electromagnetic Nanohybrids. Nano Lett. 2019; 19: 8343-56.

86. Abdalla A, Dean D, Theodore M, Fielding J, Nyairo E, Price G. Magnetically processed carbon nanotube/epoxy nanocomposites: Morphology, thermal, and mechanical properties. Polymer. 2010; 51: 1614-20.

87. Abdalla M, Dean D, Adibempe D, Nyairo E, Robinson P, Thompson G. The effect of interfacial chemistry on molecular mobility and morphology of multiwalled carbon nanotubes epoxy nanocomposite. Polymer. 2007; 48: 5662-70.

88. Maggini L, Liu M, Ishida Y, Bonifazi D. Anisotropically luminescent hydrogels containing magnetically-aligned MWCNTs-Eu(III) hybrids. Adv Mater. 2013; 25: 2462-7.

89. Kim YS, Liu M, Ishida Y, Ebina Y, Osada M, Sasaki T, et al. Thermoresponsive actuation enabled by permittivity switching in an electrostatically anisotropic hydrogel. Nat Mater. 2015; 14: 1002-7.

90. Liu M, Ishida Y, Ebina Y, Sasaki T, Hikima T, Takata M, et al. An anisotropic hydrogel with electrostatic repulsion between cofacially aligned nanosheets. Nature. 2015; 517: 68-72.

91. Dai CF, Khoruzhenko O, Zhang C, Zhu QL, Jiao D, Du M, et al. Magneto-Orientation of Magnetic Double Stacks for Patterned Anisotropic Hydrogels with Multiple Responses and Modulable Motions. Angew Chem Int Ed Engl. 2022; 61: e202207272.

92. Yan G, He S, Chen G, Tang X, Sun Y, Xu F, et al. Anisotropic, strong, self-adhesive and strain-sensitive hydrogels enabled by magnetically-oriented cellulose/polydopamine nanocomposites. Carbohydr Polym. 2022; 276: 118783.

93. Chen H, Zhang X, Shang L, Su Z. Programmable Anisotropic Hydrogels with Localized Photothermal/Magnetic Responsive Properties. Adv Sci. 2022; 9: e2202173.

94. Chen Q, Zhang X, Chen K, Wu X, Zong T, Feng C, et al. Anisotropic hydrogels with enhanced mechanical and tribological performance by magnetically oriented nanohybrids. Chemical Engineering Journal. 2022; 430: 133036.

95. Arruebo M, Fernandez-Pacheco R, Ibarra MR, Santamaria J. Magnetic nanoparticles for drug delivery. Nano Today. 2007; 2: 22-32.

96. Radvar E, Shi Y, Grasso S, Edwards-Gayle CJC, Liu X, Mauter MS, et al. Magnetic Field-Induced Alignment of Nanofibrous Supramolecular Membranes: A Molecular Design Approach to Create Tissue-like Biomaterials. ACS Appl Mater Interfaces. 2020; 12: 22661-72.

97. Wallace M, Cardoso AZ, Frith WJ, Iggo JA, Adams DJ. Magnetically aligned supramolecular hydrogels. Chemistry. 2014; 20: 16484-7.

98. Dubey N, Letourneau PC, Tranquillo RT. Neuronal contact guidance in magnetically aligned fibrin gels: effect of variation in gel mechano-structural properties. Biomaterials. 2001; 22: 1065-75.

99. Eguchi Y, Ohtori S, Sekino M, Ueno S. Effectiveness of magnetically aligned collagen for neural regeneration in vitro and in vivo. Bioelectromagnetics. 2015; 36: 233-43.

100. Torbet J, Malbouyres M, Builles N, Justin V, Roulet M, Damour O, et al. Orthogonal scaffold of magnetically aligned collagen lamellae for corneal stroma reconstruction. Biomaterials. 2007; 28: 4268-76.

101. Chen S, Hirota N, Okuda M, Takeguchi M, Kobayashi H, Hanagata N, et al. Microstructures and rheological properties of tilapia fish-scale collagen hydrogels with aligned fibrils fabricated under magnetic fields. Acta Biomater. 2011; 7: 644-52.

102. De France KJ, Yager KG, Chan KJW, Corbett B, Cranston ED, Hoare T. Injectable Anisotropic Nanocomposite Hydrogels Direct in Situ Growth and Alignment of Myotubes. Nano Lett. 2017; 17: 6487-95.

103. Frka-Petesic B, Sugiyama J, Kimura S, Chanzy H, Maret G. Negative Diamagnetic Anisotropy and Birefringence of Cellulose Nanocrystals. Macromolecules. 2015; 48: 8844-57.

104. Petrov DA, Zakhlevnykh AN. Statistical theory of magnetic field induced phase transitions in negative diamagnetic anisotropy liquid crystals doped with carbon nanotubes. J Mol Liq. 2019; 287: 110901.

105. Wu L, Ohtani M, Takata M, Saeki A, Seki S, Ishida Y, et al. Magnetically induced anisotropic orientation of graphene oxide locked by in situ hydrogelation. ACS Nano. 2014; 8: 4640-9.

106. Tian B, Lin WY, Zhuang PP, Li JZ, Shih TM, Cai WW. Magnetically-induced alignment of graphene via Landau diamagnetism. Carbon. 2018; 131: 66-71.

107. Isabettini S, Stucki S, Massabni S, Baumgartner ME, Reckey PQ, Kohlbrecher J, et al. Development of Smart Optical Gels with Highly Magnetically Responsive Bicelles. ACS Appl Mater Interfaces. 2018; 10: 8926-36.

108. Ansorge R, Graves M. Magnetic field generation. The Physics and Mathematics of MRI: Morgan & Claypool Publishers; 2016. p. 2-1-2-25.

109. Tang J, Yin Q, Qiao Y, Wang T. Shape Morphing of Hydrogels in Alternating Magnetic Field. ACS Appl Mater Interfaces. 2019; 11: 21194-200.

110. Hu K, Yu TT, Tang SJ, Xu XQ, Guo ZB, Qian J, et al. Dual anisotropicity comprising 3D printed structures and magnetic nanoparticle assemblies: towards the promotion of mesenchymal stem cell osteogenic differentiation. Npg Asia Mater. 2021; 13: 19.

111. Li Y, Huang G, Zhang X, Li B, Chen Y, Lu T, et al. Magnetic Hydrogels and Their Potential Biomedical Applications. Adv Funct Mater. 2013; 23: 660-72.

112. Liu X, Zhang J, Tang S, Sun J, Lou Z, Yang Y, et al. Growth enhancing effect of LBL-assembled magnetic nanoparticles on primary bone marrow cells. Sci China Mater. 2016; 59: 901-10.

113. Huang Q, Zou Y, Arno MC, Chen S, Wang T, Gao J, et al. Hydrogel scaffolds for differentiation of adipose-derived stem cells. Chem Soc Rev. 2017; 46: 6255-75.

114. Shuai CJ, Yang WJ, He CX, Peng SP, Gao CD, Yang YW, et al. A magnetic micro-environment in scaffolds for stimulating bone regeneration. Mater Des. 2020; 185: 108275.

115. Santhosh M, Choi JH, Choi JW. Magnetic-Assisted Cell Alignment within a Magnetic Nanoparticle-Decorated Reduced Graphene Oxide/Collagen 3D Nanocomposite Hydrogel. Nanomaterials 2019; 9: 1293.

116. Yook S, Shams Es-Haghi S, Yildirim A, Mutlu Z, Cakmak M. Anisotropic hydrogels formed by magnetically-oriented nanoclay suspensions for wound dressings. Soft Matter. 2019; 15: 9733-41.

117. Arami H, Khandhar A, Liggitt D, Krishnan KM. In vivo delivery, pharmacokinetics, biodistribution and toxicity of iron oxide nanoparticles. Chem Soc Rev. 2015; 44: 8576-607.

118. Soenen SJ, Parak WJ, Rejman J, Manshian B. (Intra)cellular stability of inorganic nanoparticles: effects on cytotoxicity, particle functionality, and biomedical applications. Chem Rev. 2015; 115: 2109-35.

119. Boraschi D, Italiani P, Palomba R, Decuzzi P, Duschl A, Fadeel B, et al. Nanoparticles and innate immunity: new perspectives on host defence. Semin Immunol. 2017; 34: 33-51.

120. Fadeel B. Hide and Seek: Nanomaterial Interactions With the Immune System. Front Immunol. 2019; 10: 133.

121. Jelena K-T, Lénaic L, Yasir J, Nathalie L, Teresa P, Claire W, et al. Biotransformations of magnetic nanoparticles in the body. Nano Today. 2016; 11: 280-4.

122. Nowak-Jary J, Machnicka B. Pharmacokinetics of magnetic iron oxide nanoparticles for medical applications. J Nanobiotechnology. 2022; 20: 305.

123. Chimene D, Kaunas R, Gaharwar AK. Hydrogel Bioink Reinforcement for Additive Manufacturing: A Focused Review of Emerging Strategies. Adv Mater. 2020; 32: e1902026.

124. Ouyang K, Zhuang J, Chen C, Wang X, Xu M, Xu Z. Gradient Diffusion Anisotropic Carboxymethyl Cellulose Hydrogels for Strain Sensors. Biomacromolecules. 2021; 22: 5033-41.

125. Dutta S, Singh AK, Pattader PSG, Bandyopadhyay D. Genesis of electric field assisted microparticle assemblage in a dielectric fluid. J Fluid Mech. 2021; 915: A6.

126. Cha H, Fallahi H, Dai Y, Yuan D, An H, Nguyen NT, et al. Multiphysics microfluidics for cell manipulation and separation: a review. Lab Chip. 2022; 22: 423-44.

127. Morales D, Bharti B, Dickey MD, Velev OD. Bending of Responsive Hydrogel Sheets Guided by Field-Assembled Microparticle Endoskeleton Structures. Small. 2016; 12: 2283-90.

128. Chiang MY, Cheng HW, Lo YC, Wang WC, Chang SJ, Cheng CH, et al. 4D spatiotemporal modulation of biomolecules distribution in anisotropic corrugated microwrinkles via electrically manipulated microcapsules within hierarchical hydrogel for spinal cord regeneration. Biomaterials. 2021; 271: 120762.

129. Ramon-Azcon J, Ahadian S, Estili M, Liang X, Ostrovidov S, Kaji H, et al. Dielectrophoretically aligned carbon nanotubes to control electrical and mechanical properties of hydrogels to fabricate contractile muscle myofibers. Adv Mater. 2013; 25: 4028-34.

130. Ahadian S, Yamada S, Ramon-Azcon J, Estili M, Liang X, Nakajima K, et al. Hybrid hydrogel-aligned carbon nanotube scaffolds to enhance cardiac differentiation of embryoid bodies. Acta Biomater. 2016; 31: 134-43.

131. Yang Y, Tan Y, Wang X, An W, Xu S, Liao W, et al. Photothermal Nanocomposite Hydrogel Actuator with Electric-Field-Induced Gradient and Oriented Structure. ACS Appl Mater Interfaces. 2018; 10: 7688-92.

132. Wang L, Song D, Zhang X, Ding Z, Kong X, Lu Q, et al. Silk-Graphene Hybrid Hydrogels with Multiple Cues to Induce Nerve Cell Behavior. ACS Biomater Sci Eng. 2019; 5: 613-22.

133. Huang K, Li Z, Lin J, Han G, Huang P. Two-dimensional transition metal carbides and nitrides (MXenes) for biomedical applications. Chem Soc Rev. 2018; 47: 5109-24.

134. Naguib M, Kurtoglu M, Presser V, Lu J, Niu J, Heon M, et al. Two-dimensional nanocrystals produced by exfoliation of Ti3 AlC2. Adv Mater. 2011; 23: 4248-53.

135. Xue P, Bisoyi HK, Chen Y, Zeng H, Yang J, Yang X, et al. Near-Infrared Light-Driven Shape-Morphing of Programmable Anisotropic Hydrogels Enabled by MXene Nanosheets. Angew Chem Int Ed Engl. 2021; 60: 3390-6.

136. Dutta P, Deb SK, Patra A, Majumdar A, Karim GM, Parashar CK, et al. Electric Field Guided Fast and Oriented Assembly of MXene into Scalable Pristine Hydrogels for Customized Energy Storage and Water Evaporation Applications. Adv Funct Mater. 2022; 32: 2204622.

137. Zhu Y-D, Ma X-Y, Li L-P, Yang Q-J, Jin F, Chen Z-N, et al. Surface Functional Modification by Ti3C2Tx MXene on PLLA Nanofibers for Optimizing Neural Stem Cell Engineering. Adv Healthc Mater. 2023; 12: 2300731.

138. Zhu QL, Dai CF, Wagner D, Khoruzhenko O, Hong W, Breu J, et al. Patterned Electrode Assisted One-Step Fabrication of Biomimetic Morphing Hydrogels with Sophisticated Anisotropic Structures. Adv Sci 2021; 8: e2102353.

139. da Silva LP, Kundu SC, Reis RL, Correlo VM. Electric Phenomenon: A Disregarded Tool in Tissue Engineering and Regenerative Medicine. Trends Biotechnol. 2020; 38: 24-49.

140. Zhu Z, Li Y, Xu H, Peng X, Chen YN, Shang C, et al. Tough and Thermosensitive Poly(N-isopropylacrylamide)/Graphene Oxide Hydrogels with Macroscopically Oriented Liquid Crystalline Structures. ACS Appl Mater Interfaces. 2016; 8: 15637-44.

141. Prince E, Alizadehgiashi M, Campbell M, Khuu N, Albulescu A, De France K, et al. Patterning of Structurally Anisotropic Composite Hydrogel Sheets. Biomacromolecules. 2018; 19: 1276-84.

142. Khuu N, Alizadehgiashi M, Gevorkian A, Galati E, Yan N, Kumacheva E. Temperature-Mediated Microfluidic Extrusion of Structurally Anisotropic Hydrogels. Adv Mater Technol. 2019; 4: 1800627.

143. Gevorkian A, Morozova SM, Kheiri S, Khuu N, Chen HY, Young E, et al. Actuation of Three-Dimensional-Printed Nanocolloidal Hydrogel with Structural Anisotropy. Adv Funct Mater. 2021; 31: 2010743.

144. Miyamoto N, Shintate M, Ikeda S, Hoshida Y, Yamauchi Y, Motokawa R, et al. Liquid crystalline inorganic nanosheets for facile synthesis of polymer hydrogels with anisotropies in structure, optical property, swelling/deswelling, and ion transport/fixation. Chem Commun 2013; 49: 1082-4.

145. Schwab A, Helary C, Richards RG, Alini M, Eglin D, D'Este M. Tissue mimetic hyaluronan bioink containing collagen fibers with controlled orientation modulating cell migration and alignment. Mater Today Bio. 2020; 7: 100058.

146. Mittal N, Benselfelt T, Ansari F, Gordeyeva K, Roth SV, Wagberg L, et al. Ion-Specific Assembly of Strong, Tough, and Stiff Biofibers. Angew Chem Int Ed Engl. 2019; 58: 18562-9.

147. Hiratani T, Kose O, Hamad WY, MacLachlan MJ. Stable and sensitive stimuli-responsive anisotropic hydrogels for sensing ionic strength and pressure. Mater Horiz. 2018; 5: 1076-81.

148. Wu Y, Jiang Z, Zan X, Lin Y, Wang Q. Shear flow induced long-range ordering of rod-like viral nanoparticles within hydrogel. Colloids and surfaces B, Biointerfaces. 2017; 158: 620-6.

149. Milani AH, Fielding LA, Greensmith P, Saunders BR, Adlam DJ, Freemont AJ, et al. Anisotropic pH-Responsive Hydrogels Containing Soft or Hard Rod-Like Particles Assembled Using Low Shear. Chem Mater. 2017; 29: 3100-10.

150. Siqueira G, Kokkinis D, Libanori R, Hausmann MK, Gladman AS, Neels A, et al. Cellulose Nanocrystal Inks for 3D Printing of Textured Cellular Architectures. Adv Funct Mater. 2017; 27: 1604619.

151. Gladman AS, Matsumoto EA, Nuzzo RG, Mahadevan L, Lewis JA. Biomimetic 4D printing. Nat Mater. 2016; 15: 413-8.

152. Prendergast ME, Davidson MD, Burdick JA. A biofabrication method to align cells within bioprinted photocrosslinkable and cell-degradable hydrogel constructs via embedded fibers. Biofabrication. 2021; 13: 044108.

153. Wang CL, Chai Y, Wen XD, Ai YJ, Zhao H, Hu WT, et al. Stretchable and Anisotropic Conductive Composite Hydrogel as Therapeutic Cardiac Patches. Acs Mater Lett. 2021; 3: 1238-48.

154. Hu DN, Cui YD, Mo KW, Wang JM, Huang YN, Miao XR, et al. Ultrahigh strength nanocomposite hydrogels designed by locking oriented tunicate cellulose nanocrystals in polymeric networks. Compos B Eng. 2020; 197: 108118.

155. Boularaoui S, Al Hussein G, Khan KA, Christoforou N, Stefanini C. An overview of extrusion-based bioprinting with a focus on induced shear stress and its effect on cell viability. Bioprinting. 2020; 20: e00093.

156. Lu KJ, Qian Y, Gong JX, Zhu ZY, Yin J, Ma L, et al. Biofabrication of aligned structures that guide cell orientation and applications in tissue engineering. Biodes Manuf. 2021; 4: 258-77.

157. Shen X, Chen L, Li D, Zhu L, Wang H, Liu C, et al. Assembly of colloidal nanoparticles directed by the microstructures of polycrystalline ice. ACS Nano. 2011; 5: 8426-33.

158. Biswas B, Misra M, Bisht AS, Kumar SK, Kumaraswamy G. Colloidal assembly by directional ice templating. Soft Matter. 2021; 17: 4098-108.

159. Radulescu DM, Neacsu IA, Grumezescu AM, Andronescu E. New Insights of Scaffolds Based on Hydrogels in Tissue Engineering. Polymers. 2022; 14: 799.

160. Qin K, Parisi C, Fernandes FM. Recent advances in ice templating: from biomimetic composites to cell culture scaffolds and tissue engineering. J Mater Chem B. 2021; 9: 889-907.

161. Darder M, Aranda P, Ferrer ML, Gutierrez MC, del Monte F, Ruiz-Hitzky E. Progress in bionanocomposite and bioinspired foams. Adv Mater. 2011; 23: 5262-7.

162. Feng YB, Liu H, Zhu WH, Guan L, Yang XT, Zvyagin AV, et al. Muscle-Inspired MXene Conductive Hydrogels with Anisotropy and Low-Temperature Tolerance for Wearable Flexible Sensors and Arrays. Adv Funct Mater. 2021; 31: 2105264.

163. Whitesides GM, Grzybowski B. Self-assembly at all scales. Science. 2002; 295: 2418-21.

164. Freeman R, Han M, Alvarez Z, Lewis JA, Wester JR, Stephanopoulos N, et al. Reversible self-assembly of superstructured networks. Science. 2018; 362: 808-13.

165. Webber MJ, Appel EA, Meijer EW, Langer R. Supramolecular biomaterials. Nat Mater. 2016; 15: 13-26.

166. Kyle S, Aggeli A, Ingham E, McPherson MJ. Production of self-assembling biomaterials for tissue engineering. Trends Biotechnol. 2009; 27: 423-33.

167. Bhorkar I, Dhoble AS. Advances in the synthesis and application of self-assembling biomaterials. Prog Biophys Mol Biol. 2021; 167: 46-62.

168. Liu L, Tanguy NR, Yan N, Wu Y, Liu X, Qing Y. Anisotropic cellulose nanocrystal hydrogel with multi-stimuli response to temperature and mechanical stress. Carbohydr Polym. 2022; 280: 119005.

169. Jiang Y, Zhao Y, Zhang AQ, Lei X, Qin SY. Solvent-tailored ordered self-assembly of oligopeptide amphiphiles to create an anisotropic meso-matrix. Chem Commun 2021; 57: 6181-4.

170. Patel A, Xue Y, Hartley R, Sant V, Eles JR, Cui XT, et al. Hierarchically aligned fibrous hydrogel films through microfluidic self-assembly of graphene and polysaccharides. Biotechnol Bioeng. 2018; 115: 2654-67.

171. Haque MA, Kamita G, Kurokawa T, Tsujii K, Gong JP. Unidirectional alignment of lamellar bilayer in hydrogel: one-dimensional swelling, anisotropic modulus, and stress/strain tunable structural color. Adv Mater. 2010; 22: 5110-4.

172. Pappas CG, Frederix PW, Mutasa T, Fleming S, Abul-Haija YM, Kelly SM, et al. Alignment of nanostructured tripeptide gels by directional ultrasonication. Chem Commun 2015; 51: 8465-8.

173. Hedegaard CL, Collin EC, Redondo-Gómez C, Nguyen LTH, Ng KW, Castrejón-Pita AA, et al. Hydrodynamically Guided Hierarchical Self-Assembly of Peptide-Protein Bioinks. Adv Funct Mater. 2018; 28: 1703716.

174. Wall BD, Diegelmann SR, Zhang S, Dawidczyk TJ, Wilson WL, Katz HE, et al. Aligned macroscopic domains of optoelectronic nanostructures prepared via shear-flow assembly of peptide hydrogels. Adv Mater. 2011; 23: 5009-14, 4967.

175. A Hill RJ, Sedman VL, Allen S, Williams P, Paoli M, Adler-Abramovich L, et al. Alignment of Aromatic Peptide Tubes in Strong Magnetic Fields. Adv Mater. 2007; 19: 4474-9.

176. Choi S, Kim J. Designed fabrication of super-stiff, anisotropic hybrid hydrogels via linear remodeling of polymer networks and subsequent crosslinking. J Mater Chem B. 2015; 3: 1479-83.

177. Choi S, Choi Y, Kim J. Anisotropic Hybrid Hydrogels with Superior Mechanical Properties Reminiscent of Tendons or Ligaments. Adv Funct Mater. 2019; 29: 1904342.

178. Chen L, Chang X, Chen J, Zhu Y. Ultrastretchable, Antifreezing, and High-Performance Strain Sensor Based on a Muscle-Inspired Anisotropic Conductive Hydrogel for Human Motion Monitoring and Wireless Transmission. ACS Appl Mater Interfaces. 2022; 14: 43833-43.

179. Park N, Kim J. Anisotropic Hydrogels with a Multiscale Hierarchical Structure Exhibiting High Strength and Toughness for Mimicking Tendons. ACS Appl Mater Interfaces. 2022; 14: 4479-89.

180. Choi S, Moon JR, Park N, Im J, Kim YE, Kim JH, et al. Bone-Adhesive Anisotropic Tough Hydrogel Mimicking Tendon Enthesis. Adv Mater. 2023; 35: e2206207.

181. Li K, Xu J, Wang J, Gu X, Li P, Fan Y. Oriented/dual-gradient in structure and mechanics chitosan hydrogel bio-films based on stretching for guiding cell orientation. Compos B Eng. 2022; 232: 109616.

182. Chen Y, Jiao C, Peng X, Liu T, Shi Y, Liang M, et al. Biomimetic anisotropic poly(vinyl alcohol) hydrogels with significantly enhanced mechanical properties by freezing–thawing under drawing. J Mater Chem B. 2019; 7: 3243-9.

183. Wang Q, Zhang Q, Wang G, Wang Y, Ren X, Gao G. Muscle-Inspired Anisotropic Hydrogel Strain Sensors. ACS Appl Mater Interfaces. 2022; 14: 1921-8.

184. Sun M, Li H, Hou Y, Huang N, Xia X, Zhu H, et al. Multifunctional tendon-mimetic hydrogels. Sci Adv. 2023; 9: eade6973.

185. Qiao LC, Du C, Gong JP, Wu ZL, Zheng Q. Programmed Diffusion Induces Anisotropic Superstructures in Hydrogels with High Mechano-Optical Sensitivity. Adv Mater Technol. 2019; 4: 1900665.

186. Mredha MTI, Tran VT, Jeong SG, Seon JK, Jeon I. A diffusion-driven fabrication technique for anisotropic tubular hydrogels. Soft Matter. 2018; 14: 7706-13.

187. Pei B, Wang Z, Nie J, Hu Q. Highly mineralized chitosan-based material with large size, gradient mineral distribution and hierarchical structure. Carbohydr Polym. 2019; 208: 336-44.

188. Kamranpour NO, Miri AK, James-Bhasin M, Nazhat SN. A gel aspiration-ejection system for the controlled production and delivery of injectable dense collagen scaffolds. Biofabrication. 2016; 8: 015018.

189. Marelli B, Ghezzi CE, James-Bhasin M, Nazhat SN. Fabrication of injectable, cellular, anisotropic collagen tissue equivalents with modular fibrillar densities. Biomaterials. 2015; 37: 183-93.

190. Park H, Nazhat SN, Rosenzweig DH. Mechanical activation drives tenogenic differentiation of human mesenchymal stem cells in aligned dense collagen hydrogels. Biomaterials. 2022; 286: 121606.

191. Shao L, Hou R, Zhu Y, Yao Y. Pre-shear bioprinting of highly oriented porous hydrogel microfibers to construct anisotropic tissues. Biomater Sci. 2021; 9: 6763-71.

192. Kim W, Kim G. A functional bioink and its application in myoblast alignment and differentiation. Chemical Engineering Journal. 2019; 366: 150-62.

193. Wang M, Yang C, Deng H, Du Y, Xiao L, Shi X. Electrically induced anisotropic assembly of chitosan with different molecular weights. Carbohydr Polym. 2023; 304: 120494.

194. Tong Y, Yang C, Qi L, Zhang J, Deng H, Du Y, et al. Tubular chitosan hydrogels with a tuneable lamellar structure programmed by electrical signals. Chem Commun 2022; 58: 5781-4.

195. Ding Z, Lu G, Cheng W, Xu G, Zuo B, Lu Q, et al. Tough Anisotropic Silk Nanofiber Hydrogels with Osteoinductive Capacity. ACS Biomater Sci Eng. 2020; 6: 2357-67.

196. Abu-Rub MT, Billiar KL, van Es MH, Knight A, Rodriguez BJ, Zeugolis DI, et al. Nano-textured self-assembled aligned collagen hydrogels promote directional neurite guidance and overcome inhibition by myelin associated glycoprotein. Soft Matter. 2011; 7: 2770-81.

197. Li L, Zhang Y, Lu H, Wang Y, Xu J, Zhu J, et al. Cryopolymerization enables anisotropic polyaniline hybrid hydrogels with superelasticity and highly deformation-tolerant electrochemical energy storage. Nat Commun. 2020; 11: 62.

198. Liang X, Chen G, Lin S, Zhang J, Wang L, Zhang P, et al. Anisotropically Fatigue-Resistant Hydrogels. Adv Mater. 2021; 33: e2102011.

199. Hua M, Wu S, Ma Y, Zhao Y, Chen Z, Frenkel I, et al. Strong tough hydrogels via the synergy of freeze-casting and salting out. Nature. 2021; 590: 594-9.

200. Wang YK, Li J, Muhammad N, Wang ZF, Wu DF. Hierarchical networks of anisotropic hydrogels based on cross-linked Poly (vinyl alcohol)/Poly(vinylpyrrolidone). Polymer. 2022; 251: 124920.

201. Dai RG, Meng L, Fu QJ, Hao SW, Yang J. Fabrication of Anisotropic Silk Fibroin-Cellulose Nanocrystals Cryogels with Tunable Mechanical Properties, Rapid Swelling, and Structural Recoverability via a Directional-Freezing Strategy. ACS Sustain Chem Eng. 2021; 9: 12274-85.

202. Rao Z, Lin T, Qiu S, Zhou J, Liu S, Chen S, et al. Decellularized nerve matrix hydrogel scaffolds with longitudinally oriented and size-tunable microchannels for peripheral nerve regeneration. Mater Sci Eng C Mater Biol Appl. 2021; 120: 111791.

203. Si Y, Wang L, Wang X, Tang N, Yu J, Ding B. Ultrahigh-Water-Content, Superelastic, and Shape-Memory Nanofiber-Assembled Hydrogels Exhibiting Pressure-Responsive Conductivity. Adv Mater. 2017; 29: 1700339.

204. Bai H, Polini A, Delattre B, Tomsia AP. Thermoresponsive composite hydrogels with aligned macroporous structure by ice-templated assembly. Chem Mater. 2013; 25: 4551-6.

205. Dong XY, Guo X, Liu QY, Zhao YJ, Qi HB, Zhai W. Strong and Tough Conductive Organo-Hydrogels via Freeze-Casting Assisted Solution Substitution. Adv Funct Mater. 2022; 32: 2203610.

206. Yuan Z, Yuan X, Zhao Y, Cai Q, Wang Y, Luo R, et al. Injectable GelMA Cryogel Microspheres for Modularized Cell Delivery and Potential Vascularized Bone Regeneration. Small. 2021; 17: e2006596.

207. Yuan X, Yuan Z, Wang Y, Wan Z, Wang X, Yu S, et al. Vascularized pulp regeneration via injecting simvastatin functionalized GelMA cryogel microspheres loaded with stem cells from human exfoliated deciduous teeth. Mater Today Bio. 2022; 13: 100209.

208. Murray KA, Gibson MI. Chemical approaches to cryopreservation. Nat Rev Chem. 2022; 6: 579-93.

209. Maral S, Albayrak M, Pala C, Yildiz A, Sahin O, Ozturk HB. Dimethyl Sulfoxide-Induced Tonic-Clonic Seizure and Cardiac Arrest During Infusion of Autologous Peripheral Blood Stem Cells. Cell Tissue Bank. 2018; 19: 831-2.

210. He H, Liu M, Wei J, Chen P, Wang S, Wang Q. Hydrogel with Aligned and Tunable Pore Via "Hot Ice" Template Applies as Bioscaffold. Adv Healthc Mater. 2016; 5: 648-52, 26.

211. Chen BK, Knight AM, Madigan NN, Gross L, Dadsetan M, Nesbitt JJ, et al. Comparison of polymer scaffolds in rat spinal cord: a step toward quantitative assessment of combinatorial approaches to spinal cord repair. Biomaterials. 2011; 32: 8077-86.

212. Hakim JS, Rodysill BR, Chen BK, Schmeichel AM, Yaszemski MJ, Windebank AJ, et al. Combinatorial tissue engineering partially restores function after spinal cord injury. J Tissue Eng Regen Med. 2019; 13: 857-73.

213. Hakim JS, Esmaeili Rad M, Grahn PJ, Chen BK, Knight AM, Schmeichel AM, et al. Positively Charged Oligo[Poly(Ethylene Glycol) Fumarate] Scaffold Implantation Results in a Permissive Lesion Environment after Spinal Cord Injury in Rat. Tissue Eng Part A. 2015; 21: 2099-114.

214. Siddiqui AM, Islam R, Cuellar CA, Silvernail JL, Knudsen B, Curley DE, et al. Newly regenerated axons via scaffolds promote sub-lesional reorganization and motor recovery with epidural electrical stimulation. NPJ Regen Med. 2021; 6: 66.

215. Dumont CM, Carlson MA, Munsell MK, Ciciriello AJ, Strnadova K, Park J, et al. Aligned hydrogel tubes guide regeneration following spinal cord injury. Acta Biomater. 2019; 86: 312-22.

216. Prang P, Muller R, Eljaouhari A, Heckmann K, Kunz W, Weber T, et al. The promotion of oriented axonal regrowth in the injured spinal cord by alginate-based anisotropic capillary hydrogels. Biomaterials. 2006; 27: 3560-9.

217. Pawar K, Mueller R, Caioni M, Prang P, Bogdahn U, Kunz W, et al. Increasing capillary diameter and the incorporation of gelatin enhance axon outgrowth in alginate-based anisotropic hydrogels. Acta Biomater. 2011; 7: 2826-34.

218. Nutzl M, Schrottenbaum M, Muller T, Muller R. Mechanical properties and chemical stability of alginate-based anisotropic capillary hydrogels. J Mech Behav Biomed Mater. 2022; 134: 105397.

219. Li C, Kuss M, Kong Y, Nie F, Liu X, Liu B, et al. 3D Printed Hydrogels with Aligned Microchannels to Guide Neural Stem Cell Migration. ACS Biomater Sci Eng. 2021; 7: 690-700.

220. Unagolla JM, Jayasuriya AC. Hydrogel-based 3D bioprinting: A comprehensive review on cell-laden hydrogels, bioink formulations, and future perspectives. Appl Mater Today. 2020; 18: 100479.

221. Ma Y, Wang X, Su T, Lu F, Chang Q, Gao J. Recent Advances in Macroporous Hydrogels for Cell Behavior and Tissue Engineering. Gels. 2022; 8.

222. Pashuck ET, Stevens M. From clinical imaging to implantation of 3D printed tissues. Nat Biotechnol. 2016; 34: 295-6.

223. Li X, Liu B, Pei B, Chen J, Zhou D, Peng J, et al. Inkjet Bioprinting of Biomaterials. Chem Rev. 2020; 120: 10793-833.

224. Derakhshanfar S, Mbeleck R, Xu K, Zhang X, Zhong W, Xing M. 3D bioprinting for biomedical devices and tissue engineering: A review of recent trends and advances. Bioact Mater. 2018; 3: 144-56.

225. Zhang M, Wang Y, Jian M, Wang C, Liang X, Niu J, et al. Spontaneous Alignment of Graphene Oxide in Hydrogel during 3D Printing for Multistimuli-Responsive Actuation. Adv Sci 2020; 7: 1903048.

226. Zhao WW, Chen LJ, Hu SM, Shi ZJ, Gao X, Silberschmidt VV. Printed hydrogel nanocomposites: fine-tuning nanostructure for anisotropic mechanical and conductive properties. Advanced Composites and Hybrid Materials. 2020; 3: 315-24.

227. Pardo A, Bakht SM, Gomez-Florit M, Rial R, Monteiro RF, Teixeira SPB, et al. Magnetically-Assisted 3D Bioprinting of Anisotropic Tissue-Mimetic Constructs. Adv Funct Mater. 2022; 32: 2208940.

228. Chiu LL, Janic K, Radisic M. Engineering of oriented myocardium on three-dimensional micropatterned collagen-chitosan hydrogel. Int J Artif Organs. 2012; 35: 237-50.

229. Tekin H, Tsinman T, Sanchez JG, Jones BJ, Camci-Unal G, Nichol JW, et al. Responsive micromolds for sequential patterning of hydrogel microstructures. J Am Chem Soc. 2011; 133: 12944-7.

230. Hu Y, You JO, Aizenberg J. Micropatterned Hydrogel Surface with High-Aspect-Ratio Features for Cell Guidance and Tissue Growth. ACS Appl Mater Interfaces. 2016; 8: 21939-45.

231. Choi YS, Vincent LG, Lee AR, Kretchmer KC, Chirasatitsin S, Dobke MK, et al. The alignment and fusion assembly of adipose-derived stem cells on mechanically patterned matrices. Biomaterials. 2012; 33: 6943-51.

232. Wang C, Yang S, Guo Q, Xu L, Xu Y, Qiu D. Wrinkled double network hydrogel via simple stretch-recovery. Chem Commun 2020; 56: 13587-90.

233. Yun YF, Guan Y, Zhang YJ. Patterned PHEMA Films Synthesized by Redox Polymerization for Multicellular Spheroid Generation. Ind Eng Chem Res. 2019; 58: 10713-23.

234. Chen Q, Cui L, Guan Y, Zhang Y. Diels-Alder Cross-Linked, Washing-Free Hydrogel Films with Ordered Wrinkling Patterns for Multicellular Spheroid Generation. Biomacromolecules. 2021; 22: 3474-85.

235. Rodríguez-Hernández J. Wrinkled interfaces: Taking advantage of surface instabilities to pattern polymer surfaces. Progress in Polymer Science. 2015; 42: 1-41.

236. Allen HG. Analysisand design of Structural Sandwich panels. Pergamon Press pp8; 1969.

237. Bowden N, Brittain S, Evans AG, Hutchinson JW, Whitesides GM. Spontaneous formation of ordered structures in thin films of metals supported on an elastomeric polymer. Nature. 1998; 393: 146-9.

238. Liu N, Sun Q, Yang Z, Shan L, Wang Z, Li H. Wrinkled Interfaces: Taking Advantage of Anisotropic Wrinkling to Periodically Pattern Polymer Surfaces. Adv Sci. 2023; 10: e2207210.

239. Kashihara Y, Asoh TA, Uyama H. Travelling Wave Generation of Wrinkles on the Hydrogel Surfaces. Macromol Rapid Commun. 2022; 43: e2100848.

240. Zou J, Wu S, Chen J, Lei X, Li Q, Yu H, et al. Highly Efficient and Environmentally Friendly Fabrication of Robust, Programmable, and Biocompatible Anisotropic, All-Cellulose, Wrinkle-Patterned Hydrogels for Cell Alignment. Adv Mater. 2019; 31: e1904762.

241. Kong W, Wang C, Jia C, Kuang Y, Pastel G, Chen C, et al. Muscle-Inspired Highly Anisotropic, Strong, Ion-Conductive Hydrogels. Adv Mater. 2021; 33: e2103732.

242. Xu RNA, Zhao XD, Ma SH, Ma ZF, Wang R, Cai MR, et al. Hydrogen bonding induced enhancement for constructing anisotropic sugarcane composite hydrogels. J Appl Polym Sci. 2021; 138: e51374.

243. Yan G, He S, Ma S, Zeng A, Chen G, Tang X, et al. Catechol-based all-wood hydrogels with anisotropic, tough, and flexible properties for highly sensitive pressure sensing. Chemical Engineering Journal. 2022; 427: 131896.

244. Yang G, Lin H, Rothrauff BB, Yu S, Tuan RS. Multilayered polycaprolactone/gelatin fiber-hydrogel composite for tendon tissue engineering. Acta Biomater. 2016; 35: 68-76.

245. Bas O, De-Juan-Pardo EM, Meinert C, D'Angella D, Baldwin JG, Bray LJ, et al. Biofabricated soft network composites for cartilage tissue engineering. Biofabrication. 2017; 9: 025014.

246. Wu Y, Wang L, Guo B, Ma PX. Interwoven Aligned Conductive Nanofiber Yarn/Hydrogel Composite Scaffolds for Engineered 3D Cardiac Anisotropy. ACS Nano. 2017; 11: 5646-59.

247. Freedman BR, Mooney DJ. Biomaterials to Mimic and Heal Connective Tissues. Adv Mater. 2019; 31: e1806695.

248. Lutolf MP, Hubbell JA. Synthetic biomaterials as instructive extracellular microenvironments for morphogenesis in tissue engineering. Nat Biotechnol. 2005; 23: 47-55.

249. Gonzalez-Fernandez T, Sikorski P, Leach JK. Bio-instructive materials for musculoskeletal regeneration. Acta Biomater. 2019; 96: 20-34.

250. Higuchi A, Ling QD, Chang Y, Hsu ST, Umezawa A. Physical cues of biomaterials guide stem cell differentiation fate. Chem Rev. 2013; 113: 3297-328.

251. Zielinski PS, Gudeti PKR, Rikmanspoel T, Wlodarczyk-Biegun MK. 3D printing of bio-instructive materials: Toward directing the cell. Bioact Mater. 2023; 19: 292-327.

252. Humphrey JD, Dufresne ER, Schwartz MA. Mechanotransduction and extracellular matrix homeostasis. Nat Rev Mol Cell Biol. 2014; 15: 802-12.

253. Desai TA. Micro- and nanoscale structures for tissue engineering constructs. Med Eng Phys. 2000; 22: 595-606.

254. Teixeira AI, Abrams GA, Bertics PJ, Murphy CJ, Nealey PF. Epithelial contact guidance on well-defined micro- and nanostructured substrates. J Cell Sci. 2003; 116: 1881-92.

255. Curtis AS, Varde M. Control of Cell Behavior: Topological Factors. J Natl Cancer Inst. 1964; 33: 15-26.

256. Luo J, Walker M, Xiao Y, Donnelly H, Dalby MJ, Salmeron-Sanchez M. The influence of nanotopography on cell behaviour through interactions with the extracellular matrix - A review. Bioact Mater. 2022; 15: 145-59.

257. Gumbiner BM. Cell adhesion: the molecular basis of tissue architecture and morphogenesis. Cell. 1996; 84: 345-57.

258. Kechagia JZ, Ivaska J, Roca-Cusachs P. Integrins as biomechanical sensors of the microenvironment. Nat Rev Mol Cell Biol. 2019; 20: 457-73.

259. Karimi F, O'Connor AJ, Qiao GG, Heath DE. Integrin Clustering Matters: A Review of Biomaterials Functionalized with Multivalent Integrin-Binding Ligands to Improve Cell Adhesion, Migration, Differentiation, Angiogenesis, and Biomedical Device Integration. Adv Healthc Mater. 2018; 7: e1701324.

260. Horton ER, Astudillo P, Humphries MJ, Humphries JD. Mechanosensitivity of integrin adhesion complexes: role of the consensus adhesome. Exp Cell Res. 2016; 343: 7-13.

261. Biggs MJ, Richards RG, Gadegaard N, Wilkinson CD, Oreffo RO, Dalby MJ. The use of nanoscale topography to modulate the dynamics of adhesion formation in primary osteoblasts and ERK/MAPK signalling in STRO-1+ enriched skeletal stem cells. Biomaterials. 2009; 30: 5094-103.

262. Goult BT, Yan J, Schwartz MA. Talin as a mechanosensitive signaling hub. J Cell Biol. 2018; 217: 3776-84.

263. Grashoff C, Hoffman BD, Brenner MD, Zhou R, Parsons M, Yang MT, et al. Measuring mechanical tension across vinculin reveals regulation of focal adhesion dynamics. Nature. 2010; 466: 263-6.

264. Sawada Y, Tamada M, Dubin-Thaler BJ, Cherniavskaya O, Sakai R, Tanaka S, et al. Force sensing by mechanical extension of the Src family kinase substrate p130Cas. Cell. 2006; 127: 1015-26.

265. Marcus M, Baranes K, Park M, Choi IS, Kang K, Shefi O. Interactions of Neurons with Physical Environments. Adv Healthc Mater. 2017; 6: 1700267.

266. Dalby MJ, Gadegaard N, Oreffo RO. Harnessing nanotopography and integrin-matrix interactions to influence stem cell fate. Nat Mater. 2014; 13: 558-69.

267. Tonazzini I, Meucci S, Faraci P, Beltram F, Cecchini M. Neuronal differentiation on anisotropic substrates and the influence of nanotopographical noise on neurite contact guidance. Biomaterials. 2013; 34: 6027-36.

268. Seo CH, Furukawa K, Montagne K, Jeong H, Ushida T. The effect of substrate microtopography on focal adhesion maturation and actin organization via the RhoA/ROCK pathway. Biomaterials. 2011; 32: 9568-75.

269. Ozasa R, Matsugaki A, Matsuzaka T, Ishimoto T, Yun H-S, Nakano T. Superior Alignment of Human iPSC-Osteoblasts Associated with Focal Adhesion Formation Stimulated by Oriented Collagen Scaffold. Int J Mol Sci; 2021; 22, 6232.

270. Ray A, Lee O, Win Z, Edwards RM, Alford PW, Kim DH, et al. Anisotropic forces from spatially constrained focal adhesions mediate contact guidance directed cell migration. Nat Commun. 2017; 8: 14923.

271. Ballester-Beltrán J, Biggs MJP, Dalby MJ, Salmerón-Sánchez M and Leal-Egaña A. Sensing the Difference: The Influence of Anisotropic Cues on Cell Behavior. Front Mater. 2015; 2: 39.

272. Paluch EK, Aspalter IM, Sixt M. Focal Adhesion-Independent Cell Migration. Annu Rev Cell Dev Biol. 2016; 32: 469-90.

273. Shellard A, Mayor R. All Roads Lead to Directional Cell Migration. Trends Cell Biol. 2020; 30: 852-68.

274. Bear JE, Haugh JM. Directed migration of mesenchymal cells: where signaling and the cytoskeleton meet. Curr Opin Cell Biol. 2014; 30: 74-82.

275. Lammermann T, Sixt M. Mechanical modes of 'amoeboid' cell migration. Curr Opin Cell Biol. 2009; 21: 636-44.

276. Ladoux B, Mege RM. Mechanobiology of collective cell behaviours. Nat Rev Mol Cell Biol. 2017; 18: 743-57.

277. Liu YJ, Le Berre M, Lautenschlaeger F, Maiuri P, Callan-Jones A, Heuze M, et al. Confinement and low adhesion induce fast amoeboid migration of slow mesenchymal cells. Cell. 2015; 160: 659-72.

278. Ruprecht V, Wieser S, Callan-Jones A, Smutny M, Morita H, Sako K, et al. Cortical contractility triggers a stochastic switch to fast amoeboid cell motility. Cell. 2015; 160: 673-85.

279. Lou HY, Zhao W, Zeng Y, Cui B. The Role of Membrane Curvature in Nanoscale Topography-Induced Intracellular Signaling. Acc Chem Res. 2018; 51: 1046-53.

280. Driscoll MK, Sun X, Guven C, Fourkas JT, Losert W. Cellular contact guidance through dynamic sensing of nanotopography. ACS Nano. 2014; 8: 3546-55.

281. Le Maout E, Lo Vecchio S, Kumar Korla P, Jinn-Chyuan Sheu J, Riveline D. Ratchetaxis in Channels: Entry Point and Local Asymmetry Set Cell Directions in Confinement. Biophys J. 2020; 119: 1301-8.

282. Ramirez-San Juan GR, Oakes PW, Gardel ML. Contact guidance requires spatial control of leading-edge protrusion. Mol Biol Cell. 2017; 28: 1043-53.

283. Jang KJ, Kim MS, Feltrin D, Jeon NL, Suh KY, Pertz O. Two distinct filopodia populations at the growth cone allow to sense nanotopographical extracellular matrix cues to guide neurite outgrowth. PLoS One. 2010; 5: e15966.

284. Lou HY, Zhao W, Li X, Duan L, Powers A, Akamatsu M, et al. Membrane curvature underlies actin reorganization in response to nanoscale surface topography. Proc Natl Acad Sci U S A. 2019; 116: 23143-51.

285. Lomakin AJ, Cattin CJ, Cuvelier D, Alraies Z, Molina M, Nader GPF, et al. The nucleus acts as a ruler tailoring cell responses to spatial constraints. Science. 2020; 370: eaba2894.

286. Kim HN, Hong Y, Kim MS, Kim SM, Suh KY. Effect of orientation and density of nanotopography in dermal wound healing. Biomaterials. 2012; 33: 8782-92.

287. Doron G, Temenoff JS. Culture Substrates for Improved Manufacture of Mesenchymal Stromal Cell Therapies. Adv Healthc Mater. 2021; 10: e2100016.

288. Oh S, Daraio C, Chen LH, Pisanic TR, Finones RR, Jin S. Significantly accelerated osteoblast cell growth on aligned TiO2 nanotubes. J Biomed Mater Res A. 2006; 78: 97-103.

289. Tan X, Xu A, Zhao T, Zhao Q, Zhang J, Fan C, et al. Simulated microgravity inhibits cell focal adhesions leading to reduced melanoma cell proliferation and metastasis via FAK/RhoA-regulated mTORC1 and AMPK pathways. Sci Rep. 2018; 8: 3769.

290. Moreno-Layseca P, Streuli CH. Signalling pathways linking integrins with cell cycle progression. Matrix Biol. 2014; 34: 144-53.

291. Izadpanahi M, Seyedjafari E, Arefian E, Hamta A, Hosseinzadeh S, Kehtari M, et al. Nanotopographical cues of electrospun PLLA efficiently modulate non-coding RNA network to osteogenic differentiation of mesenchymal stem cells during BMP signaling pathway. Mater Sci Eng C Mater Biol Appl. 2018; 93: 686-703.

292. Lee MS, Lee DH, Jeon J, Oh SH, Yang HS. Topographically Defined, Biodegradable Nanopatterned Patches to Regulate Cell Fate and Acceleration of Bone Regeneration. ACS Appl Mater Interfaces. 2018; 10: 38780-90.

293. Xiao Q-R, Zhang N, Wang X, Man X-Y, Yang K, Lü L-X, et al. Oriented Surface Nanotopography Promotes the Osteogenesis of Mesenchymal Stem Cells. Adv Mater Interfaces. 2017; 4: 1600652.

294. McNamara LE, McMurray RJ, Biggs MJ, Kantawong F, Oreffo RO, Dalby MJ. Nanotopographical control of stem cell differentiation. J Tissue Eng. 2010; 2010: 120623.

295. Lauria I, Kramer M, Schroder T, Kant S, Hausmann A, Boke F, et al. Inkjet printed periodical micropatterns made of inert alumina ceramics induce contact guidance and stimulate osteogenic differentiation of mesenchymal stromal cells. Acta Biomater. 2016; 44: 85-96.

296. Seo CH, Jeong H, Feng Y, Montagne K, Ushida T, Suzuki Y, et al. Micropit surfaces designed for accelerating osteogenic differentiation of murine mesenchymal stem cells via enhancing focal adhesion and actin polymerization. Biomaterials. 2014; 35: 2245-52.

297. Zhou C, Zhang D, Zou J, Li X, Zou S, Xie J. Substrate Compliance Directs the Osteogenic Lineages of Stem Cells from the Human Apical Papilla via the Processes of Mechanosensing and Mechanotransduction. ACS Appl Mater Interfaces. 2019; 11: 26448-59.

298. Yang LL, Ge L, Zhou QH, Mokabber T, Pei YT, Bron R, et al. Biomimetic Multiscale Hierarchical Topography Enhances Osteogenic Differentiation of Human Mesenchymal Stem Cells. Adv Mater Interfaces. 2020; 7: 2000385.

299. Paris JL, Lafuente-Gomez N, Cabanas MV, Roman J, Pena J, Vallet-Regi M. Fabrication of a nanoparticle-containing 3D porous bone scaffold with proangiogenic and antibacterial properties. Acta Biomater. 2019; 86: 441-9.

300. Medvedeva EV, Grebenik EA, Gornostaeva SN, Telpuhov VI, Lychagin AV, Timashev PS, et al. Repair of Damaged Articular Cartilage: Current Approaches and Future Directions. Int J Mol Sci. 2018; 19: 2366.

301. Mendler M, Eich-Bender SG, Vaughan L, Winterhalter KH, Bruckner P. Cartilage contains mixed fibrils of collagen types II, IX, and XI. J Cell Biol. 1989; 108: 191-7.

302. Parsons P, Gilbert SJ, Vaughan-Thomas A, Sorrell DA, Notman R, Bishop M, et al. Type IX collagen interacts with fibronectin providing an important molecular bridge in articular cartilage. J Biol Chem. 2011; 286: 34986-97.

303. Sartore L, Manferdini C, Saleh Y, Dey K, Gabusi E, Ramorino G, et al. Polysaccharides on gelatin-based hydrogels differently affect chondrogenic differentiation of human mesenchymal stromal cells. Mater Sci Eng C Mater Biol Appl. 2021; 126: 112175.

304. Makris EA, Gomoll AH, Malizos KN, Hu JC, Athanasiou KA. Repair and tissue engineering techniques for articular cartilage. Nat Rev Rheumatol. 2015; 11: 21-34.

305. Im GI, Cho CS. Updates in Cartilage Tissue Regeneration. Tissue Eng Regen Med. 2019; 16: 325-6.

306. Zhang Q, Xu ZY, Zhang XP, Liu CJ, Yang R, Sun YG, et al. 3D Printed High-Strength Supramolecular Polymer Hydrogel-Cushioned Radially and Circumferentially Oriented Meniscus Substitute. Adv Funct Mater. 2022; 32: 2200360.

307. Dey K, Agnelli S, Re F, Russo D, Lisignoli G, Manferdini C, et al. Rational Design and Development of Anisotropic and Mechanically Strong Gelatin-Based Stress Relaxing Hydrogels for Osteogenic/Chondrogenic Differentiation. Macromol Biosci. 2019; 19: e1900099.

308. Liu DL, Dong XF, Han BG, Huang H, Qi M. Cellulose nanocrystal/collagen hydrogels reinforced by anisotropic structure: Shear viscoelasticity and related strengthening mechanism. Composites Communications. 2020; 21: 100374.

309. Chen Q, Zhang X, Chen K, Feng C, Wang D, Qi J, et al. Bilayer Hydrogels with Low Friction and High Load-Bearing Capacity by Mimicking the Oriented Hierarchical Structure of Cartilage. ACS Appl Mater Interfaces. 2022; 14: 52347-58.

310. Wu X, Ding J, Xu P, Feng X, Wang Z, Zhou T, et al. A cell-free ROS-responsive hydrogel/oriented poly(lactide-co-glycolide) hybrid scaffold for reducing inflammation and restoring full-thickness cartilage defectsin vivo. Biomed Mater. 2021; 16: 064101.

311. Gossla E, Bernhardt A, Tonndorf R, Aibibu D, Cherif C, Gelinsky M. Anisotropic Chitosan Scaffolds Generated by Electrostatic Flocking Combined with Alginate Hydrogel Support Chondrogenic Differentiation. Int J Mol Sci. 2021; 22: 9341.

312. Wang DQ, Xu H, Liu JM, Chen ZX, Li YY, Hu BH, et al. Bio-inspired cellulose reinforced anisotropic composite hydrogel with zone-dependent complex mechanical adaptability and cell recruitment characteristics. Compos B Eng. 2020; 202: 108418.

313. Wang S, Zhao S, Yu J, Gu Z, Zhang Y. Advances in Translational 3D Printing for Cartilage, Bone, and Osteochondral Tissue Engineering. Small. 2022; 18: e2201869.

314. Burr DB. Bone Morphology and Organization. In: Burr DB, Allen MR, editors. Basic and Applied Bone Biology: Academic Press; 2019. 3-26.

315. Gao C, Peng S, Feng P, Shuai C. Bone biomaterials and interactions with stem cells. Bone Res. 2017; 5: 17059.

316. Wildemann B, Ignatius A, Leung F, Taitsman LA, Smith RM, Pesantez R, et al. Non-union bone fractures. Nat Rev Dis Primers. 2021; 7: 57.

317. Qu M, Wang C, Zhou X, Libanori A, Jiang X, Xu W, et al. Multi-Dimensional Printing for Bone Tissue Engineering. Adv Healthc Mater. 2021; 10: e2001986.

318. Zhang X, Hang Y, Ding Z, Xiao L, Cheng W, Lu Q. Macroporous Silk Nanofiber Cryogels with Tunable Properties. Biomacromolecules. 2022; 23: 2160-9.

319. Xu T, Zhao W, Zhu JM, Albanna MZ, Yoo JJ, Atala A. Complex heterogeneous tissue constructs containing multiple cell types prepared by inkjet printing technology. Biomaterials. 2013; 34: 130-9.

320. Sithole MN, Kumar P, du Toit LC, Marimuthu T, Choonara YE, Pillay V. A 3D bioprinted in situ conjugated-co-fabricated scaffold for potential bone tissue engineering applications. J Biomed Mater Res A. 2018; 106: 1311-21.

321. Lin XH, Xing X, Li SS, Wu XY, Jia QQ, Tu H, et al. Anisotropic Hybrid Hydrogels Constructed by the Noncovalent Assembly for Biomimetic Tissue Scaffold. Adv Funct Mater. 2022; 32: 2112685.

322. He XH, Li WY, Liu K, Wen W, Lu L, Liu MX, et al. Anisotropic and robust hydrogels combined osteogenic and angiogenic activity as artificial periosteum. Compos B Eng. 2022; 233: 109627.

323. Chen J, Chen J, Zhu Z, Sun T, Liu M, Lu L, et al. Drug-Loaded and Anisotropic Wood-Derived Hydrogel Periosteum with Super Antibacterial, Anti-Inflammatory, and Osteogenic Activities. ACS Appl Mater Interfaces. 2022; 14: 50485-98.

324. Ruiz-Alonso S, Lafuente-Merchan M, Ciriza J, Saenz-Del-Burgo L, Pedraz JL. Tendon tissue engineering: Cells, growth factors, scaffolds and production techniques. J Control Release. 2021; 333: 448-86.

325. Bosworth LA. Tendon tissue regeneration. In: Bosworth LA, Downes S, editors. Electrospinning for Tissue Regeneration: Woodhead Publishing; 2011. 148-67.

326. Lipman K, Wang C, Ting K, Soo C, Zheng Z. Tendinopathy: injury, repair, and current exploration. Drug Des Devel Ther. 2018; 12: 591-603.

327. Maganaris CN, Narici MV. Mechanical Properties of Tendons. In: Maffulli N, Renström P, Leadbetter WB, editors. Tendon Injuries: Basic Science and Clinical Medicine. London: Springer London; 2005. 14-21.

328. Paredes JJ, Andarawis-Puri N. Therapeutics for tendon regeneration: a multidisciplinary review of tendon research for improved healing. Ann N Y Acad Sci. 2016; 1383: 125-38.

329. Linderman SW, Gelberman RH, Thomopoulos S, Shen H. Cell and Biologic-Based Treatment of Flexor Tendon Injuries. Oper Tech Orthop. 2016; 26: 206-15.

330. Linderman SW, Shen H, Yoneda S, Jayaram R, Tanes ML, Sakiyama-Elbert SE, et al. Effect of connective tissue growth factor delivered via porous sutures on the proliferative stage of intrasynovial tendon repair. J Orthop Res. 2018; 36: 2052-63.

331. Prabhath A, Vernekar VN, Sanchez E, Laurencin CT. Growth factor delivery strategies for rotator cuff repair and regeneration. Int J Pharm. 2018; 544: 358-71.

332. Rinoldi C, Costantini M, Kijenska-Gawronska E, Testa S, Fornetti E, Heljak M, et al. Tendon Tissue Engineering: Effects of Mechanical and Biochemical Stimulation on Stem Cell Alignment on Cell-Laden Hydrogel Yarns. Adv Healthc Mater. 2019; 8: e1801218.

333. Screen HR, Berk DE, Kadler KE, Ramirez F, Young MF. Tendon functional extracellular matrix. J Orthop Res. 2015; 33: 793-9.

334. Ackermann PW, Salo P, Hart DA. Tendon Innervation. Adv Exp Med Biol. 2016; 920: 35-51.

335. Calejo I, Costa-Almeida R, Reis RL, Gomes ME. A Textile Platform Using Continuous Aligned and Textured Composite Microfibers to Engineer

Tendon-to-Bone Interface Gradient Scaffolds. Adv Healthc Mater. 2019; 8: e1900200.

336. Lin Z, Zhao X, Chen S, Du C. Osteogenic and tenogenic induction of hBMSCs by an integrated nanofibrous scaffold with chemical and structural mimicry of the bone-ligament connection. J Mater Chem B. 2017; 5: 1015-27.

337. Kim BS, Kim EJ, Choi JS, Jeong JH, Jo CH, Cho YW. Human collagen-based multilayer scaffolds for tendon-to-bone interface tissue engineering. J Biomed Mater Res A. 2014; 102: 4044-54.

338. Sensini A, Cristofolini L. Biofabrication of Electrospun Scaffolds for the Regeneration of Tendons and Ligaments. Materials 2018; 11: 1963.

339. Frontera WR, Ochala J. Skeletal muscle: a brief review of structure and function. Calcif Tissue Int. 2015; 96: 183-95.

340. Mukund K, Subramaniam S. Skeletal muscle: A review of molecular structure and function, in health and disease. Wiley Interdiscip Rev Syst Biol Med. 2020; 12: e1462.

341. Gholobova D, Terrie L, Gerard M, Declercq H, Thorrez L. Vascularization of tissue-engineered skeletal muscle constructs. Biomaterials. 2020; 235: 119708.

342. Ostrovidov S, Salehi S, Costantini M, Suthiwanich K, Ebrahimi M, Sadeghian RB, et al. 3D Bioprinting in Skeletal Muscle Tissue Engineering. Small. 2019; 15: e1805530.

343. Grogan BF, Hsu JR, Skeletal Trauma Research C. Volumetric muscle loss. J Am Acad Orthop Surg. 2011; 19 Suppl 1: S35-7.

344. Russell CS, Mostafavi A, Quint JP, Panayi AC, Baldino K, Williams TJ, et al. In Situ Printing of Adhesive Hydrogel Scaffolds for the Treatment of Skeletal Muscle Injuries. ACS Appl Bio Mater. 2020; 3: 1568-79.

345. Shandalov Y, Egozi D, Koffler J, Dado-Rosenfeld D, Ben-Shimol D, Freiman A, et al. An engineered muscle flap for reconstruction of large soft tissue defects. Proc Natl Acad Sci U S A. 2014; 111: 6010-5.

346. Costantini M, Testa S, Mozetic P, Barbetta A, Fuoco C, Fornetti E, et al. Microfluidic-enhanced 3D bioprinting of aligned myoblast-laden hydrogels leads to functionally organized myofibers in vitro and in vivo. Biomaterials. 2017; 131: 98-110.

347. Virani SS, Alonso A, Aparicio HJ, Benjamin EJ, Bittencourt MS, Callaway CW, et al. Heart Disease and Stroke Statistics-2021 Update: A Report From the American Heart Association. Circulation. 2021; 143: e254-e743.

348. Ye H, Zhang K, Kai D, Li Z, Loh XJ. Polyester elastomers for soft tissue engineering. Chem Soc Rev. 2018; 47: 4545-80.

349. Zhuang RZ, Lock R, Liu B, Vunjak-Novakovic G. Opportunities and challenges in cardiac tissue engineering from an analysis of two decades of advances. Nat Biomed Eng. 2022; 6: 327-38.

350. Walker BW, Lara RP, Yu CH, Sani ES, Kimball W, Joyce S, et al. Engineering a naturally-derived adhesive and conductive cardiopatch. Biomaterials. 2019; 207: 89-101.

351. Montgomery M, Ahadian S, Davenport Huyer L, Lo Rito M, Civitarese RA, Vanderlaan RD, et al. Flexible shape-memory scaffold for minimally invasive delivery of functional tissues. Nat Mater. 2017; 16: 1038-46.

352. Feiner R, Engel L, Fleischer S, Malki M, Gal I, Shapira A, et al. Engineered hybrid cardiac patches with multifunctional electronics for online monitoring and regulation of tissue function. Nat Mater. 2016; 15: 679-85.

353. Ren J, Xu Q, Chen X, Li W, Guo K, Zhao Y, et al. Superaligned Carbon Nanotubes Guide Oriented Cell Growth and Promote Electrophysiological Homogeneity for Synthetic Cardiac Tissues. Adv Mater. 2017; 29: 1702713.

354. Kharaziha M, Nikkhah M, Shin SR, Annabi N, Masoumi N, Gaharwar AK, et al. PGS:Gelatin nanofibrous scaffolds with tunable mechanical and structural properties for engineering cardiac tissues. Biomaterials. 2013; 34: 6355-66.

355. Tijore A, Irvine SA, Sarig U, Mhaisalkar P, Baisane V, Venkatraman S. Contact guidance for cardiac tissue engineering using 3D bioprinted gelatin patterned hydrogel. Biofabrication. 2018; 10: 025003.

356. Navaei A, Moore N, Sullivan RT, Truong D, Migrino RQ, Nikkhah M. Electrically conductive hydrogel-based micro-topographies for the development of organized cardiac tissues. RSC Adv. 2017; 7: 3302-12.

357. Mehrotra S, de Melo BAG, Hirano M, Keung W, Li RA, Mandal BB, et al. Nonmulberry Silk Based Ink for Fabricating Mechanically Robust Cardiac Patches and Endothelialized Myocardium-on-a-Chip Application. Adv Funct Mater. 2020; 30: 1907436.

358. Nunes SS, Miklas JW, Liu J, Aschar-Sobbi R, Xiao Y, Zhang B, et al. Biowire: a platform for maturation of human pluripotent stem cell-derived cardiomyocytes. Nat Methods. 2013; 10: 781-7.

359. Fleischer S, Shapira A, Feiner R, Dvir T. Modular assembly of thick multifunctional cardiac patches. Proc Natl Acad Sci U S A. 2017; 114: 1898-903.

360. Sousa AMM, Meyer KA, Santpere G, Gulden FO, Sestan N. Evolution of the Human Nervous System Function, Structure, and Development. Cell. 2017; 170: 226-47.

361. Wieringa PA, Goncalves de Pinho AR, Micera S, van Wezel RJA, Moroni L. Biomimetic Architectures for Peripheral Nerve Repair: A Review of Biofabrication Strategies. Adv Healthc Mater. 2018; 7: e1701164.

362. Georgiou M, Bunting SC, Davies HA, Loughlin AJ, Golding JP, Phillips JB. Engineered neural tissue for peripheral nerve repair. Biomaterials. 2013; 34: 7335-43.

363. Du J, Chen H, Qing L, Yang X, Jia X. Biomimetic neural scaffolds: a crucial step towards optimal peripheral nerve regeneration. Biomater Sci. 2018; 6: 1299-311.

364. Liu J, Zhang B, Li L, Yin J, Fu J. Additive-lathe 3D bioprinting of bilayered nerve conduits incorporated with supportive cells. Bioact Mater. 2021; 6: 219-29.

365. Dodla MC, Alvarado-Velez M, Mukhatyar VJ, Bellamkonda RV. Peripheral Nerve Regeneration. In: Atala A, Lanza R, Mikos AG, Nerem R, editors. Principles of Regenerative Medicine. Boston: Academic Press; 2019. 1223-36.

366. Gu X, Ding F, Yang Y, Liu J. Construction of tissue engineered nerve grafts and their application in peripheral nerve regeneration. Prog Neurobiol. 2011; 93: 204-30.

367. Zhang Y, Chen H, Li J. Recent advances on gelatin methacrylate hydrogels with controlled microstructures for tissue engineering. Int J Biol Macromol. 2022; 221: 91-107.

368. Park J, Jeon J, Kim B, Lee MS, Park S, Lim J, et al. Electrically Conductive Hydrogel Nerve Guidance Conduits for Peripheral Nerve Regeneration. Adv Funct Mater. 2020; 30: 2003759.

369. Wu Z, Xie S, Kang Y, Shan X, Li Q, Cai Z. Biocompatibility evaluation of a 3D-bioprinted alginate-GelMA-bacteria nanocellulose (BNC) scaffold laden with oriented-growth RSC96 cells. Mater Sci Eng C Mater Biol Appl. 2021; 129: 112393.

370. Arslantunali D, Dursun T, Yucel D, Hasirci N, Hasirci V. Peripheral nerve conduits: technology update. Med Devices 2014; 7: 405-24.

371. AxoGen. 2020. https://www.axogeninc.com/avance-nerve-graft/

372. Leipzig ND, Shoichet MS. The effect of substrate stiffness on adult neural stem cell behavior. Biomaterials. 2009; 30: 6867-78.

373. Babu S, Chen I, Vedaraman S, Gerardo-Nava J, Licht C, Kittel Y, et al. How do the Local Physical, Biochemical, and Mechanical Properties of an Injectable Synthetic Anisotropic Hydrogel Affect Oriented Nerve Growth? Adv Funct Mater. 2022; 32, 2202468.

374. Ghaderinejad P, Najmoddin N, Bagher Z, Saeed M, Karimi S, Simorgh S, et al. An injectable anisotropic alginate hydrogel containing oriented fibers for nerve tissue engineering. Chemical Engineering Journal. 2021; 420: 130465.

375. Lu Q, Zhang F, Cheng W, Gao X, Ding Z, Zhang X, et al. Nerve Guidance Conduits with Hierarchical Anisotropic Architecture for Peripheral Nerve Regeneration. Adv Healthc Mater. 2021; 10: e2100427.

376. Traumatic spinal cord injury. Nature Reviews Disease Primers. 2017; 3: 17019.

377. Carelli S, Giallongo T, Rey F, Colli M, Tosi D, Bulfamante G, et al. Neuroprotection, Recovery of Function and Endogenous Neurogenesis in Traumatic Spinal Cord Injury Following Transplantation of Activated Adipose Tissue. Cells. 2019; 8: 329.

378. Venkatesh K, Ghosh SK, Mullick M, Manivasagam G, Sen D. Spinal cord injury: pathophysiology, treatment strategies, associated challenges, and future implications. Cell Tissue Res. 2019; 377: 125-51.

379. Xue W, Shi W, Kong Y, Kuss M, Duan B. Anisotropic scaffolds for peripheral nerve and spinal cord regeneration. Bioact Mater. 2021; 6: 4141-60.

380. Rose JC, Camara-Torres M, Rahimi K, Kohler J, Moller M, De Laporte L. Nerve Cells Decide to Orient inside an Injectable Hydrogel with Minimal Structural Guidance. Nano Lett. 2017; 17: 3782-91.

381. Kim BJ, Choi JY, Choi H, Han S, Seo J, Kim J, et al. Astrocyte-Encapsulated Hydrogel Microfibers Enhance Neuronal Circuit Generation. Adv Healthc Mater. 2020; 9: e1901072.

382. Chen Z, Zhang H, Fan C, Zhuang Y, Yang W, Chen Y, et al. Adhesive, Stretchable, and Spatiotemporal Delivery Fibrous Hydrogels Harness Endogenous Neural Stem/Progenitor Cells for Spinal Cord Injury Repair. ACS Nano. 2022; 16: 1986-98.

383. Gao X, Cheng W, Zhang X, Zhou Z, Ding Z, Zhou X, et al. Nerve Growth Factor-Laden Anisotropic Silk Nanofiber Hydrogels to Regulate Neuronal/Astroglial Differentiation for Scarless Spinal Cord Repair. ACS Appl Mater Interfaces. 2022; 14: 3701-15.

384. Orive G, Anitua E, Pedraz JL, Emerich DF. Biomaterials for promoting brain protection, repair and regeneration. Nat Rev Neurosci. 2009; 10: 682-92.

385. Jiang JY, Gao GY, Feng JF, Mao Q, Chen LG, Yang XF, et al. Traumatic brain injury in China. Lancet Neurol. 2019; 18: 286-95.

386. Zhu W, Chen L, Wu Z, Li W, Liu X, Wang Y, et al. Bioorthogonal DOPA-NGF activated tissue engineering microunits for recovery from traumatic brain injury by microenvironment regulation. Acta Biomater. 2022; 150: 67-82.

387. Li F, Ducker M, Sun B, Szele FG, Czernuszka JT. Interpenetrating polymer networks of collagen, hyaluronic acid, and chondroitin sulfate as scaffolds for brain tissue engineering. Acta Biomater. 2020; 112: 122-35.

388. Gao P, Postiglione MP, Krieger TG, Hernandez L, Wang C, Han Z, et al. Deterministic progenitor behavior and unitary production of neurons in the neocortex. Cell. 2014; 159: 775-88.

389. Jinnou H, Sawada M, Kawase K, Kaneko N, Herranz-Perez V, Miyamoto T, et al. Radial Glial Fibers Promote Neuronal Migration and Functional Recovery after Neonatal Brain Injury. Cell Stem Cell. 2018; 22: 128-37 e9.

390. Chai Y, Zhao H, Yang S, Gao X, Cao Z, Lu J, et al. Structural alignment guides oriented migration and differentiation of endogenous neural stem cells for neurogenesis in brain injury treatment. Biomaterials. 2022; 280: 121310.

391. Shah A, Brugnano J, Sun S, Vase A, Orwin E. The development of a tissue-engineered cornea: biomaterials and culture methods. Pediatr Res. 2008; 63: 535-44.

392. Thomas MB, Selvam S, Agrawal P, Bellur P, Waghmare N, Chowdhury SK, et al. Print me a cornea - Are we there yet? Bioprinting. 2022; 28: e00227.

393. Kilic Bektas C, Hasirci V. Cell loaded 3D bioprinted GelMA hydrogels for corneal stroma engineering. Biomater Sci. 2019; 8: 438-49.

394. Kim H, Jang J, Park J, Lee KP, Lee S, Lee DM. Shear-induced alignment of collagen fibrils using 3D cell printing for corneal stroma tissue engineering. Biofabrication. 2019; 11: 035017.

395. He B, Wang J, Xie M, Xu M, Zhang Y, Hao H, et al. 3D printed biomimetic epithelium/stroma bilayer hydrogel implant for corneal regeneration. Bioact Mater. 2022; 17: 234-47.

396. Dellaquila A, Le Bao C, Letourneur D, Simon-Yarza T. In Vitro Strategies to Vascularize 3D Physiologically Relevant Models. Adv Sci 2021; 8: e2100798.

397. Guo YN, Huang J, Fang YF, Huang H, Wu J. 1D, 2D, and 3D scaffolds promoting angiogenesis for enhanced wound healing. Chemical Engineering Journal. 2022; 437: 134690.

398. Seifu DG, Purnama A, Mequanint K, Mantovani D. Small-diameter vascular tissue engineering. Nat Rev Cardiol. 2013; 10: 410-21.

399. Alexandre N, Costa E, Coimbra S, Silva A, Lopes A, Rodrigues M, et al. In vitro and in vivo evaluation of blood coagulation activation of polyvinyl alcohol hydrogel plus dextran-based vascular grafts. J Biomed Mater Res A. 2015; 103: 1366-79.

400. Jia W, Gungor-Ozkerim PS, Zhang YS, Yue K, Zhu K, Liu W, et al. Direct 3D bioprinting of perfusable vascular constructs using a blend bioink. Biomaterials. 2016; 106: 58-68.

401. Attalla R, Ling C, Selvaganapathy P. Fabrication and characterization of gels with integrated channels using 3D printing with microfluidic nozzle for tissue engineering applications. Biomed Microdevices. 2016; 18: 17.

402. Gao Q, He Y, Fu JZ, Liu A, Ma L. Coaxial nozzle-assisted 3D bioprinting with built-in microchannels for nutrients delivery. Biomaterials. 2015; 61: 203-15.

403. Dolati F, Yu Y, Zhang Y, De Jesus AM, Sander EA, Ozbolat IT. In vitro evaluation of carbon-nanotube-reinforced bioprintable vascular conduits. Nanotechnology. 2014; 25: 145101.

404. Tabriz AG, Hermida MA, Leslie NR, Shu W. Three-dimensional bioprinting of complex cell laden alginate hydrogel structures. Biofabrication. 2015; 7: 045012.

405. Zhou Y, Gui Q, Yu W, Liao S, He Y, Tao X, et al. Interfacial Diffusion Printing: An Efficient Manufacturing Technique for Artificial Tubular Grafts. ACS Biomater Sci Eng. 2019; 5: 6311-8.

406. Bertassoni LE, Cecconi M, Manoharan V, Nikkhah M, Hjortnaes J, Cristino AL, et al. Hydrogel bioprinted microchannel networks for vascularization of tissue engineering constructs. Lab Chip. 2014; 14: 2202-11.

407. McCoy MG, Wei JM, Choi S, Goerger JP, Zipfel W, Fischbach C. Collagen Fiber Orientation Regulates 3D Vascular Network Formation and Alignment. ACS Biomater Sci Eng. 2018; 4: 2967-76.

408. Sun T, Shi Q, Liang Q, Yao Y, Wang H, Sun J, et al. Fabrication of vascular smooth muscle-like tissues based on self-organization of circumferentially aligned cells in microengineered hydrogels. Lab Chip. 2020; 20: 3120-31.

409. McClendon MT, Stupp SI. Tubular hydrogels of circumferentially aligned nanofibers to encapsulate and orient vascular cells. Biomaterials. 2012; 33: 5713-22.

410. Pi Q, Maharjan S, Yan X, Liu X, Singh B, van Genderen AM, et al. Digitally Tunable Microfluidic Bioprinting of Multilayered Cannular Tissues. Adv Mater. 2018; 30: e1706913.

411. Yu JR, Navarro J, Coburn JC, Mahadik B, Molnar J, Holmes JHt, et al. Current and Future Perspectives on Skin Tissue Engineering: Key Features of Biomedical Research, Translational Assessment, and Clinical Application. Adv Healthc Mater. 2019; 8: e1801471.

412. Wei C, Feng YH, Che DZ, Zhang JH, Zhou X, Shi YB, et al. Biomaterials in skin tissue engineering. International Journal of Polymeric Materials and Polymeric Biomaterials. 2022; 71: 993-1011.

413. Kim HS, Sun X, Lee JH, Kim HW, Fu X, Leong KW. Advanced drug delivery systems and artificial skin grafts for skin wound healing. Adv Drug Deliv Rev. 2019; 146: 209-39.

414. Tang G, Zhou B, Li F, Wang W, Liu Y, Wang X, et al. Advances of Naturally Derived and Synthetic Hydrogels for Intervertebral Disk Regeneration. Front Bioeng Biotechnol. 2020; 8: 745.

415. Nakamichi R, Ito Y, Inui M, Onizuka N, Kayama T, Kataoka K, et al. Mohawk promotes the maintenance and regeneration of the outer annulus fibrosus of intervertebral discs. Nat Commun. 2016; 7: 12503.

416. Vos T, Flaxman AD, Naghavi M, Lozano R, Michaud C, Ezzati M, et al. Years lived with disability (YLDs) for 1160 sequelae of 289 diseases and injuries 1990-2010: a systematic analysis for the Global Burden of Disease Study 2010. Lancet. 2012; 380: 2163-96.

417. Sakai D, Andersson GB. Stem cell therapy for intervertebral disc regeneration: obstacles and solutions. Nat Rev Rheumatol. 2015; 11: 243-56.

418. Liu J, Wang D, Li Y, Zhou Z, Zhang D, Li J, et al. Overall Structure Construction of an Intervertebral Disk Based on Highly Anisotropic Wood Hydrogel Composite Materials with Mechanical Matching and Buckling Buffering. ACS Appl Mater Interfaces. 2021; 13: 15709-19.